Oncology and Translational Medicine

Volume 7 • Number 3 • June 2021

Oncology and Translational Medicine Volume 7 • Number 3 • June 2021 pp 99–147

邮发代号：38-121
ISSN 2095-9621

GENERAL INFORMATION
≫otm.tjh.com.cn

ISSN 2095-9621
CN 42-1865/R

Oncology and Translational Medicine

肿瘤学与转化医学（英文）

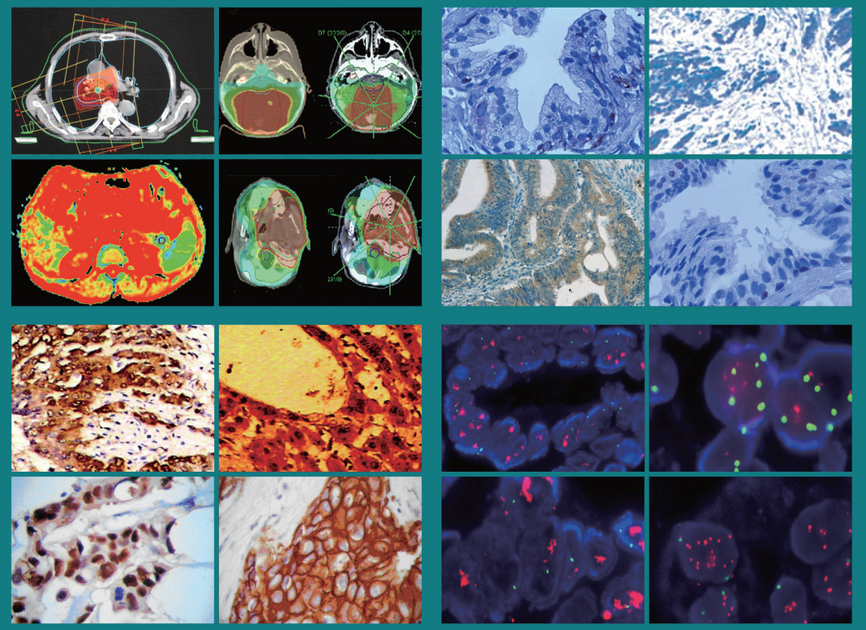

Volume 7
Number 3
June 2021

Oncology and Translational Medicine

Oncology and Translational Medicine
June 2021 Volume 7 Number 3

Contents

Oncology and Translational Medicine

Volume 7 • Number 3 • June 2021

Aims & Scope

Oncology and Translational Medicine is an international professional academic periodical. The Journal is designed to report progress in research and the latest findings in domestic and international oncology and translational medicine, to facilitate international academic exchanges, and to promote research in oncology and translational medicine as well as levels of service in clinical practice. The entire journal is published in English for a domestic and international readership.

Copyright

Supervised by

Ministry of Education of the People's Republic of China.

Administered by

Tongji Medical College, Huazhong University of Science and Technology.

Submission information

Manuscripts should be submitted to:
http://otm.tjh.com.cn
dmedizin@sina.com

Subscription information

ISSN edition: 2095-9621
CN: 42-1865/R

■ Subscription rates

Subscription may begin at any time. Remittances made by check, draft or express money order should be made payable to this journal. The price for 2021 is as follows: US $ 30 per issue; RMB ￥28.00 per issue.

Database

Oncology and Translational Medicine is abstracted and indexed in EMBASE, Index Copernicus, Chinese Science and Technology Paper Citation Database (CSTPCD), Chinese Core Journals Database, Chinese Journal Full-text Database (CJFD), Wanfang Data; Weipu Data; Chinese Academic Journal Comprehensive Evaluation Database.

Business correspondence

All matters relating to orders, subscriptions, back issues, offprints, advertisement booking and general enquiries should be addressed to the editorial office.

Mailing address

Editorial office of
Oncology and Translational Medicine
Tongji Hospital
Tongji Medical College
Huazhong University of Science and Technology
Jie Fang Da Dao 1095
430030 Wuhan, China
Tel.: +86-27-69378388
Email: dmedizin@sina.com

Printer

Changjiang Spatial Information Technology Engineering Co., Ltd. (Wuhan) Hangce Information Cartorgraphy Printing Filial, Wuhan, China
Printed in People's Republic of China

Editors-in-Chief

Managing director

Executive editors

Oncology and Translational Medicine
DOI 10.1007/s10330-021-0505-5

June 2021, Vol. 7, No. 3, P99–P101

SPECIAL CONTRIBUTION

In memory of Academician Mengchao Wu, the pioneer of Chinese hepatobiliary surgery

Xiaoping Chen (✉)

Hepatic Surgery Center, Tongji Hospital, Tongji Medical College, Huazhong University of Science and Technology, Wuhan 430030, China

Received: 16 June 2021
Accepted: 17 June 2021

I have two important reasons for writing this. First, I want to commemorate the Academician Mengchao Wu I knew – a venerable man who, though gone, has left behind a spirit that will continue to inspire people forever. He was a man of conviction with a resolute sense of his mission; he brought honor to his country and his generation. Second, I want people to know about his contributions, character, teachings, and influence and see them as a legacy to be embraced and passed down to younger generations as a beacon and stars that light the way and continue to shine into the future.

Acadamician Mengchao Wu (left) and Acadamician Xiaoping Chen (right)

On May 22, 2021, Academician Mengchao Wu passed away in Shanghai. Words can't even begin to describe the grief I felt when I heard the news. Thoughts churned inside my mind in the middle of night. The memories of our friendship had never been so clear. There is a Chinese saying: "No matter whom you meet, he is destined to appear in your life; there are no coincidences." Some people are born to be a beam of light – admired, respected, and followed by others. Mengchao Wu was one of those people.

Academician Wu once said, "What concerns me most is that others look down on us Chinese people. Because humiliation is rampant overseas, the country should be strengthened." He was an overseas Chinese residing in Malaysia. An impoverished country where the people were weak brought him bitter anguish. After the outbreak of the Chinese People's War of Resistance against Japanese Aggression, the Chinese living in Malaysia fervently discussed the decision by the Communist Party of China (CPC) to resist the Japanese invaders and Party members' heroic deeds in combat. Ever patriotic, Academician Wu resolutely vowed to return to China to join the national efforts in fighting against the Japanese invaders. Unfortunately, battles and turmoil prevented him from going to Yan'an (the base of the CPC then), so he decided to "save the country through education" and applied to the School of Medicine of Tongji University. His affectionate love for the country and his unwavering determination to serve the country supported him throughout his entire life. His selfless devotion to China's medical development made him a legend. I often encourage young doctors by telling them that only when intellectuals integrate their own pursuits into the nation's great causes will they make the best use of their knowledge and ultimately have successful careers. This epiphany inspired by Academician Mengchao Wu has stood the test of time.

✉ Correspondence to: Xiaoping Chen. Email: chenxpchenxp@163.com

In 2011, Wu received the Moving China award. At the ceremony, he was praised for "having an undying flame of passion that ever guides him to fulfill his oath; this flame has been ever burning and has never been put out." This aptly described the academician, a man of faith who carved out his career as needed by the country and the people. He once said, "I made three right decisions in my life: "returning to China, joining the army, and joining the Party. By going back to my motherland, my aspiration took root in the soil; by dedicating myself to medical science, I had an ideal to strive for; by becoming a Party member, I had a lofty ambition to guide me; by joining the army, I had a great school to teach me." In 1956, after applying 19 times with the faith and enthusiasm of a communist fighter, Wu was finally approved to join the CPC. From that moment, he began to fulfill his commitments to the Party. His original aspiration remained unchanged for 65 years.

In the early 1950s, Mengchao Wu asked his mentor Fazu Qiu about his future career. Professor Qiu told him, "There is little development in hepatobiliary surgery in China. You might seek progress in this direction." At that time, hepatobiliary surgery was an uncharted territory in China, a specialty eschewed by many because patients could easily die from heavy bleeding during the operations. Yet Mengchao Wu did not hesitate when Professor Qiu asked him to lead a three-person team committed to solving the technical problems associated with hepatobiliary surgery. That three-person research team has since developed into the largest professional institute of liver surgery, hepatobiliary clinic, and scientific research. Most theories and techniques for surgical treatment of liver cancer were created in China. Over the decades, Academician Mengchao Wu achieved numerous firsts in hepatobiliary surgery in China and worldwide. He helped build China's prepotency in hepatobiliary surgery from the ground up, embodying the quest for excellence in the field as the pioneer of Chinese hepatobiliary surgery. In 2005, he won the State Supreme Science and Technology Award of China. Academician Mengchao Wu epitomizes the professional ethics and bright future of Chinese medical science. I am honored to carry forward my esteemed colleague's precious spiritual legacy.

Academician Wu's beloved mentor Professor Qiu and him – the father of Chinese hepatobiliary surgery and the master of Chinese surgery, respectively – shared many common traits and experiences that touched many people's hearts and lives. In them, I see unwavering dedication to the medical cause and the well-being of humankind. Such undistracted devotion is priceless and deeply moving. Professor Qiu once commended Academician Wu: "He is a man of great virtue in that he loves his wife, respects his teachers, and works very hard." Academician Qiu was eight years older than Academician Wu. When Academician Qiu turned ninety, Academician Mengchao Wu was in his eighties, yet we often saw Academician Wu voluntarily supporting Qiu to walk in public, a touching scene and a lesson for us all. His respect for his teacher was evident in every moment he spent with his teacher, a respect that came from the bottom of his heart. His reverence profoundly impressed me and was praised widely in the medical circle. We Chinese have a saying: "The country will be prosperous if teachers are respected and honored." Their deep and abiding mentor-student relationship embodied the profound and time-honored humanistic spirit of the Chinese nation and should be a model for us all.

Academician Wu was committed to assimilating Professor Qiu's medical knowledge, ethics, and skills. One of the walls in Academician Wu's office was adorned with a motto by Professor Qiu that read, "Able to speak, able to do, and able to write." At the end of 2017, Wu led a team at the seventh session of the Chinese branch of the International Hepato-Pancreato-Biliary Association, which also marked the Second Seminar on Fazu Qiu's academic thinking. At the event, speaking to top hepato-pancreato-biliary experts in China, Wu said that by discussing the latest developments and cutting-edge technologies in China and pooling their strengths to improve the diagnosis and treatment of such diseases, they were practicing Academician Fazu Qiu's teachings and repaying him for what he had done for the development of Chinese surgery. Academician Wu did the same throughout his life. He had more than mastered Professor Qiu's surgical skills, yet he always drove himself to learn more, and he instilled in me the importance of passing on our skills and knowledge.

Academician Wu frequently emphasized the importance of cultivating young talent. He hoped his students would become more

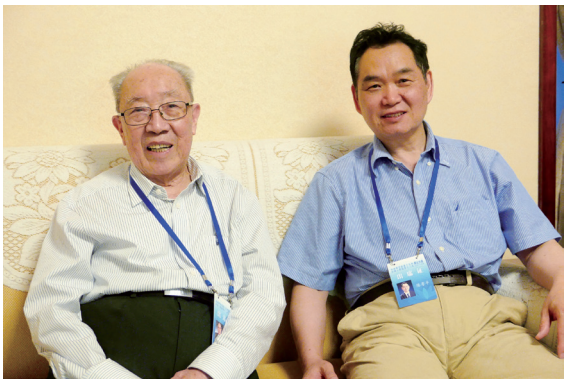

than just doctors who only perform operations and continue to pursue excellence and become true masters. He said that the healthy development of Chinese hepatobiliary surgery depended on the next generation. If young people do well, there is great cause for hope. He groomed and influenced many high-caliber professionals with his knowledge and virtues. He imparted knowledge, but, more importantly, he taught us ethics – not only by teaching and lecturing but by making himself an example for students. He accomplished each task meticulously, no matter how trivial it was or how easily overlooked. By succeeding at even the most menial of tasks, he helped young people internalize the correct values and perceptions of life on which their futures rely. Academician Wu mentored and guided four generations of students. Most of the doctors and post-doctors he mentored have become the quintessence of liver surgery in China.

When I was a student, "Mengchao Wu" was already a famous name. He was a great professor in our eyes, yet he was disarmingly humble. My first contact with Professor Wu was in December 1985, when my doctoral dissertation defense was scheduled, and I was asked to pick him up at the Wangjiadun Airport. I was young and tended to judge people from their appearance. He was a soldier, so I presumed that he would be tall and strongly built. I waited for a long time at the airport exit and still hadn't been able to identify when passengers were all gone. I finally gave up and returned to the university, nervous and worried that my adviser, Professor Qiu, would criticize me. When I returned, I saw that Professor Wu had already settled in the school's guesthouse and was talking with Professor Qiu. Professor Wu's gray Chinese tunic suit and hat were obviously not new, nor was the briefcase in his hand. He was plain-looking and modest, completely different from what I had imagined. I entered the room with great nervousness, but he greeted me and said, "You must be my junior, Xiaoping Chen, right?" The tension suddenly disappeared. (He called me "junior" for decades until I was approaching 70.) I defended my graduation dissertation, and his amiable demeanor confirmed my first impression of Mengchao Wu. He asked critical questions and was happy when I gave him answers; he guided and inspired me when I could not answer immediately. He really wanted to help young people.

In the course of our subsequent contacts, we became more familiar with one another. Sometimes, I visited him in Shanghai and ate at his home. I liked to see his clear eyes. He chatted with me in plain language, often helping me resolve and clarify problems and confusion. When I visited, he always asked me the same question: "Xiaoping, how are you doing recently? What difficulties do you have?" The simple questions made me feel that my teacher cared about me. Although he was in Shanghai and I was in Wuhan, he still had a great influence on me in a subtle way. I owe my achievements today to his teachings and behaviors.

Academician Wu's colleagues and patients called his hands the hands of God. He saved lives throughout his lifetime. In our conversations, he talked most about his patients' illnesses, how they improved after receiving treatments, and what he learned in the process. He focused his mind on diagnosing diseases, but he set his heart on caring for people. Academician Wu always treated patients with utmost care and sincerity. In his 75 years of being a doctor, he was in charge of more than 16,000 operations and treated more than 20,000 patients. These numbers are living stories of Wu's outstanding medical achievements as a doctor who saved lives and was committed to the well-being of humanity. For him, becoming a doctor was like the self-cultivation required to become an ascetic monk. There is no global shortage of experts and authority, but many lack the "human" quality – the willingness to give themselves to a greater cause. What Wu held dear to his heart was "carrying every patient across the river on his back." He was the one who gave himself to the greater cause.

"Those who are not as virtuous as Buddha cannot be doctors, and those who are not as knowledgeable as sages cannot be doctors." Professor Qiu's words made us cautious and self-disciplined. Mengchao Wu followed his teacher's lesson and became a true medical master just like his teacher: benevolent, righteous, and selfless. As his junior, what kind of mission do I inherit? What kind of responsibilities do I now bear? I often think about this, and the answer is self-evident.

May the legacy of Academician Mengchao Wu live on forever!

Xiaoping Chen

Oncology and Translational Medicine
DOI 10.1007/s10330-020-0470-0

June 2021, Vol. 7, No. 3, P102–P107

REVIEW ARTICLE

Future of targeted therapy for gastrointestinal cancer: Claudin 18.2

Qian Niu, Jiamin Liu (Co-first author), Xiaoxiao Luo, Beibei Su, Xianglin Yuan (✉)

Department of Oncology, Tongji Hospital, Tongji Medical College, Huazhong University of Science and Technology, Wuhan 430030, China

Abstract

The treatment of gastrointestinal cancer has always been a crucial research area, and targeted therapy has been receiving increasing attention. At present, the effect of targeted therapy is unsatisfactory for gastric cancer. Thus, the discovery of new targets is crucial. Claudin 18.2 (CLDN18.2), a member of the claudin family, belongs to the tight junction protein family that controls the flow of molecules between cell layers. CLDN18.2 expression has been discussed in many studies. In recent years, there have been many studies on targeted therapy with CLDN18.2-ideal monoclonal antibody 362. Furthermore, CLDN18.2-specific chimeric antigen receptor T therapy has been used for CLDN18.2-positive tumors, such as gastric and pancreatic cancers. Considerable research has been focused on CLDN18.2. CLDN18.2, a newly discovered marker for precise targeted therapy of gastric cancer, could offer new hope for the treatment of gastric cancer.

Received: 16 November 2020
Revised: 24 January 2021
Accepted: 15 March 2021

Key words: gastrointestinal cancer; claudin 18.2 (CLDN18.2); targeted therapy; ideal monoclonal antibody 362 (IMAB362); chimeric antigen receptor (CAR) T cells treatment

Gastric cancer is the fifth most common cancer and the third leading cause of cancer-related deaths worldwide, with almost one million new cases diagnosed every year [1]. The early symptoms of gastric cancer are not easily observed, and hence, it is usually diagnosed at an advanced stage. Surgery and chemotherapy, which are the main treatments for advanced gastric cancer, cannot provide striking survival benefits [2].

To improve the treatment of gastric cancer, an increasing number of studies are being conducted on targeted therapy. The monoclonal antibody, trastuzumab, which targets anti-human epidermal growth factor receptor 2 (HER2), is listed as a targeted drug for gastric cancer by the National Comprehensive Cancer Network [3]. Other drugs, such as pertuzumab, an anti-HER2 monoclonal antibody [4], ramucirumab, an anti-vascular endothelial growth factor receptor 2 monoclonal antibody [5], and pembrolizumab, an anti-procedural cell death protein 1 monoclonal antibody [6], also showed satisfactory results in clinical trials. For targeted therapy, claudin 18.2 (CLDN18.2), a newly discovered target, is expected to become a breakthrough in the treatment of gastric cancer.

Claudin protein belongs to the family of tight junction proteins that can control the flow of molecules between cell layers. Claudin 18 (CLDN18) is a protein encoded by the CLDN18 gene in humans, with two splicing variants, claudin 18.1 (CLDN18.1) and CLDN18.2. CLDN18.2 is primarily expressed in differentiated gastric parietal cells [7].

Ideal monoclonal antibody (IMAB) 362 (claudiximab/zolbetuximab) is a therapeutic monoclonal antibody against CLDN18.2 [8]. The safety and efficacy of IMAB362 have been demonstrated in completed phase I and II clinical trials [9–10], indicating that CLDN18.2 is a very valuable target. Moreover, a large number of phase III studies have been conducted. Additional treatments associated with CLDN18.2 are also being developed. In this review, we focus on the progress of CLDN18.2.

Characteristics of the claudin protein

In 1998, Furuse *et al* [11] first discovered the claudin protein in chicken liver. Claudins are the major

✉ Correspondence to: Xianglin Yuan. Email: xlyuan1020@163.com

transmembrane protein components of tight junctions in human endothelia and epithelia [12]. The functions of claudins include adherence to cells, maintenance of cell polarity, regulation of cell permeability, and participation in the regulation of cell proliferation and differentiation [13]. To date, 27 members of the claudin protein family have been discovered in mammals, with expression in different tissues. For example, claudin 1 is highly expressed in the liver, lungs, and kidneys, and although, claudin 3 is present in the lung and liver, it is rarely expressed in the kidney. In tumor cells, related studies have shown that the occurrence of colon cancer is related to claudin 1, 3, 4 [14]. Claudin 7 is expressed in gastric [15], renal [16] and ovarian cancers [17]. The decreased expression of claudin 10 benefits the prognosis of hepatocellular carcinoma [18]. In addition, the distribution of CLDN18.1 and CLDN18.2 expression is different because of the differences in the eight amino acids of the two sequences. CLDN18.1, which is selectively expressed in normal lung cells, and CLDN18.2 are expressed in differentiated gastric parietal cells, but not in stem cells [7]. In addition, CLDN18.2 is retained during the malignant transformation of gastric cancer. Moreover, the ectopic activation of CLDN18.2 has been observed in gastric cancer and its metastatic foci [19]. CLDN18.2 can also be expressed in pancreatic, esophageal, ovarian, and lung cancers.

The claud in protein consists of four transmembrane regions, including two extracellular rings. The N-terminal and C-terminal regions of the protein are located in the cytoplasm [20]. The two extracellular rings make it a potential antibody target. As an ideal therapeutic target, a monoclonal antibody, IMAB362, has been developed against CLDN18.2.

CLDN18.2 expression in gastric cancer patients

Clinical and therapeutic features of CLDN18.2 in a gastric cancer population have been studied.

Dottermusch *et al* conducted a cohort study on Caucasians [21]. They investigated the association between CLDN18.2 expression and clinicopathological features including survival time in gastric cancer patients. CLDN18.2 expression was observed in 42.2% of the patients (n = 203/481), and 14.8% (n = 71/481) showed weak immunostaining (ICH 1+). The study also pointed out that CLDN18.2 expression is associated with mucin phenotype, EBV status, integrin αvβ5, EpCAM extracellular domain EPEX, and lysozyme.

Gastric cancer is more common in the Asian population. A recent study in Japan [22] compared CLDN18.2 expression in primary gastric cancer patients with that in patients with lymph node metastasis. In the study, 52% of primary tumors (n = 135/262) and 45% of cancers with LN metastases (n = 61/135) had moderate to strong CLDN18.2 membrane staining (≥ 40% tumor cells with CLDN18.2 expression ≥ 2+). They also found a higher expression of CLDN18.2 in diffuse gastric cancer and high-grade (G3) tumors, which was not consistent with the results of Dottermusch *et al*. In addition, the positive rate of CLDN18.2 in gastric cancer patients in Japan (87%, n = 228/262) was higher than that in Europe (77%, n = 51/66) [7].

Based on the aforementioned study, Baek *et al* explored the expression of CLDN18.2 in gastric cancer in Korea [23]. The study included 367 gastric cancer patients (pathological stage II to III) who had undergone radical surgery. The authors carried out immunohistochemical staining for CLDN18.2, followed by a semi-quantitative analysis based on the intensity and percentage of staining. They reported that CLDN18.2 expression was observed in 237 patients, with 108 patients (29.4%) categorized as CLDN18.2-positive cases, based on staining scores of 51%–100% and moderate to strong staining intensity. The results demonstrated that there was a higher expression of CLDN18.2 in diffuse and HER2-positive (HER2 2+ or 3+) gastric cancer. In addition, they reported that CLDN18.2 expression was independent of survival outcome, age, sex, primary tumor location, or TNM stage.

A significant difference in the expression rate of CLDN18.2 in different studies may be related to ethnic characteristics. Different testing methods and contemporary standards for determining CLDN18.2 expression have also produced varied results (Table 1). High expression of CLDN18.2 in gastric cancer patients in Asia indicates that it might be a potential and exclusive therapeutic target for gastric cancer.

Therapy

Mechanism of targeted therapy

IMAB362 (zolbetuximab/claudiximab) is a new IgG-1 antibody that is highly specific to CLDN18.2 [25]. Studies have shown that IMAB362 mediates cell killing through a series of immune mechanisms [20], which stimulates the activation of antibody-dependent cytotoxicity and complement-dependent cytotoxicity-induced cellular and soluble immune effects [26]. In addition, it could interfere with the biological function of CLDN18.2 in cancer cells, resulting in anti-proliferation and pro-apoptosis effects [27]. However, further exploration of the mechanism is still necessary. Furthermore, IMAB362 combined with chemotherapy plays a role in the recruitment of T cells, alteration of the tumor microenvironment, and prolongation of the overall survival time (OS) and progression-free survival time (PFS) [9].

Table 1 The expression of CLND18.2 in different studies

Author	Population	CLDN18.2+ expression rate	Definition of positive	Test method
Al-Batran SE [24] (FAST study)	German	48% (334/686)	Moderate to strong CLDN18.2 expression and membrane staining intensity ≥ 2+ in ≥ 40% of cancer cells	CLAUDETECT™ 18.2 kit
Rohde C [22]	Japanese	52% (135/262)	The same as above	CLAUDETECT™ 18.2 kit
Dottermusch M [21]	Caucasian	42.2% (203/481) 10% If use FAST criteria	Used histoscore for expression scoring	Anti CLDN18.2 monoclonal antibody, Abcam
Baek JH [23]	Korean	29.4% (108/367)	Semi-quantitative scoring method: a percentage of staining score of 3 (51%–100%) and with moderate to strong staining intensity (2 or 3)	Anti CLDN18.2 monoclonal antibody, Abcam

Application of IMAB362/claudiximab/zolbetuximab

Many studies have investigated the effect of IMAB362 in various types of tumors, including advanced gastric [28], pancreatic [29], non-small-cell lung [30], and esophagogastric cancers [31]. Clinical studies on IMAB362 have also yielded encouraging results.

Clinical trials on IMAB362/claudiximab/zolbetuximab

In a phase I clinical study (PILOT, NCT01671774) [32], the safety and efficacy of claudiximab in combination with zoledronic acid (ZA) and interleukin-2 in the treatment of esophageal and gastric adenocarcinoma were investigated. In the study, 28 patients were included, and in 11 of the 20 evaluable patients, disease control was achieved. One patient showed partial response and the other 10 patients stable disease. The OS and PFS were 40 weeks and 12.7 weeks, respectively, which suggests that claudiximab, as a single therapy, has anti-tumor effect and can be used in combination with ZA for the treatment of tumors.

In a phase II clinical study (MONO, NCT01197885) [10], the safety and efficacy of zolbetuximab in the treatment of metastatic, refractory, and recurrent adenocarcinoma of the stomach or the lower esophagus were investigated. Patients with CLDN18.2 expression in more than 50% of tumor cells were intravenously injected with zolbetuximab five times every 2 weeks (two dose levels: four received 300 mg/m^2 in cohort 1 and 50 received 600 mg/m^2 in cohort 2/3). A total of 54 patients were evaluated. The antitumor activity data of 43 patients were finally obtained; the objective response rate, partial remission rate, and clinical benefit rate were 9%, 9%, and 23%, respectively. The effect was more significant in the subgroup; out of 29 patients with CLDN18.2 expression in ≥ 70% of tumor cells, 14% (four of 29) achieved partial response and 17% (five of 29) had stable disease. This study confirmed the efficacy of zolbetuximab monotherapy.

In a phase IIb clinical study (FAST, NCT01630083) [24], the researchers evaluated IMAB362 as a first-line treatment for advanced, recurrent gastric cancer and gastroesophageal junction adenocarcinoma. Patients with CLDN18.2 expression (with immunohistochemical score ≥ 2+) in ≥ 40% tumor cells were included and randomly assigned to the first-line standard EOX (epi-doxorubicin, oxaliplatin, and capecitabine) group; chemotherapy was administered once every three weeks, with or without IMAB362 (the loading dose was 800 mg/m^2, 600 mg/m^2 on the first day).

There was also an exploratory third arm in which a high-dose monoclonal antibody (1000 mg/m^2) plus EOX was administered. IMAB362 combined with EOX significantly improved the PFS of patients compared with EOX alone (PFS: 7.9 months *vs.* 4.8 months; HR 0.47, P = 0.0001 and OS: 13.2 months *vs.* 8.4 months; HR 0.51, P = 0.0001). Patients with high CLDN18.2 expression (≥ 70% tumor cells with CLDN18.2 expression ≥ 2+) had a better prognosis (PFS: 7.2 months *vs.* 5.6 months; HR 0.36, P < 0.0005; OS: 16.6 months *vs.* 9.3 months; HR 0.45, P < 0.0005). PFS was significantly improved in the IMAB362 high-dose group compared with the chemotherapy group (PFS: 7.1 months *vs.* 4.8 months; HR 0.59, P = 0.0026). The study demonstrated that IMAB362 combined with EOX is a safe and effective therapeutic strategy. The FAST study also provided a solid foundation for large-scale phase III clinical studies.

A phase III clinical study on the first-line treatment of CLDN18.2-positive, HER2-negative, locally progressive, metastatic gastric cancer or gastroesophageal junction adenocarcinoma with mFOLFOX in combination with zolbetuximab or placebo (NCT03504397) is ongoing. A clinical study on CAPOX plus zolbetuximab (NCT03653507) has also been conducted.

All clinical studies showed good prospects for IMAB326, and the results of the phase III clinical study are anticipated. Previous studies are limited to Western countries; however, the high expression of CLDN18.2 in gastric cancer patients in Asia has encouraged the exploration of the effect of zolbetuximab in Asian

populations.

CLDN18.2-specific chimeric antigen receptor (CAR) T cell therapy

Dr. Li Zonghai's team explored the use of CLDN18.2-specific CAR T cells for gastric cancer treatment, and they published their findings in the Journal of the National Cancer Institute in 2018 [33]. In their study, they developed specific humanized antibodies 8E5 (hu8E5) scFv, using the hybridoma and humanization techniques, and prepared CLDN18.2-specific CAR T cells – CAR (hu8E5-28Z, hu8E5-BBZ, and hu8E5-2I-28Z) T, using the lentiviral vector transduction method. Cytotoxicity test and enzyme-linked immunosorbent assay were then performed to detect the antitumor activity and cytokine-producing ability of CAR T cells against gastric cancer cells *in vitro*. The *in vivo* antitumor activity of CAR T cells was evaluated using a mouse gastric cancer cell line and a human transplanted tumor (PDX) model. CAR T cells could lyse CLDN18.2-positive cells *in vitro*, but not CLDN18.2-negative cells. In the PDX model of gastric cancer (GA0006), the hu8E5-2I-28Z group was compared with the untransduced T (UTD) group. The tumor size (hu8E5-2I-28Z group *vs.* UTD group: 252.6 (158.6) mm^3 *vs.* 1029.1 (852.7) mm^3, $P < 0.001$) and weight ($P < 0.007$) were significantly lower in the hu8E5-2I-28Z group than in the UTD group. All the results showed that CAR T cell therapy is an effective way to treat CLDN18.2-positive gastric cancer. Furthermore, after treatment with hu8E5-2I T cells, no obvious damage was observed in the stomach tissue or other organs of the mice.

Similarly, some researchers conducted a clinical study (NCT03159819) in which CAR T cells targeted CLDN18.2 in gastric and pancreatic cancers. According to their mid-term data, 12 patients with advanced gastric and pancreatic cancers were enrolled in the study. Most of the patients had multiple organ metastases and eight patients had different degrees of tumor regression. In particular, in a modified treatment subgroup, according to RECIST 1.1, five of the six patients achieved objective remission, including one complete remission.

Targeting CLDN18.2 using antibody drug conjugates (ADCs) or CD3-bispecifc modality

Zhu *et al* demonstrated that targeting CLDN18.2 using ADCs and CD3-bispecifc modality may be an effective treatment strategy for gastric and pancreatic cancers [34]. The anti-CLDN18.2 ADC and CD3-bispecifc molecules inhibited tumor cell growth *in vitro*. In addition, the efficacy and safety of the strategy have been demonstrated *in vivo* in PDX animal models of gastric and pancreatic cancers.

Conclusion and prospect

The treatment of advanced gastric cancer remains challenging. To date, chemotherapy has been the mains treamtreatment for advanced tumors [35]. With the innovation of surgical methods and the emergence of new chemotherapy regimens, the 5-year survival rate of patients with advanced gastric cancer has improved to some extent, but it is still low, approximately 5%–20%, and the median OS is approximately 10 months [36]. Targeted therapy is an effective treatment and has become the most promising therapy in oncology. Especially in gastric cancer, the variety of targeted drugs has become increasingly abundant [37]. Currently, some progress has been made in the use of trastuzumab for the treatment of HER2-positive tumor cells [3, 38]. We expect that CLDN18.2 will be explored in the development of a targeted therapy for gastric cancer and other CLDN18.2-positive tumors.

Existing studies have pointed out the different expression characteristics of CLDN18.2. Some studies have shown that the downregulation of CLDN18.2 is a characteristic of gastric cancer [21, 39]. This is mainly due to the destruction of tight junctions, which leads to the disruption of epithelial cell cohesion [40] and promotes the invasive potential and metastasis of tumor cells [41–42]. However, in the study by Rohde *et al*, CLDN18.2 expression remained the same with the presence of lymph node metastasis [22], which is consistent with the results of the FAST study. Jun *et al* found that reduced expression of CLDN18.2 was associated with peripheral invasion and poor OS [42]. However, Baek *et al* showed that CLDN18.2 expression in gastric cancer patients was independent of survival outcome [23]. Thus, more studies are required to elucidate the role of CLDN18.2 in gastric cancer metastasis.

Moreover, CLDN18.2 and HER2 co-expression has been mentioned in some studies [23–24]. The dual-target therapy (monoclonal antibody of anti-HER2 and anti-CLDN18.2) creates a combination treatment mode for gastric cancer patients, which could provide additional survival benefits to specific patients.

Presently, IMAB is a better choice for the treatment of solid tumors and hematological tumors, as IMAB binds to the selective target of the tumor [43]. It is mainly expressed in tumor cells and rarely expressed in healthy tissues. The limited expression of IMAB in normal tissues can reduce adverse events and improve curative effect [29].

CLDN18.2-specific CAR T cells also provide a new strategy for the treatment of gastric cancer and other CLDN18.2-positive tumors in clinical practice. This therapeutic approach should provide great benefit to cancer patients, such as those with pancreatic or gastric cancer [44].

At present, treatments for pancreatic and gastric cancers are not effective. CLDN18.2 expression in these cancers brings more options for treatment. However, there is still a need to further explore how much survival benefits CLDN18.2 could provide for patients with pancreatic or gastric cancer. In addition, the role of CLDN18.2 in tumor progression is also worth investigating. Furthermore, the combination of targeted therapy and radiotherapy has not been studied in depth. We hope to find more clinical applications of this strategy for the treatment of tumors.

Conflicts of interest

The authors indicated no potential conflicts of interest.

References

1. Bray F, Ferlay J, Soerjomataram I, *et al*. Global cancer statistics 2018: GLOBOCAN estimates of incidence and mortality worldwide for 36 cancers in 185 countries. CA Cancer J Clin, 2018, 68: 394–424.
2. Lazăr DC, Tăban S, Cornianu M, *et al*. New advances in targeted gastric cancer treatment. World J Gastroenterol, 2016, 22: 6776–6799.
3. Bang YJ, Van Cutsem E, Feyereislova A, *et al*. Trastuzumab in combination with chemotherapy versus chemotherapy alone for treatment of HER2-positive advanced gastric or gastro-oesophageal junction cancer (ToGA): a phase 3, open-label, randomised controlled trial. Lancet, 2010, 376: 687–697.
4. Tabernero J, Hoff PM, Shen L, *et al*. Pertuzumab plus trastuzumab and chemotherapy for HER2-positive metastatic gastric or gastro-oesophageal junction cancer (JACOB): final analysis of a double-blind, randomised, placebo-controlled phase 3 study. Lancet Oncol, 2018, 19: 1372–1384.
5. Khan U, Shah MA. Ramucirumab for the treatment of gastric or gastro-esophageal junction cancer. Expert Opin Biol Ther, 2019, 19: 1135–1141.
6. Shitara K, Özgüroğlu M, Bang YJ, *et al*. Pembrolizumab versus paclitaxel for previously treated, advanced gastric or gastro-oesophageal junction cancer (KEYNOTE-061): a randomised, open-label, controlled, phase 3 trial. Lancet, 2018, 392: 123–133.
7. Sahin U, Koslowski M, Dhaene K, *et al*. Claudin-18 splice variant 2 is a pan-cancer target suitable for therapeutic antibody development. Clin Cancer Res, 2008, 14: 7624–7634.
8. Shitara K, Ohtsu A. Advances in systemic therapy for metastatic or advanced gastric cancer. J Natl Compr Canc Netw, 2016, 14: 1313–1320.
9. Al-Batran SE, Schuler M, Zvirbule Z, *et al*. IMAB362: a novel immunotherapeutic antibody targeting the tight-junction protein component CLAUDIN 18.2 in gastric cancer. Ann Oncol, 2016, 27: 141–142.
10. Türeci O, Sahin U, Schulze-Bergkamen H, *et al*. A multicentre, phase IIa study of zolbetuximab as a single agent in patients with recurrent or refractory advanced adenocarcinoma of the stomach or lower oesophagus: the MONO study. Ann Oncol, 2019, 30: 1487–1495.
11. Furuse M, Fujita K, Hiiragi T, *et al*. Claudin-1 and -2: novel integral membrane proteins localizing at tight junctions with no sequence similarity to occludin. J Cell Biol, 1998, 141: 1539–1550.
12. Liu F, Koval M, Ranganathan S, *et al*. Systems proteomics view of the endogenous human claudin protein family. J Proteome Res, 2016, 15: 339–359.
13. Swisshelm K, Macek R, Kubbies M. Role of claudins in tumorigenesis. Adv Drug Deliv Rev, 2005, 57: 919–928.
14. Mees ST, Mennigen R, Spieker T, *et al*. Expression of tight and adherens junction proteins in ulcerative colitis associated colorectal carcinoma: upregulation of claudin-1, claudin-3, claudin-4, and beta-catenin. Int J Colorectal Dis, 2009, 24: 361–368.
15. Johnson AH, Frierson HF, Zaika A, *et al*. Expression of tight-junction protein claudin-7 is an early event in gastric tumorigenesis. Am J Pathol, 2005, 167: 577–584.
16. Hornsby CD, Cohen C, Amin MB, *et al*. Claudin-7 immunohistochemistry in renal tumors: a candidate marker for chromophobe renal cell carcinoma identified by gene expression profiling. Arch Pathol Lab Med, 2007, 131: 1541–1546.
17. Tassi RA, Bignotti E, Falchetti M, *et al*. Claudin-7 expression in human epithelial ovarian cancer. Int J Gynecol Cancer, 2008, 18: 1262–1271.
18. Cheung ST, Leung KL, Ip YC, *et al*. Claudin-10 expression level is associated with recurrence of primary hepatocellular carcinoma. Clin Cancer Res, 2005, 11 (2 Pt 1): 551–556.
19. Tabariès S, Siegel PM. The role of claudins in cancer metastasis. Oncogene, 2017, 36: 1176–1190.
20. Singh P, Toom S, Huang YW. Anti-claudin 18.2 antibody as new targeted therapy for advanced gastric cancer. J Hematol Oncol, 2017, 10: 105.
21. Dottermusch M, Krüger S, Behrens HM, *et al*. Expression of the potential therapeutic target claudin-18.2 is frequently decreased in gastric cancer: results from a large Caucasian cohort study. Virchows Arch, 2019, 475: 563–571.
22. Rohde C, Yamaguchi R, Mukhina S, *et al*. Comparison of Claudin 18.2 expression in primary tumors and lymph node metastases in Japanese patients with gastric adenocarcinoma. Jpn J Clin Oncol, 2019, 49: 870–876.
23. Baek JH, Park DJ, Kim GY, *et al*. Clinical implications of claudin 18.2 expression in patients with gastric cancer. Anticancer Res, 2019, 39: 6973–6979.
24. Al-Batran SE, Schuler MH, Zvirbule Z, *et al*. FAST: an international, multicenter, randomized, phase II trial of epirubicin, oxaliplatin, and capecitabine (EOX) with or without IMAB362, a first-in-class anti-CLDN18.2 antibody, as first-line therapy in patients with advanced CLDN18.2+ gastric and gastroesophageal junction (GEJ) adenocarcinoma. J Clin Oncol, 2016, 34: 18 Suppl. doi: 10.1200/JCO.2016.34.18_suppl.LBA4001.
25. Sahin U, Schuler M, Richly H, *et al*. A phase I dose-escalation study of IMAB362 (Zolbetuximab) in patients with advanced gastric and gastro-oesophageal junction cancer. Eur J Cancer, 2018, 100: 17–26.
26. Kellner C, Otte A, Cappuzzello E, *et al*. Modulating cytotoxic effector functions by Fc engineering to improve cancer therapy. Transfus Med Hemother, 2017, 44: 327–336.
27. Türeci Ö, Mitnacht-Kraus R, Wöll S, *et al*. Characterization of zolbetuximab in pancreatic cancer models. Oncoimmunology, 2018, 8: e1523096.
28. Lordick F, Shitara K, Janjigian YY. New agents on the horizon in gastric cancer. Ann Oncol, 2017, 28: 1767–1775.
29. Wöll S, Schlitter AM, Dhaene K, *et al*. Claudin 18.2 is a target for IMAB362 antibody in pancreatic neoplasms. Int J Cancer, 2014, 134: 731–739.
30. Micke P, Mattsson JSM, Edlund K, *et al*. Aberrantly activated claudin 6 and 18.2 as potential therapy targets in non-small-cell lung cancer. Int J Cancer, 2014, 135: 2206–2214.

31. Lyons TG, Ku GY. Systemic therapy for esophagogastric cancer: targeted therapies. Chin Clin Oncol, 2017, 6: 48.
32. Sahin U, Al-Batran SE, Hozaeel W, *et al*. IMAB362 plus zoledronic acid (ZA) and interleukin-2 (IL-2) in patients (pts) with advanced gastroesophageal cancer (GEC): clinical activity and safety data from the PILOT phase I trial. J Clin Oncol, 2015, 33: e15079.
33. Jiang H, Shi ZM, Wang P, *et al*. Claudin 18.2-specific chimeric antigen receptor engineered T cells for the treatment of gastric cancer. J Natl Cancer Inst, 2019, 111: 409–418.
34. Zhu GY, Foletti D, Liu XH, *et al*. Targeting CLDN18.2 by CD3 bispecific and ADC modalities for the treatments of gastric and pancreatic cancer. Sci Rep, 2019, 9: 8420.
35. Waddell T, Verheij M, Allum W, *et al*. Gastric cancer: ESMO-ESSO-ESTRO clinical practice guidelines for diagnosis, treatment and follow-up. Eur J Surg Oncol, 2014, 40: 584–591.
36. Ferlay J, Soerjomataram I, Dikshit R, *et al*. Cancer incidence and mortality worldwide: sources, methods and major patterns in GLOBOCAN 2012. Int J Cancer, 2015, 136: E359–E386.
37. Huang TT, Qiu H, Yuan XL. Targeted therapy of gastric cancer: current and prospective strategies. Oncol Transl Med, 2018, 4: 41–47.
38. Cameron D, Piccart-Gebhart MJ, Gelber RD, *et al*. 11 years' follow-up of trastuzumab after adjuvant chemotherapy in HER2-positive early breast cancer: final analysis of the HERceptin Adjuvant (HERA) trial. Lancet, 2017, 389: 1195–1205.
39. Hagen SJ, Ang LH, Zheng Y, *et al*. Loss of tight junction protein claudin 18 promotes progressive neoplasia development in mouse stomach. Gastroenterology, 2018, 155: 1852–1867.
40. Yang LL, Sun X, Meng XW. Differences in the expression profiles of claudin proteins in human gastric carcinoma compared with non-neoplastic mucosa. Mol Med Rep, 2018, 18: 1271–1278.
41. Oshima T, Shan J, Okugawa T, *et al*. Down-regulation of claudin-18 is associated with the proliferative and invasive potential of gastric cancer at the invasive front. PLoS One, 2013, 8: e74757.
42. Jun KH, Kim JH, Jung JH, *et al*. Expression of claudin-7 and loss of claudin-18 correlate with poor prognosis in gastric cancer. Int J Surg, 2014, 12: 156–162.
43. Scott AM, Wolchok JD, Old LJ. Antibody therapy of cancer. Nat Rev Cancer, 2012, 12: 278–287.
44. Chang ZL, Chen YY. CARs: Synthetic immunoreceptors for cancer therapy and beyond. Trends Mol Med, 2017, 23: 430–450.

DOI 10.1007/s10330-020-0470-0
Cite this article as: Niu Q, Liu JM, Luo XX, *et al*. Future of targeted therapy for gastrointestinal cancer: Claudin 18.2. Oncol Transl Med, 2021, 7: 102–107.

Oncology and Translational Medicine
DOI 10.1007/s10330-021-0488-8

June 2021, Vol. 7, No. 3, P108–P114

ORIGINAL ARTICLE

Seroprevalence of severe acute respiratory syndrome coronavirus 2 (SARS-CoV-2) in patients with cancer and the impact of anti-tumor treatment on antibodies*

Bili Wu[1], Bo Liu[1], Xueyan Jiang[1], Ye Yuan[2], Wan Qin[1], Kai Qin[1], Qi Mei[1], Li Zhang[1], Huilan Zhang[3], Guangyuan Hu[1] (✉), Xianglin Yuan[1] (✉)

[1] Department of Oncology, Tongji Hospital, Tongji Medical College, University of Science and Technology, Wuhan 430030, China
[2] Department of Gastroenterology, Tongji Hospital, Tongji Medical College, Huazhong University of Science and Technology, Wuhan 430030, China
[3] Department of Respiratory and Critical Care Medicine, Tongji Hospital, Tongji Medical College, Huazhong University of Science and Technology, Wuhan 430030, China

Abstract

Objective The aim of this study was to examine the seroprevalence of severe acute respiratory syndrome coronavirus 2 (SARS-CoV-2) among patients with cancer and followed up changes in SARS-CoV-2-specific antibodies to explore the impact of anti-tumor treatment in patients.

Methods Patients with cancer who visited the Outpatient Clinic of Oncology, Tongji Hospital, Tongji Medical College, Huazhong University of Science and Technology, Wuhan, China between March 9 and April 30, 2020 were enrolled in this retrospective cohort study. SARS-CoV-2 immunoglobulin (Ig) G, IgM, and viral load at various time points during the disease course were determined.

Results We examined the serological results of 779 patients with cancer. The overall seroprevalence (IgG-positive or IgM-positive) rate of SARS-CoV-2 was 3.4%. The probability of seropositivity was significantly higher in patients with gastric cancer than in those without gastric cancer (odds ratio: 6.349, 95% confidence interval: 2.191–18.396). Follow-up data showed that SARS-CoV-2 IgM and IgG levels decreased and the polymerase chain reaction test result remained negative in seropositive patients with cancer.

Conclusion This study investigated the seroprevalence of SARS-CoV-2 in coronavirus disease (COVID-19)-positive patients with cancer in Wuhan, China. The seropositivity in patients with cancer was lower than or similar to that in the general population. Irrespective of anti-tumor therapy, the levels of SARS-CoV-2 antibodies decreased in these patients. More studies are needed to better understand the impact of anti-tumor therapy on change in the levels of SARS-CoV-2 antibodies.

Received: 3 April 2021
Revised: 20 April 2021
Accepted: 15 May 2021

Key words: coronavirus disease (COVID-19); cancer; immunoglobulin (Ig) G; IgM

Coronavirus disease (COVID-19), caused by severe acute respiratory syndrome coronavirus 2 (SARS-CoV-2), has spread rapidly worldwide. As of January 16, 2021, 98459 and 92506811 confirmed COVID-19 cases and 4803 and 2001773 deaths were reported in China and worldwide, respectively [1]. The main symptoms of COVID-19 include fever, dry cough, and fatigue. Patients with COVID-19 are categorized to have mild, moderate, severe, and critically severe disease according to the severity of clinical symptoms. However, some people

✉ Correspondence to: Xianglin Yuan. Email: yuanxianglin@hust.edu.cn; Guangyuan Hu. Email: h.g.y.121@163.com
* Supported by the research grants from the National Natural Science Foundation of China (No. 81773360, and No. 81902619) and COVID-19 Emergency Project of Huazhong University of Science and Technology (No. 2020kfyXGYJ062).

present with no obvious clinical symptoms [2]. SARS-CoV-2 infection can be diagnosed by the detection of the viral RNA or antibodies. Serological tests help to monitor the overall seroprevalence of SARS-CoV-2 in the population and evaluate immune response after viral infection.

Patients with cancer, as a special population, are prone to viral or bacterial infections due to immune suppression [3–4]. Previous studies on COVID-19 have revealed that patients with cancer have a poor prognosis, which is treatment related; however, recent studies do not support this notion [5–10].

Currently, several studies have investigated the seroprevalence of SARS-CoV-2 in the general population. However, limited studies have been conducted in patients with cancer. It is unclear whether COVID-19-positive patients can be administered anti-tumor treatment [11]. Therefore, in this study, we examined the seroprevalence of SARS-CoV-2 among patients with cancer and followed up changes in SARS-CoV-2-specific antibodies to explore the impact of anti-tumor treatment in patients.

Patients and methods

Study design and participants

This retrospective study was conducted in Tongji Hospital, Tongji Medical College, Huazhong University of Science and Technology, Wuhan, China from March 9 to April 30, 2020 and included 852 patients who presented to our outpatient oncology clinic. Detailed data were obtained from the electronic medical records. Tumor diagnosis was established based on clinical manifestation and laboratory examinations. After excluding 73 patients who lacked data on the results of the throat swab or serological tests, 779 patients were included in the study. We investigated the seroprevalence of SARS-CoV-2 in the population. Twenty-five patients were positive for SARS-CoV-2-specific antibodies (Fig. 1). We dynamically observed the change in the antibodies during anti-tumor treatment, with the cutoff date set on September 9, 2020.

This study was approved by the Ethics Committee of Tongji Hospital, Tongji Medical College, Huazhong University of Science and Technology, Wuhan, China, which waived the requirement of informed consent.

Observation indicators and data collection

Epidemiological data, such as data on sex, age, and tumor type, were obtained from the electronic medical records and through patient interviews. Data on radiological findings and treatment information of the patients positive for SARS-CoV-2 antibodies were also included. All data were separately reviewed and verified by two physicians. Any missing or uncertain data were retrieved by contacting the physicians or the patients themselves. Data on laboratory examinations, including chest computed tomography (CT), were obtained at the first outpatient visit. No patients were lost-to-follow-up.

Cancer stage was categorized according to the tumor-node-metastasis staging system [12]. Using quantitative real-time (RT) polymerase chain reaction (PCR) and next-generation gene sequencing, SARS-CoV-2 can be detected using nasopharyngeal swab samples [13]. Wantai kits were used for antibody detection [14]. The serum antibody level was standardized against the ratio of the signal value to the cut-off point (S/CO). The ratio was measured using the optical density (OD) value generated by the sample relative to the cut-off point OD value. When the ratio was > 1, the sample was considered positive for SARS-CoV-2.

Statistical analysis

Quantitative variables are expressed as medians [interquartile range (IQR)], and qualitative variables are presented as frequencies. The Mann-Whitney *U*-test, the chi-square test, and Fisher's exact test were used to compare seropositive and seronegative patients in terms of demographic statistics where appropriate. Univariable and multivariable Logistic regression models were used to screen or identify the risk factors of seropositivity. To follow the 10 events per variable (EPV) principle to avoid overfitting, we eventually entered three factors in the multivariate model. The normality of data was tested using the Shapiro-Wilk test. The Wilcoxon signed-rank (nonparametric) test was used for the comparison of paired data. All statistical tests were two-sided and $P \leq 0.05$ was considered statistically significant. SPSS version 22.0 statistics software package (IBM Corp., Armonk, NY, USA) was used for statistical analysis.

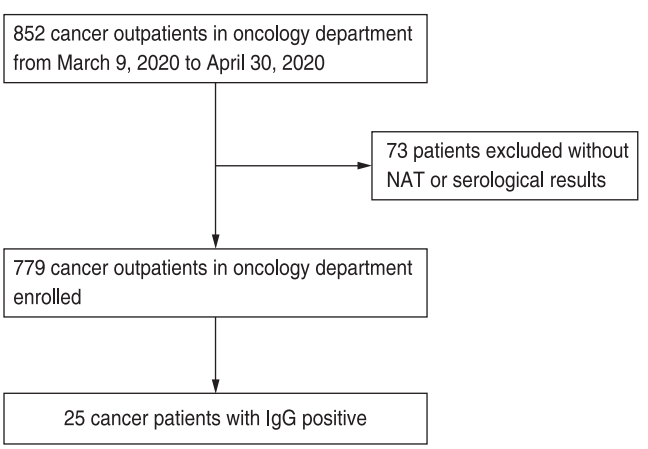

Fig. 1 Patient flow diagram. NAT: nucleic acid tests

Results

Clinical features of patients with cancer and influencing factors of positive SARS-CoV-2 antibodies

Among the 779 patients with tumors, 384 (49.3%) were men, and the median patient age was 54.0 (45.0–62.0) years. The most common tumor types were lung cancer (n = 201), breast cancer (n = 132), cervical cancer (n = 65), and nasopharyngeal carcinoma (n = 48; Table 1).

Of the 779 patients, 25 (3.2%) were positive for SARS-CoV-2 IgG antibody and four (0.5%) were positive for SARS-CoV-2 IgM antibody, with an overall seropositive rate of 3.2% (Table 2).

Univariable analysis showed that the rate of seropositivity was higher in patients with gastric cancer than in those without gastric cancer; however, it was not significantly different among other tumor types, sexes, and age groups. Univariable logistics analysis revealed that gastric cancer was associated with seropositivity. Considering the seropositive patients (n = 25), we included three variables in the multivariable logistic regression model to avoid over-fitting the model. The results showed that gastric cancer was associated with a higher rate of seropositivity than the other cancer types (Tables 3 and 4).

None of the patients presented with typical COVID-19 symptoms according to the Chinese Clinical Guidelines for COVID-19 Pneumonia Diagnosis and Treatment (8th edition). PCR test results of all patients remained negative.

Clinical characteristics and dynamic changes in SARS-CoV-2 antibodies in seropositive patients

Table 5 presents the clinical characteristics of 25 seropositive patients. Among them, 14 (56%) patients were men, and the median patient age was 56.0 (48.0–61.0) years. The most common tumor types were lung cancer

Table 1 Demographic and baseline clinical characteristics of cancer patients [n (%)]

Characteristics	Patients (n = 779)
Median age (years)	54.0 (45.0–62.0)
Sex	
Male	384 (49.3)
Female	395 (50.7)
Tumour diagnosis	
Lung cancer	201 (25.8)
Breast cancer	132 (17.0)
Cervical cancer	65 (8.3)
Nasopharynx cancer	48 (6.2)
Other	333 (42.7)

Note: Data are presented as median (IQR) or n (%) unless noted otherwise

Table 2 Rates of the serological test results [n (%)]

Results	Patients (n = 779)
IgM– /IgG–	754 (96.8)
IgM+ /IgG–	0 (0)
IgM– /IgG+	21 (2.7)
IgM+ /IgG+	4 (0.5)

Table 3 Demographic characteristics of the patients based on seroprevalence

Characteristics	SARS-COV2 seropositive (n = 25)	SARS-COV2 seronegative (n = 754)	P value
Age (years)	56.0 (48.0–61.0)	54.0 (45.0–62.0)	0.868
Sex			0.495
Male (n = 384)	14	370	
Female (n = 395)	11	384	
Cancer type			
Lung cancer (n = 201)	5	196	0.500
Breast cancer (n = 132)	2	130	0.288
Cervical cancer (n = 65)	3	62	0.457
Nasopharynx cancer (n = 48)	3	45	0.195
Gastric cancer (n = 34)	5	29	0.003
Other (n = 299)	7	292	0.278

Note: Data are presented as median (IQR) or n (%) unless noted otherwise. P values were calculated by Mann-Whitney U test, χ^2 test, or Fisher's exact test, as appropriate

Table 4 Risk factors associated with seropositivity

	Univariable OR (95% CI)	P value	Multivariable OR (95% CI)	P value
Male sex (*vs* female)	1.321 (0.592–2.947)	0.497	1.263 (0.551–2.893)	0.581
Age (years)	0.995 (0.966–1.025)	0.737	0.989 (0.959–1.020)	0.481
Cancer type present (*vs* not present)				
Lung cancer	0.712 (0.264–1.922)	0.502		
Breast cancer	0.417 (0.097–1.792)	0.240		
Cervical cancer	1.522 (0.443–5.228)	0.505		
Nasopharynx cancer	2.148 (0.620–7.449)	0.228		
Gastric cancer	6.250 (2.192–17.823)	0.001	6.349 (2.191–18.396)	0.001
Other	0.615 (0.254–1.491)	0.282		

Note: OR = odds ratio; CI = confidence interval

(n = 5), gastric cancer (n = 5), nasopharyngeal cancer (n = 3), and cervical cancer (n = 3). Thirteen patients were diagnosed with stage IV cancer. Two patients had been surgically treated, 12 patients had received chemotherapy, seven patients had undergone radiotherapy, five patients were receiving target therapy, and two patients received immunotherapy. At their first visit to the hospital, radiological examinations showed that 22 patients had nodules, 10 patients had pleural thickening, nine patients had fibrous stripes, four patients had patchy shadows, and one patient had ground-glass opacity.

We followed up 25 patients seropositive for SARS-CoV-2 for a median period of 60 (16–141) days. All patients were tested for SARS-CoV-2 antibodies and SARS-CoV-2 RNA using nasopharyngeal swab samples. Their RT-PCR test yielded negative results. The IgM levels in four SARS-CoV-2 IgM-positive patients showed a downward trend, and in three of them, the level shifted from above to below the cut-off point. Twenty-five SARS-CoV-2 IgG-positive patients also showed a downward trend in IgG levels during the follow-up period (Fig. 2). However, the results of five patients eventually turned negative. One patient received radiotherapy, one cycle of tegaful, and one cycle of capecitabine; one patient was administered osimertinib; one patient received three cycles of tegaful, and one patient was initiated on one cycle of PP (pemetrexed and cisplatin) protocol; and one patient was treated with one cycle of XELOX (oxaliplatin and cisplatin) regime in combination with bevacizumab, one cycle of capecitabine plus bevacizumab, one cycle of concurrent capecitabine and radiotherapy, and three cycles of capecitabine and bevacizumab therapy. Fig. 3 shows the SARS-CoV-2 IgG and IgM antibody levels at the first and last tests. The antibody levels conspicuously reduced at the last test and the difference in IgG level was

Table 5 Demographic and baseline clinical characteristics of cancer patients with SARS-COV-2 IgG positive

Characteristics	Patients (n = 25)
Median age (years)	56.0 (48.0–61.0)
Sex	
Male	14 (56.0)
Female	11 (44.0)
Tumour diagnosis	
Lung cancer	5 (20.0)
Oesophagus cancer	2 (8.0)
Breast cancer	2 (8.0)
Cervical cancer	3 (12.0)
Gastric cancer	5 (20.0)
Colon cancer	1 (4.0)
Rectum cancer	2 (8.0)
Thyroid cancer*	1 (4.0)
Nasopharynx cancer	3 (12.0)
Hodgkin lymphoma	1 (4.0)
Glioblastoma	1 (4.0)
Tumour stage	
Stage I/II/III	12 (48.0)
Stage IV	13 (52.0)
Cancer treatment during Covid-19 pandemic	
Operation	2 (8.0)
Chemotherapy	12 (48.0)
Radiotherapy	7 (28.0)
Target therapy	5 (20.0)
Immunotherapy	2 (8.0)
Radiological findings	
Ground-glass opacity	1 (4.0)
Patchy shadows	4 (16.0)
Fibrous stripes	9 (36.0)
Pleural thickening	10 (40.0)
Nodules	22 (88.0)

Note: *, one patient has nasopharynx cancer and thyroid cancer, and the tumor stage is stage II; Data are presented as median (IQR) or n (%) unless noted otherwise

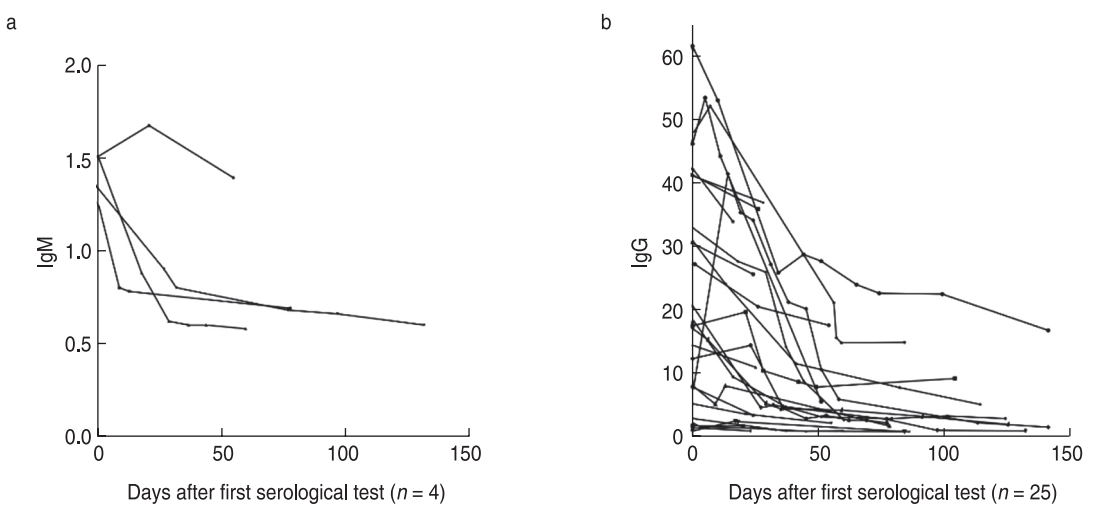

Fig. 2 Serological courses and decline in (a) IgM and (b) IgG levels in patients with cancer who were initially seropositive

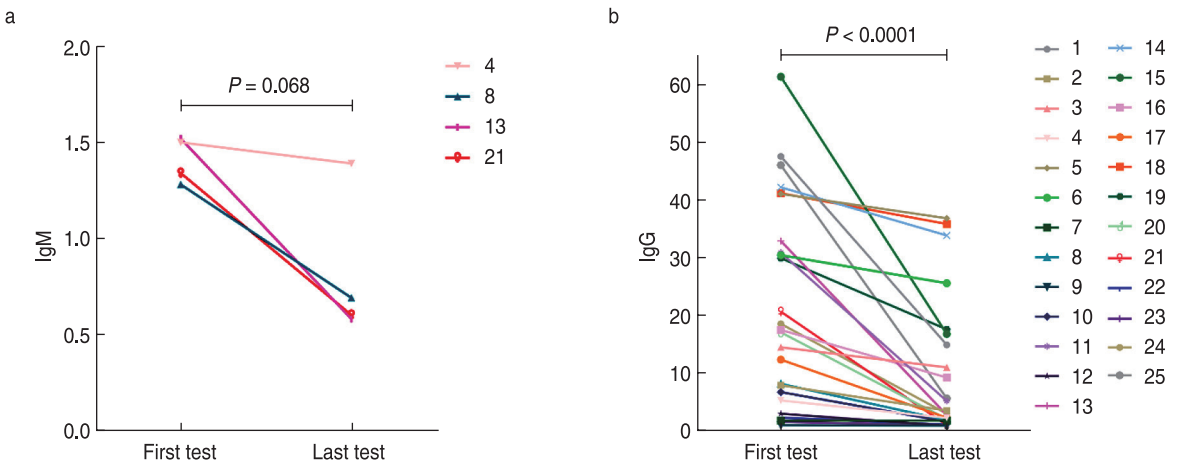

Fig. 3 Changes in SARS-CoV-2 serum IgM and IgG levels in patients with cancer who were seropositive at the first and last test. The *P* value for the difference between first and last test is 0.068 and < 0.0001 for IgM and IgG, respectively

statistically significant.

Discussion

Patients with cancer, as a special population, are vulnerable to COVID-19. The effect of anti-tumor treatment on this population was still unclear. To provide evidence regarding the prognosis and treatment of patients with cancer infected with SARS-CoV-2, we investigated the clinical characteristics, treatment, and serological results of 779 patients with cancer between March 9 and April 30, 2020 at our oncology clinic at Tongji Hospital, Tongji Medical College, Huazhong University of Science and Technology, Wuhan, China. We found that 25 asymptomatic individuals were positive for SARS-CoV-2 IgG antibodies. An association was found between the seropositivity of the SARS-CoV-2 antibodies and gastric cancer. Serological follow-up revealed a declining trend in both IgG and IgM levels.

Among the 779 patients with cancer enrolled in this study, 25 were positive for SARS-CoV-2 IgG and four were positive for IgM. The overall seropositivity rate was 3.2%. In a study involving medical workers and their close contacts in Wuhan from March to April 2020, the seropositivity was approximately 3.2%–3.8% [15]. Another study examined Wuhan citizens during the same period and found a positivity rate of 3.57% [16]. The seropositivity in patients with cancer is lower than or similar to that in the general population. In Madrid, Spain, the positive rate of SARS-CoV-2 antibodies in outpatients of a cancer center was 31.4%, whereas the IgG positive rate in the general population in the same area was 20.18% [17]. Compared to the seroprevalence of SARS-CoV-2 in other regions, that in Wuhan was lower. This might be contributed to the different infection rates of SARS-CoV-2 in different regions. The immunity of patients with cancer is impaired after receiving chemotherapy, immunotherapy, or other anti-tumor treatment. They have to frequently visit the hospital, and such visits make them more susceptible to COVID-19, as demonstrated by previous studies [4, 18]. In a previous study, the SARS-CoV-2 positivity rate was higher in patients with cancer than in the general population [17]; however, this was not the case in China. Such discrepancy might be attributed to the difference in the study populations. Early studies on COVID-19 mainly focused on symptomatic patients. A study conducted in Spain also included patients with pneumonia. However, in our study, all SARS-CoV-2-infected patients were asymptomatic. Moreover, each patient was followed up for >14 days and they could be regarded as "truly asymptomatic" patients. Therefore, the possibility of patients being symptomatic in the incubation period was excluded.

In addition, we showed that gastric cancer was associated with a higher positivity rate of SARS-CoV-2 antibodies. The invasion of SARS-CoV-2 into host cells relies on the combination of spike protein and angiotensin-converting enzyme 2 (ACE-2). Transmembrane protease serine 2, cathepsin L, and cathepsin B (CTSL/B) assist in the binding, tailoring, and activation of the spike protein. Both ACE-2 and CTSL/B are highly expressed in stomach adenocarcinoma [19–20]. These might facilitate the entry of SARS-CoV-2 into the host cells, thereby causing viral infection in patients with stomach adenocarcinoma.

Further, we conducted a follow-up study on patients with cancer positive for SARS-CoV-2 antibodies. Their antibody levels showed a declining pattern. An asymptomatic patient was defined as a patient who tested positive on the nucleic acid test but did not show clinical symptoms throughout the infection. At present,

the serological changes in these patients are not clear. Patients with COVID-19 were mainly screened by nucleic acid testing and antibody testing. Nucleic acid tests are most commonly used for detection of the SARS-CoV-2 RNA in the nasopharynx and oropharynx by RT-PCR and can yield positive results before and within a few weeks of symptom onset. Three types of antibodies (IgA, IgM, and IgG) are produced by the human body in response to SARS-CoV-2 infection. The first two tend to appear within 1 week of symptom onset and their levels gradually decrease after reaching a plateau. IgG is produced within 2 weeks of symptom onset and persists in the serum for some time, serving as an indication of host immunity to SARS-CoV-2 [21–22]. The nucleic acid test results of the patients in our study were negative, but the receptor-binding domain (RBD) in the spike proteins IgG and IgM showed a downward trend. The current long-term follow-up study on antibodies against the spike protein or RBD of SARS-CoV-2 shows that IgG level stay positive for a long time or decrease gradually. The IgM level stays negative for a shorter time than the IgG level [23–25]. Flehmig and Crawford examined the ability of antibodies to neutralize the virus and found that 3–4 months after symptom onset, the neutralizing ability of antibodies diminished [26–28]. These findings are consistent with the antibody results in our study, suggesting that human immunity against SARS-CoV-2 dropped gradually over time.

Many studies have demonstrated that patients with cancer are more likely to have adverse events or a higher mortality rate after being infected with SARS-CoV-2. The risk factors include sex, age, complications, tumor types, and disease stage [29–30]. Thus far, researchers have failed to agree on the impact of anti-tumor therapy on the prognosis of the disease. Some researchers believe that receiving anti-tumor treatments such as recent chemotherapy are unfavorable factors for the prognosis of patients, while other researchers do not believe in this phenomenon [6, 9]. The inconsistencies might be attributed to the differences in patient selection. Few studies investigated the impact of anti-tumor therapy on SARS-CoV-2 infection. Our study investigated changes in antibody levels in cancer patients with asymptomatic infection. Although we could not definitively determine the exact time point of the viral infection, based on a sufficiently long follow-up, we could assume that most people were in the convalescent period of the infection. During follow-up, none of the patients died or experienced any adverse event. Some patients received chemotherapy, radiotherapy, targeted therapy, immunotherapy, and other treatments, while others did not receive any anti-tumor therapy. We observed that SARS-CoV-2 antibodies of both groups presented a downward trend. In some patients, the IgG antibody level was transiently elevated. Patients 1, 16, 17, and 25 did not receive anti-tumor therapy during the high antibody level period, while patient 8 was administered icotinib orally and patient 9 was administered radiotherapy, patient 15 was treated with capecitabine plus radiotherapy, patient 21 was administered oral tegaful; patient 24 was initiated on the EP protocol (etoposide + cisplatin). The reason for the elevated antibody level might have been the IgG spiked in response to a recent infection. Antibody levels in patients 8, 15, 21, and 24 increased after decreasing for some time, which might be related to the anti-tumor treatment the patient received. Recent studies have demonstrated that patients with cancer have a lower positive rate of serum IgG than patients without cancer. Immunosuppressive therapy has been shown to be related to a lower rate of seropositivity in patients with a history of COVID-19 [31]. Further studies are needed to evaluate whether anti-tumor therapy can cause transient elevations in antibody levels.

Further, there is another question, can anti-tumor treatment cause the recurrence of SARS-CoV-2 infection? The PCR test performed using nasopharyngeal swab samples from the patients in our study all yielded negative results. No close contacts of these patients developed SARS-CoV-2 infection. At present, articles on SARS-CoV-2 recurrence are mostly case reports. In study, asymptomatic patients with COVID-19 developed symptoms after treatment with high-dose glucocorticoids [32]. In another study, COVID-19 symptoms appeared after immunosuppressive treatment in patients with acute B-lymphocytic leukemia [33]. Therefore, for patients on anti-tumor treatment, a longer period of follow-up is needed.

This study has several limitations. First, this study was a single-center retrospective nonrandomized study and only included 25 SARS-CoV-2 seropositive patients. The patients were heterogeneous in terms of factors such as tumor type, age, and treatment. Second, because most of the patients were outpatients, data on anti-tumor treatment received by seronegative patients, tumor stages, and other information were lacking, and the time and frequency of serological testing varied among patients during the follow-up. Finally, the method used in our study could only detect antibody quantity, not titers, and could not reflect the virus-neutralizing ability of the antibodies.

Conclusion

At present, the precise mechanism underlying the role of SARS-CoV-2 antibodies in COVID-19 infection is poorly understood. This study explored the seroprevalence of asymptomatic patients with cancer infected with SARS-CoV-2 in the Wuhan area and tracked antibody changes in seropositive patients. More studies are needed to better understand the impact of anti-tumor therapy on

antibody changes.

Conflicts of interest

The authors indicated no potential conflicts of interest.

References

1. WHO coronavirus disease (COVID-19) dashboard [Accessed 16 Jan 2021]. Available from: https://covid19.who.int/.
2. Diagnosis and treatment protocol for novel coronavirus pneumonia (Trial Version 8) [Accessed 20 Oct 2020]. Available from: http://www.gov.cn/zhengce/zhengceku/2020-08/19/content_5535757.htm.
3. Kamboj M, Sepkowitz KA. Nosocomial infections in patients with cancer. Lancet Oncol, 2009, 10: 589–597.
4. Liang WH, Guan WJ, Chen RC, *et al*. Cancer patients in SARS-CoV-2 infection: a nationwide analysis in China. Lancet Oncol, 2020, 21: 335–337.
5. Zhang L, Zhu F, Xie L, *et al*. Clinical characteristics of COVID-19-infected cancer patients: a retrospective case study in three hospitals within Wuhan, China. Ann Oncol, 2020, 31: 894–901.
6. Yang KY, Sheng YH, Huang CL, *et al*. Clinical characteristics, outcomes, and risk factors for mortality in patients with cancer and COVID-19 in Hubei, China: a multicentre, retrospective, cohort study. Lancet Oncol, 2020, 21: 904–913.
7. Kuderer NM, Choueiri TK, Shah DP, *et al*. Clinical impact of COVID-19 on patients with cancer (CCC19): a cohort study. Lancet, 2020, 395: 1907–1918.
8. Lee LY, Cazier JB, Angelis V, *et al*. COVID-19 mortality in patients with cancer on chemotherapy or other anticancer treatments: a prospective cohort study. Lancet, 2020, 395: 1919–1926.
9. Jee J, Foote MB, Lumish M, *et al*. Chemotherapy and COVID-19 outcomes in patients with cancer. J Clin Oncol, 2020, 38: 3538–3546.
10. Peng H, Wang S, Mei Q, *et al*. Comparable outcomes but higher risks of prolonged viral RNA shedding duration and secondary infection in cancer survivors with COVID-19: A multi-center, matched retrospective cohort study. Oncol Transl Med, 2020, 6: 237–246.
11. Bakouny Z, Hawley JE, Choueiri TK, *et al*. COVID-19 and cancer: current challenges and perspectives. Cancer Cell, 2020, 38: 629–646.
12. Amin MB, American Joint Committee on Cancer, American Cancer Society. AJCC cancer staging manual. Amin MB, Edge SB, Gress DM, *et al* (eds). 8th ed. Chicago IL: American Joint Committee on Cancer, Springer, 2017. pp1024.
13. Huang CL, Wang YM, Li XW, *et al*. Clinical features of patients infected with 2019 novel coronavirus in Wuhan, China. Lancet, 2020, 395: 497–506.
14. Abravanel F, Miédouge M, Chapuy-Regaud S, *et al*. Clinical performance of a rapid test compared to a microplate test to detect total anti SARS-CoV-2 antibodies directed to the spike protein. J Clin Virol, 2020, 130: 104528.
15. Xu X, Sun J, Nie S, *et al*. Seroprevalence of immunoglobulin M and G antibodies against SARS-CoV-2 in China. Nat Med, 2020, 26: 1193–1195.
16. Han XY, Wei X, Alwalid O, *et al*. Severe acute respiratory syndrome coronavirus 2 among asymptomatic workers screened for work resumption, China. Emerg Infect Dis, 2020, 26: 2265–2267.
17. Cabezón-Gutiérrez L, Custodio-Cabello S, Palka-Kotlowska M, *et al*. Seroprevalence of SARS-CoV-2-specific antibodies in cancer outpatients in Madrid (Spain): A single center, prospective, cohort study and a review of available data. Cancer Treat Rev, 2020, 90: 102102.
18. Yu J, Ouyang W, Chua MLK, *et al*. SARS-CoV-2 transmission in patients with cancer at a tertiary care hospital in Wuhan, China. JAMA Oncol, 2020, 6: 1108–1110.
19. Li HM, Xie LX, Chen L, *et al*. Genomic, epigenomic, and immune subtype analysis of CTSL/B and SARS-CoV-2 receptor ACE2 in pan-cancer. Aging (Albany NY), 2020, 12: 22370–22389.
20. Katopodis P, Anikin V, Randeva HS, *et al*. Pan-cancer analysis of transmembrane protease serine 2 and cathepsin L that mediate cellular SARS-CoV-2 infection leading to COVID-19. Int J Oncol, 2020, 57: 533–539.
21. He X, Lau EHY, Wu P, *et al*. Temporal dynamics in viral shedding and transmissibility of COVID-19. Nat Med, 2020, 26: 672–675.
22. Tantuoyir MM, Rezaei N. Serological tests for COVID-19: Potential opportunities. Cell Biol Int, 2021, 45: 740–748.
23. Ibarrondo FJ, Fulcher JA, Goodman-Meza D, *et al*. Rapid decay of anti-SARS-CoV-2 antibodies in persons with mild Covid-19. N Engl J Med, 2020, 383: 1085–1087.
24. Liu CM, Yu XQ, Gao CM, *et al*. Characterization of antibody responses to SARS-CoV-2 in convalescent COVID-19 patients. J Med Virol, 2021, 93: 2227–2233.
25. Röltgen K, Powell AE, Wirz OF, *et al*. Defining the features and duration of antibody responses to SARS-CoV-2 infection associated with disease severity and outcome. Sci Immunol, 2020, 5: eabe0240.
26. Crawford KHD, Dingens AS, Eguia R, *et al*. Dynamics of neutralizing antibody titers in the months after severe acute respiratory syndrome coronavirus 2 infection. J Infect Dis, 2021, 223: 197–205.
27. Seow J, Graham C, Merrick B, *et al*. Longitudinal observation and decline of neutralizing antibody responses in the three months following SARS-CoV-2 infection in humans. Nat Microbiol, 2020, 5: 1598–1607.
28. Flehmig B, Schindler M, Ruetalo N, *et al*. Persisting neutralizing activity to SARS-CoV-2 over months in sera of COVID-19 patients. Viruses, 2020, 12: 1357.
29. Giannakoulis VG, Papoutsi E, Siempos II. Effect of cancer on clinical outcomes of patients with COVID-19: A meta-analysis of patient data. JCO Glob Oncol, 2020, 6: 799–808.
30. Saini KS, Tagliamento M, Lambertini M, *et al*. Mortality in patients with cancer and coronavirus disease 2019: A systematic review and pooled analysis of 52 studies. Eur J Cancer, 2020, 139: 43–50.
31. Petersen LR, Sami S, Vuong N, *et al*. Lack of antibodies to SARS-CoV-2 in a large cohort of previously infected persons. Clin Infect Dis, 2020, ciaa1685.
32. Patrocínio de Jesus R, Silva R, Aliyeva E, *et al*. Reactivation of SARS-CoV-2 after asymptomatic infection while on high-dose corticosteroids. Case report. SN Compr Clin Med, 2020: 1–4.
33. Lancman G, Mascarenhas J, Bar-Natan M. Severe COVID-19 virus reactivation following treatment for B cell acute lymphoblastic leukemia. J Hematol Oncol, 2020, 13: 131.

DOI 10.1007/s10330-021-0488-8
Cite this article as: Wu BL, Liu B, Jiang XY, *et al*. Seroprevalence of severe acute respiratory syndrome coronavirus 2 (SARS-CoV-2) in patients with cancer and the impact of anti-tumor treatment on antibodies. Oncol Transl Med, 2021, 7: 108–114.

Oncology and Translational Medicine
DOI 10.1007/s10330-021-0489-9

June 2021, Vol. 7, No. 3, P115–P122

ORIGINAL ARTICLE

Recombinant human vascular endostatin injection to synchronize craniospinal radiotherapy for the treatment of recurrent medulloblastoma in children: A retrospective clinical study*

Yang Song[1], He Xiao[1], Chuan Chen[1], Ping Liang[2], Wenyuan Ji[2], Mingying Geng[1] (✉)

[1] Cancer Center, Institute of Surgery Research, Daping Hospital, Army Medical University (Third Military Medical University), Chongqing 400042, China
[2] Department of Neurosurgery, Children's Hospital Affiliated to Chongqing Medical University, Chongqing 400014, China

Abstract

Objective Medulloblastoma (MB) is the most common primary central nervous system malignancy in children. Nonetheless, there is no standard treatment for recurrent MB. The purpose of this study was to investigate the clinical value and toxicity of recombinant human endostatin injection (Endostar®) combined with craniospinal radiotherapy for the treatment of recurrent MB in children.

Methods This study retrospectively analyzed 13 patients with recurrent MB aged 5–18 years. Endostar® 7.5 mg/m^2/d was synchronized during craniospinal radiotherapy for 7 children with a portable micro uniform speed infusion pump. Endostar® was applied 3 days prior to the initiation of radiotherapy. The drug was in continuous use for 7 days. Similarly, the withdrawal of the drug took place over 7 days. This represented a cycle. During radiotherapy, the application was repeated until the end of radiotherapy (experimental group). In the other 6 cases, only craniospinal radiotherapy was used (control group).

Results The complete remission rate was 71.4% in the experimental group and 16.7% in the control group. The median progression-free survival (PFS) was 14 months (95% CI: 0.0–29.60) and 19 months (95% CI: 0.0–39.53) in the experimental and control groups, respectively. The median overall survival (OS) was 19 months (95% CI: 0.0–38.20) and 23 months (95% CI: 2.47–43.53) in the experimental and control groups, respectively. The most common adverse events included grade 1 thrombocytopenia (7.7%), grade 3 neutropenia (38.5%), and grade 1 anemia (30.8%).

Conclusion Endostar® synchronizing craniospinal radiotherapy significantly improved the complete response rate of children with recurrent MB. It did not increase the side effects of radiation therapy. However, it did not improve the PFS or OS.

Received: 12 April 2021
Revised: 21 May 2021
Accepted: 15 June 2021

Key words: recombinant human vascular endostatin; craniospinal radiotherapy; medulloblastoma

Medulloblastoma (MB) is the most common primary neurological malignancy in children. It mainly occurs in the vermis of the cerebellum and accounts for approximately 20% of intracranial tumors in children [1]. Prior to the combined treatment with surgical radiotherapy and chemotherapy, there was less than a 20% event-free survival for 3–5 years [2]. With improvements in surgical and radiotherapy techniques the survival rate of MB in children has significantly improved [3]. Children aged 5–14 years have a relatively good prognosis, with a 5-year OS rate of approximately 67% [4]. However, the prognosis is poor for patients who relapse after treatment.

✉ Correspondence to: Mingying Geng. Email: 380904661@qq.com
* Supported by a grant from the Chongqing Science and Health Joint Medical Research Foundation of China (No. 2019MSXM079).

The median survival time is only approximately 1 year after the secondary surgery, secondary radiotherapy, or high-dose chemotherapy supplemented with stem cells. This results in a 2-year OS rate of 25% [1, 5–6]. Consequently, it is essential to develop a new comprehensive treatment method for recurrent MB.

Recently, molecular targeting therapy has become a novel way to treat tumors. Molecular targeting plays an anti-tumor role by inhibiting key molecules in the tumor signal transduction pathway. In 1971, Folkman first proposed the hypothesis that tumor growth and infiltration depend on tumor angiogenesis [7]. Subsequently, anti-angiogenesis therapy targeting tumor angiogenesis has become one of the most important anti-tumor strategies. Recombinant human endostatin injection (Endostar®) is one of the most effective angiogenesis inhibitors. Its' pan-target anti-angiogenesis effect reduces abnormal angiogenesis and remodeling by affecting the dynamic balance of angiogenesis in the tumor microenvironment. This promotes the normalization of the tumor microenvironment, reducing tumor hypoxia and improving drug delivery. Thus, it plays a sensitization role in radiotherapy and chemotherapy [8–14]. Vascular endothelial growth factor receptor 2 (VEGFR-2) is a kinase insert domain-containing receptor (KDR). Studies have confirmed that Endostar® can be combined with radiotherapy for the simultaneous treatment of brain metastatic tumors resulting from lung cancer. This has a significant effect in patients with a high expression of VEGFR2 protein or increased copy numbers of the KDR gene [15–16]. The VEGFR gene not only has expression in the MB vascular endothelial cells, but it also has high expression in tumor cells. In patients with a poor prognosis, the KDR gene expression level is higher. Endostar® combined with radiotherapy and chemotherapy for the treatment of metastatic intracranial tumor glioma and other tumors has achieved good efficacy with a satisfactory safety profile [15–16]. This brings the hope of an effective treatment for central nervous system tumors with endostatin. Combining Endostar®'s anti-angiogenesis characteristics with classical radiotherapy synchronous treatment has important clinical value. This combination will pave the way for the exploration of new strategies for the treatment of recurrent MB in children.

Materials and methods

Patients

From February 2018 to July 2019, a total of 13 recurrent MB children were treated in the cancer center of the Daping Hospital of the Army, Military Medical University. These children were diagnosed with MB by pathology after tumor resection by a neurosurgeon. The median age at diagnosis for the 13 patients who relapsed was 10 years (range, 5–18 years). Eight of 13 (61.5%) were male and 2 (15.4%) had the desmoplastic subtype. No secondary surgery was performed in the recurrent children (Table 1). After recurrence, M stage (Chang stage) [17] was observed in 10 M3 cases (76.9%), in 2 M2 cases (15.4%), and in 1 M0 case (7.7%) in the total group of children. According to the molecular subtype results, 6 cases were classified into Group 3 (46.2%), 5 cases were classified into Group 4 (38.5%), 1 was WNT (7.7%), and 1 was a SHH type associated with TP53 gene mutations (7.7%). According to the patients' physical condition or personal wishes of the patients' family, 3 patients (23.1%) received only surgery, 4 patients (30.8%) underwent surgery and chemotherapy, 1 patient (7.7%) underwent surgery and radiotherapy, and 5 patients (38.5%) underwent surgery followed by radiotherapy and chemotherapy for the initial treatment (Tables 1, 2). Initial chemotherapy regimens included nitrosourea compounds, vincristine, methotrexate, etoposide, cyclophosphamide, or platinum derivatives (carboplatin cisplatin).

Inclusion criteria

Patients received an enhanced MRI scan of the craniospinal area and were confirmed to have myeloblastoma recurrence or tumor spread. This was confirmed prior to the initiation of treatment in our department. These patients also had measurable tumor lesions. There were no hematology contraindications prior to the initiation of radiotherapy treatment. Informed consent was obtained from the patient and legal guardian.

- Experimental group: Endostar® synchronizing craniospinal radiotherapy.
- Control group: Craniospinal radiotherapy.

The experimental group received continuous intravenous Endostar® via an infusion pump during craniospinal radiotherapy: 7.5 mg/m^2/d. A portable micro constant speed infusion pump was used for continuous intravenous infusion. Drug administration was initiated 3 days prior to the beginning of radiotherapy. This was followed by continuous infusion for 7 d. Drug withdrawal over the next 7 days completed the cycle. This cyclic application was conducted during radiotherapy until the end of radiotherapy.

Radiotherapy: All the children received irradiation, 8MV X-ray, 3 fields, conventional segmentation (1.6–2.0 Gy) using three-dimensional conformal radiotherapy technology. The radiotherapy dose was adjusted according to the total dose of the first radiotherapy, tumor size, neurological symptoms, tumor site, the child's age, and a limited dose considering the major organs.

Main purpose: To evaluate the objective response rate (ORR) and complete remission rate (CRR) of Endostar® combined with craniospinal radiotherapy for recurrent MB in children. Secondary purpose: the progression-free

Table 1 Characteristics of all 13 Patients With Relapse of Medulloblastoma

	Initial diagnosis			Treatment before relapse				Relapse			Treatment after relapse		
	Sex/Age (years)	Histology	Molecular typing	Treatment	Chemotherapy cycles (Times)	Scope of radiation	Radiotherapy dose	Time to Relapse (monthes)	Time to the end of the last radiation treatment time (monthes)	Relapse Site	Treatment	Scope of radiation	Radiotherapy dose
1	Male/6	Classic	Group3	CT + RT	3	SCI	SCI:36Gy/20f, boost:42Gy/23f	13	12	Metastatic	Experimental group	CSI	CSI:32.4gy/18f
2	Female/8	Classic	Group3	S + CT	1	None	None	2	None	Metastatic	Experimental group	CSI	CSI:36.0Gy/20f, boost45Gy
3	Male/8	Classic	Group4	S+CT + RT	9	SCI	SCI:32.4Gy/18f, boost:50.4Gy/28f	20	26	Metastatic	Experimental group	CSI	CSI:32Gy/20f
4	Male/18	Desmoplastic	Group3	S+CT + RT	4	SCI	SCI:36Gy/20f, boost:45Gy/25f	23	22	Metastatic	Experimental group	CSI	CSI:32Gy/20f
5	Male/18	Classic	WNT	S+CT + RT	1	SCI	SCI:36Gy/20f, boost:45Gy/25f	15	12	Metastatic	Experimental group	CSI	CSI:30.6Gy/17f, Boost36Gy
6	Female/13	Classic	Group4	S	None	None	None	4	None	Metastatic	Experimental group	CSI	CSI:36Gy/20f, Boost 50.4Gy
7	Male/10	Classic	Group3	S + CT	1	None	None	2	None	Metastatic	Experimental group	CSI	CSI:32Gy/24f
8	Female/19	Classic	Group4	S + CT	1	None	None	2	None	Metastatic	Control group	CSI	CSI:32.4Gy/18f, boost45Gy
9	Female/12	Classic	Group4	S	None	None	None	2	None	Metastatic	Control group	CSI	CSI:32.4Gy/18f, boost45Gy
10	Male/4	Classic	Group4	S	None	None	None	22	None	Primary	Control group	CSI	CSI:32.4Gy/18f, boost45Gy
11	Female/12	Classic	SHH/ TP53gene mutation	S + CT	11	None	None	11	None	Primary	Control group	CSI	CSI:36.0Gy/20f, boost54Gy
12	Male/5	Classic	Group3	S + CT + RT	12	None	None	10	None	Primary	Control group	CSI	CSI:32.4Gy/18f, boost:43.2Gy
13	Male/11	Desmoplastic	Group3	S + RT	None	SCI	SCI:36Gy/18f, boost:40Gy/20f	39	37	Metastatic	Control group	CSI	CSI:36Gy/20f, boost40Gy

S: Surgery; CT: Chemotherapy; RT: Radiotherapy; Experimental group: Endostar synchronizing craniospinal radiotherapy; Control group: Craniospinal radiotherapy; CSI: Craniospinal irradiation; ost: metastatic focus added to

Table 2 Baseline characteristics of control group and experimental group [*n* (%)]

Characteristics	Total number	Control group	Experimental group
Gender			
Female	5 (38.5)	3 (50.0)	2 (28.6)
Male	8 (61.5)	3 (50.0)	5 (71.4)
Diagnosis			
Classical	11 (84.6)	5 (83.3)	6 (85.7)
Desmoplastic	2 (15.4)	1 (16.7)	1 (14.3)
Molecular subtype			
Group3	6 (46.2)	2 (33.3)	4 (57.1)
Group 4	5 (38.5)	3 (50.0)	2 (28.6)
SHH/TP53	1 (7.7)	1 (16.7)	0 (0.0)
WNT	1 (7.7)	0 (0.0)	1 (14.3)
Previous treatment			
S	3 (23.1)	2 (33.3)	1 (14.3)
S, CT	4 (30.8)	2 (33.3)	2 (28.6)
S, RT	1 (7.7)	1 (16.7)	0 (0.0)
S, RT, CT	5 (38.5)	1 (16.7)	4 (57.1)
M stage			
M2	2 (15.4)	2 (33.3)	0 (0.0)
M3	11 (84.6)	4 (66.7)	7 (100)
Anemia			
Grade 0	9 (69.2)	4 (66.7)	5 (71.4)
Grade 1	4 (30.8)	2 (33.3)	2 (28.6)
Neutropenia			
Grade 1	3 (23.1)	1 (16.7)	2 (28.6)
Grade 2	5 (38.5)	2 (33.3)	3 (42.9)
Grade 3	5 (38.5)	3 (50.0)	2 (28.6)
Thrombopenia			
Grade 0	12 (92.3)	6 (100)	6 (85.7)
Grade 1	1 (7.7)	0 (0.0)	1 (14.3)
ORR			
SD	1 (7.7)	1 (16.7)	0 (0.0)
CR + PR	12 (92.3)	5 (83.3)	7 (100)
Complete response			
Non-CR	7 (53.8)	5 (83.3)	2 (28.6)
CR	6 (46.2)	1 (16.7)	5 (71.4)

survival (PFS), OS, and side effects of the treatment were also analyzed.

Therapeutic evaluation

The baseline assessment included a complete history of the child's general condition, a neurological examination, and blood work. Routine blood work was performed at least once a week. A physical and nervous system examination was also performed at least once a week. Every 2–3 weeks a blood, liver, and kidney function biochemistry was performed. Toxicity ratings were based on the third edition of the National Cancer Institute's conventional toxicity criteria (NCICTCAE, version 3.0).

An enhanced MRI scan of the whole brain and whole spine was completed within 2 weeks prior to the initiation of treatment. An additional MRI was conducted 1 week after the termination of radiotherapy. If signs or symptoms of suspected MB clinical progression occurred during treatment, an MRI scan was required.

Efficacy was evaluated according to RANO criteria.

Statistical method

Statistical analysis was performed using SPSS 20.0. Kaplan-Meier curves were used to evaluate PFS rates, overall survival (OS) rates, median PFS, OS, and corresponding 95% confidential intervals between the experimental and control groups.

Results

Overall, 13 children with MB were treated with a secondary radiotherapy after MB recurrence. This included 7 in an experimental group (53.8%) and 6 in a control group (46.2%). The craniospinal radiotherapy was 30.6–36.0 Gy (experimental group, 30.6–36.0 Gy; control group, 32.0–36.0 Gy) plus metastatic focus added to 32.0–54.0 Gy (experimental group 32.0–50.4 Gy, 40.0–54.0 Gy) (Table 1). Subsequent chemotherapy was administered post-radiotherapy.

The CRR of the experimental and control groups was 71.4% and 16.7% and ORR was 100% and 83.3%, respectively. In the entire population, the median PFS was 19.0 months (95% CI: 8.431–29.569) and median OS was 23 months (95% CI: 11.257–34.743). The median PFS was 14 months (95% CI: 0.0–29.60) and 19 months (95% CI: 0.0–39.53) in the experimental and control groups, respectively. The median OS was 19 months (95% CI: 0.0–38.20) and 23 months (95% CI: 2.47–43.53) in the experimental and control groups, respectively. The PFS rates at 6, 12, and 18 months in the experimental and control groups were 71.4%, 55.4%, 44.6%, and 83.3%, 54.8%, and 38.9%, respectively. The OS rates at 6, 12, and 18 months in the experimental and control groups were 85.7%, 71.4%, 51.8%, and 66.7%, 61.7%, and 51.7%, respectively. After radiotherapy, the efficacy of one child was evaluated as the SD. The histology test of one case indicated desmoplastic MB. The disease progressed, and the child died after 9 months. (Table 2; Fig. 1)

Toxic manifestations and side effects: None of the patients had grade 3–4 hematologic extrinsic toxicity or life-threatening events. Bone marrow suppression usually occurs 1 week after radiotherapy. The most common adverse events included grade 3 tropenia (two in the experimental group and three in the control group), grade 1 thrombocytopenia (one in the experimental group) and grade 1 anemia (two in the experimental group and two in the control group) (Table 2).

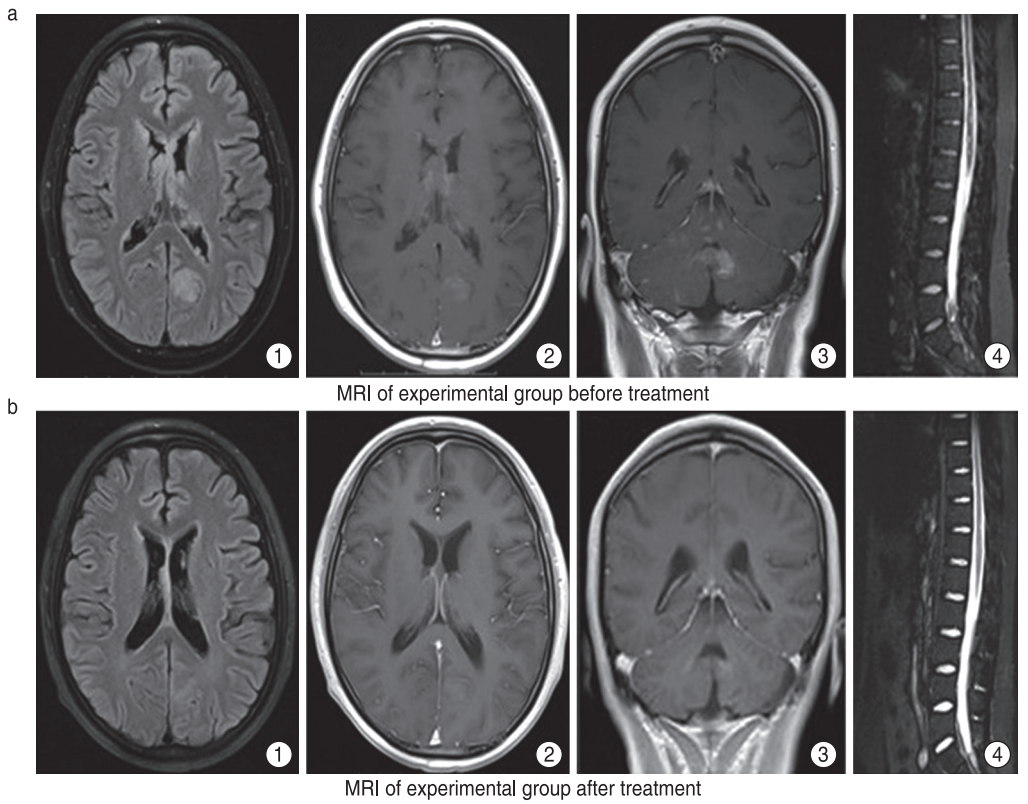

Fig. 1 (a) MRI of experimental group before treatment, multiple nodular or long T1 long T2 signals were seen in the cerebellum and left occipital lobe of bilateral lateral ventricles. (a1) FLAIR showed hyperintensity and (a2) obvious nodular abnormal enhancement, (a3) the largest was about 1.5 × 1.2 cm located in the left cerebellopontine foot, (a4) also multiple abnormal signals were seen in the medulla of cervical, thoracic and lumbar segments; (b) MRI of experimental group after treatment, intracranial lesions and spinal cord lesions were significantly reduced and some nodules disappeared

Discussion

Treatment options for children with recurrent MB are limited. Although all patients with postoperative recurrence or implantable dissemination receive active surgery and chemotherapy, the prognosis remains poor. Few children can receive radical treatment after recurrence. Unfortunately, there is a lack of standard treatment for recurrent MB.

In this study, 13 children with recurrent MB were enrolled. Of these, 5 patients underwent surgery followed by radiotherapy and chemotherapy during the initial treatment. Four children received surgery and chemotherapy. One child received surgery and radiotherapy, whereas three patients received only surgery. In 2016, MB was divided into four molecular subtypes, including Wnt, SHH (TP53 wild type and TP53 mutant type), G3, and G4 by WHO. This was based on molecular biology and histomathology [18]. Patients with G3, MYC amplification, or TP53 mutations have a poor overall prognosis [19]. Group3 was the most common subtype in this study. One child had SHH with a TP53 mutation. One child with WNT underwent only surgery and radiotherapy without chemotherapy. Among the five G4 patients, only three children underwent surgical treatment without radiotherapy or chemotherapy.

Secondary radiotherapy, targeted therapy, and other comprehensive therapies are being investigated for the treatment of recurrent MB. Zhao *et al* [20] used bevacizumab combined with stereotactic radiotherapy to treat CR in children with relapsed MB. Rao *et al* [21] performed secondary radiotherapy on 67 children with recurrent brain tumors (including 20 MB cases). The average OS was 12.8 months in the entire cohort, while the median OS was 8.4 months in MB. Gupta *et al* [22] treated 28 patients with recurrent MB with secondary radiotherapy in combination with platinum-based chemotherapy. This yielded a 46% 2-year PFS rate and 51% OS rate. In recent years, targeted therapy has become a promising therapeutic approach for the treatment of recurrent MB.

Endostar® is one of the most effective angiogenesis inhibitors discovered thus far. Its' mechanism may be related to the following factors. The mechanism by which Endostar® achieves radiosensitization may be: (1) Normalization of tumor blood vessels [12, 23–25]; (2)

blockade of the cell cycle at the radiotherapy sensitive stage [26–30]; (3) Induction of apoptosis of endothelial cells and tumor cells [31], and (4) Improvement of the tumor microenvironment (TME) [8–11]. In addition, the molecular mechanism of Endostar® anti-angiogenesis may be related to the inhibition of tyrosine phosphorylation of KDR/ flk-1 (vegfr-2) and the activation of ERK, p38 MAPK, and AKT [32]. In addition, clinical studies have shown that Endostar® combined with radiotherapy in the simultaneous treatment of brain metastatic tumors from lung cancer has a significant effect in patients with high expression of VEGFR2 protein (or increased copy number of the KDR gene) [15–16]. VEGFR is not only expressed in MB vascular endothelial cells but it is also highly expressed in tumor cells. The worse the prognosis, the higher the expression level of the KDR gene. Targeted VEGF signaling may be a new treatment option for MB [33]. Taken together, the combination of radiotherapy and Endostar® may have a synergistic effect.

The blood brain barrier (BBB) regulates homeostasis of the central nervous system by forming a tightly regulated neurovascular unit [34–35]. However, these same features also hinder the delivery of systemic therapies to brain tumors. The BBB is disrupted during tumor progression and is referred to as the blood tumor barrier (BTB). Although the BTB is more permeable than the BBB, its' heterogeneous permeability to small and large molecules as well as heterogeneous perfusion contribute to suboptimal drug accumulation in brain tumors [36–39]. As such, the BBB is one of the rate-limiting factors in clinically effective therapies. Radiotherapy can cause damage to the BBB [40]. This may increase the concentration of the drug within the tumor tissue and improve the effectiveness of treatment. In this study, the CRR and ORR of the experimental group were better than those of the control group.

Secondary radiotherapy for recurrent MB remains controversial due to its' potential for toxicity and the uncertainty of improving overall viability [41–43]. MB spreads easily within the cerebrospinal fluid. Total central or subtotal central radiotherapy remains an important guarantee to reduce the recurrence of irradiation in this area [44]. The survival rate of children who received radiotherapy was significantly higher than that of those who did not [45]. Radiobiology data showed that age, chemotherapy use, radiated volume, total dose of radiotherapy, and the time interval between the first and second radiotherapy were important factors in determining survival. This data was also important in determining the recovery of the central nervous system from radiation injury. Although there are several case reports of severe brain damage caused by conventional radiotherapy doses [46], Lawrence *et al* [47] discovered that for patients receiving brain radiation therapy, the biologically effective dose of 150 Gy (BED) was 10%. Patients with symptomatic radioactive necrosis accumulated BED doses of 204 Gy and were born with irreversible complications [48]. For the second radiotherapy of the spinal cord, if the BED dose of each radiotherapy is 98 Gy and the interval between the two radiotherapies is no less than 6 months, the accumulated BED dose can reach 120 Gy without causing spinal cord injury [49–51]. In our study, the cumulative dose of craniospinal radiotherapy was less than 72.0 Gy. None of the patients had grade 3–4 hematological extrinsic toxicities or life-threatening events. Bone marrow suppression often occurs 1 week after radiotherapy. The most common adverse events include thrombocytopenia, neutropenia, and anemia. Compared with the control group, the experimental group did not show acute toxicity or side effects, including hematological toxicity. Hematological toxicity was more closely related to early chemotherapy and total central radiotherapy. The critical functional areas of the brain are not suitable for excessive irradiation. Therefore the radiation dose is limited. Certain scholars believe that reducing the radiation dose, combined with chemotherapy, can reduce the neurotoxicity caused by high-dose radiotherapy. This is accomplished without reducing the curative effect. It also further improves the curative effect compared to chemotherapy alone [4, 52]. In this study, PFS and OS of patients in the experimental group did not benefit from the increase in ORR and CRR. We speculated that subsequent treatment of recurrent MB may play an crucial role in influencing PFS and OS. In addition, statistical bias was inevitable due to the small sample size in this study.

In conclusion, Endostar® combined craniospinal radiotherapy may be an effective treatment for the management of recurrent MB in children. Considering that this therapy has a high clinical remission rate and acceptable tolerance, all patients in the control group were radiotherapy-naive prior to recurrence. Compared to the treatment group, there was a selective statistical bias. Therefore, in a future study we will expand the sample size and multi-center enrollment to confirm the efficacy and safety of Endostar®. We will include this in a future study as well as a discussion of a maintenance program for recurrent MB in children.

References

1. Rolland A, Aquilina K. Surgery for recurrent medulloblastoma: A review. Neurochirurgie, 2021, 67: 69–75.
2. Araujo OL, Trindade KM, Trompieri NM, *et al*. Analysis of survival and prognostic factors of pediatric patients with brain tumor. J Pediatr (Rio J), 2011, 87: 425–432.
3. Evans AE, Jenkin RD, Sposto R, *et al*. The treatment of medulloblastoma. Results of a prospective randomized trial of radiation therapy with and without CCNU, vincristine, and prednisone.

J Neurosurg, 1990, 72: 572–582.
4. Massimino M, Biassoni V, Gandola L, *et al*. Childhood medulloblastoma. Crit Rev Oncol Hematol, 2016, 105: 35–51.
5. Aguilera D, Mazewski C, Fangusaro J, *et al*. Response to bevacizumab, irinotecan, and temozolomide in children with relapsed medulloblastoma: a multi-institutional experience. Childs Nerv Syst, 2013, 29: 589–596.
6. Sabel M, Fleischhack G, Tippelt S, *et al*. SIOP-E Brain Tumour Group. Relapse patterns and outcome after relapse in standard risk medulloblastoma: a report from the HIT-SIOP-PNET4 study. J Neurooncol, 2016, 129: 515–524.
7. Folkman J. Tumor angiogenesis: therapeutic implications. N Engl J Med, 1971, 285: 1182–1186.
8. Liu X, Nie W, Xie Q, *et al*. Endostatin reverses immunosuppression of the tumor microenvironment in lung carcinoma. Oncol Lett, 2018, 15: 1874–1880.
9. Wu J, Zhao X, Sun Q, *et al*. Synergic effect of PD-1 blockade and endostar on the PI3K/AKT/mTOR-mediated autophagy and angiogenesis in Lewis lung carcinoma mouse model. Biomed Pharmacother, 2020, 125: 109746.
10. Huang Y, Kim BYS, Chan CK, *et al*. Improving immune-vascular crosstalk for cancer immunotherapy. Nat Rev Immunol, 2018, 18: 195–203.
11. Diegeler S, Hellweg CE. Intercellular communication of tumor cells and immune cells after exposure to different Ionizing radiation qualities. Front Immunol, 2017, 8: 664.
12. Jain RK. Normalization of tumor vasculature: an emerging concept in antiangiogenic therapy. Science, 2005, 307: 58–62.
13. Zhu H, Yang X, Ding Y, *et al*. Recombinant human endostatin enhances the radioresponse in esophageal squamous cell carcinoma by normalizing tumor vasculature and reducing hypoxia. Sci Rep, 2015, 28, 5: 14503.
14. Ricard-Blum S, Vallet SD. Matricryptins network with matricellular receptors at the surface of endothelial and tumor cells. Front Pharmacol, 2016, 7: 11.
15. Jiang XD, Ding MH, Qiao Y, *et al*. Study on lung cancer cells expressing VEGFR2 and the impact on the effect of RHES combined with radiotherapy in the treatment of brain metastases. Clin Lung Cancer, 2014, 15: e23–29.
16. Zhang F, Xu CL, Liu CM. Drug delivery strategies to enhance the permeability of the blood-brain barrier for treatment of glioma. Drug Des Devel Ther, 2015, 9: 2089–2100.
17. Chang CH, Housepian EM, Herbert C Jr. An operative staging system and a megavoltage radiotherapeutic technic for cerebellar medulloblastomas. Radiology, 1969, 93: 1351–1359.
18. Louis DN, Perry A, Reifenberger G, *et al*. The 2016 World Health Organization Classification of Tumors of the Central Nervous System: a summary. Acta Neuropathol, 2016, 131: 803–820.
19. Ramaswamy V, Remke M, Bouffet E, *et al*. Risk stratification of childhood medulloblastoma in the molecular era: the current consensus. Acta Neuropathol, 2016, 131: 821–831.
20. Zhao M, Wang X, Fu X, *et al*. Bevacizumab and stereotactic radiosurgery achieved complete response for pediatric recurrent medulloblastoma. J Cancer Res Ther, 2018, 14 (Supplement): S789–S792.
21. Rao AD, Rashid AS, Chen Q, *et al*. Reirradiation for recurrent pediatric central nervous system malignancies: A multi-institutional review. Int J Radiat Oncol Biol Phys, 2017, 99: 634–641.
22. Gupta T, Maitre M, Sastri GJ, *et al*. Outcomes of salvage re-irradiation in recurrent medulloblastoma correlate with age at initial diagnosis, primary risk-stratification, and molecular subgrouping. J Neurooncol, 2019, 144: 283–291.
23. Vaupel P, Multhoff G. Fatal Alliance of Hypoxia-/HIF-1α-Driven Microenvironmental Traits Promoting Cancer Progression. Adv Exp Med Biol, 2020, 1232: 169–176.
24. Multhoff G, Vaupel P. Hypoxia Compromises anti-cancer immune responses. Adv Exp Med Biol, 2020, 1232: 131–143.
25. Peng F, Xu Z, Wang J, *et al*. Recombinant human endostatin normalizes tumor vasculature and enhances radiation response in xenografted human nasopharyngeal carcinoma models. PLoS One, 2012, 7: e34646.
26. Shi L, Zhang S, Wu H, *et al*. MiR-200c increases the radiosensitivity of non-small-cell lung cancer cell line A549 by targeting VEGF-VEGFR2 pathway. PLoS One, 2013, 8: e78344.
27. Liu C, Nie J, Wang R, *et al*. The cell cycle G2/M block is an indicator of cellular radiosensitivity. Dose Response, 2019, 9, 17: 1559325819891008.
28. Zhang L, Ge W, Hu K, *et al*. Endostar down-regulates HIF-1 and VEGF expression and enhances the radioresponse to human lung adenocarcinoma cancer cells. Mol Biol Rep, 2012, 39: 89–95.
29. Liu GF, Chang H, Li BT, *et al*. Effect of recombinant human endostatin onradiotherapy for esophagus cancer. Asian Pac J Trop Med, 2016, 9: 86–90.
30. Toulany M. Targeting DNA double-strand break repair pathways to improve radiotherapy response. Genes (Basel), 2019, 10: 25.
31. Yan H, Guo W, Li K, *et al*. Combination of DESI2 and endostatin gene therapy significantly improves antitumor efficacy by accumulating DNA lesions, inducing apoptosis and inhibiting angiogenesis. Exp Cell Res, 2018, 371: 50–62.
32. Ling Y, Yang Y, Lu N, *et al*. Endostar, a novel recombinant human endostatin, exerts antiangiogenic effect via blocking VEGF-induced tyrosine phosphorylation of KDR/Flk-1 of endothelial cells. Biochem Biophys Res Commun, 2007, 361: 79–84.
33. Slongo ML, Molena B, Brunati AM, *et al*. Functional VEGF and VEGF receptors are expressed in human medulloblastomas. Neuro Oncol, 2007, 9: 384–392.
34. O'Brown NM, Pfau SJ, Gu C. Bridging barriers: a comparative look at the blood-brain barrier across organisms. Genes Dev, 2018, 32: 466–478.
35. Abbott NJ. Blood-brain barrier structure and function and the challenges for CNS drug delivery. J Inherit Metab Dis, 2013, 36: 437–449.
36. Hobbs SK, Monsky WL, Yuan F, *et al*. Regulation of transport pathways in tumor vessels: role of tumor type and microenvironment. Proc Natl Acad Sci U S A, 1998, 95: 4607–4612.
37. Monsky WL, Mouta Carreira C, Tsuzuki Y, *et al*. Role of host microenvironment in angiogenesis and microvascular functions in human breast cancer xenografts: mammary fat pad versus cranial tumors. Clin Cancer Res, 2002, 8: 1008–1013.
38. Pitz MW, Desai A, Grossman SA, *et al*. Tissue concentration of systemically administered antineoplastic agents in human brain tumors. J Neurooncol, 2011, 104: 629–638.
39. Sarkaria JN, Hu LS, Parney IF, *et al*. Is the blood-brain barrier really disrupted in all glioblastomas? A critical assessment of existing clinical data. Neuro Oncol, 2018, 20: 184–191.
40. Qin DX, Zheng M, Tang J, *et al*. The effect of brain radiotherapy on the blood-brain barrier. Chin Radiat Oncol (Chinese), 1990, 4: 29–31.
41. Padovani L, Andre N, Gentet JC, *et al*. Reirradiation and concomitant metronomic temozolomide: an efficient combination for local control in medulloblastoma disease? J Pediatr Hematol Oncol, 2011, 33:

600–604.
42. Bakst RL, Dunkel IJ, Gilheeney S, *et al*. Reirradiation for recurrent medulloblastoma. Cancer, 2011, 117: 4977–4982.
43. Massimino M, Gandola L, Spreafico F, *et al*. No salvage using high-dose chemotherapy plus/minus reirradiation for relapsing previously irradiated medulloblastoma. Int J Radiat Oncol Biol Phys, 2009, 73: 1358–1363.
44. Wetmore C, Herington D, Lin T, *et al*. Reirradiation of recurrent medulloblastoma: does clinical benefit outweigh risk for toxicity? Cancer, 2014, 120: 3731–3737.
45. Johnston DL, Keene D, Bartels U, *et al*. Medulloblastoma in children under the age of three years: A retrospective Canadian review. J Neurooncol, 2009, 94: 51–56.
46. Zhang Q, Tang J, Du J, *et al*. Radiation-induced brain injury after a conventional dose of intensity-modulated radiotherapy for nasopharyngeal carcinoma:a case report and literature review. Oncol Transl Med, 2020, 6: 30–35.
47. Lawrence YR, Li XA, el Naqa I, *et al*. Radiation dose-volume effects in the brain. Int J Radiat Oncol Biol Phys, 2010, 76 (3 Suppl): S20–27.
48. Veninga T, Langendijk HA, Slotman BJ, *et al*. Reirradiation of primary brain tumours: survival, clinical response and prognostic factors. Radiother Oncol, 2001, 59: 127–137.
49. Nieder C, Milas L, Ang KK. Tissue tolerance to reirradiation. Semin Radiat Oncol, 2000, 10: 200–209.
50. Nieder C, Grosu AL, Andratschke NH, *et al*. Update of human spinal cord reirradiation tolerance based on additional data from 38 patients. Int J Radiat Oncol Biol Phys, 2006, 66: 1446–1449.
51. Nieder C, Andratschke NH, Grosu AL. Increasing frequency of reirradiation studies in radiation oncology: systematic review of highly cited articles. Am J Cancer Res, 2013, 3: 152–158.
52. Ris MD, Packer R, Goldwein J, *et al*. Intellectual outcome after reduced-dose radiation therapy plus adjuvant chemotherapy for medulloblastoma: a Children's Cancer Group study. J Clin Oncol, 2001, 19: 3470–3476.

DOI 10.1007/s10330-021-0489-9
Cite this article as: Song Y, Xiao H, Chen C, *et al*. Recombinant human vascular endostatin injection to synchronize craniospinal radiotherapy for the treatment of recurrent medulloblastoma in children: A retrospective clinical study. Oncol Transl Med, 2021, 7: 115–122.

Oncology and Translational Medicine
DOI 10.1007/s10330-021-0486-6

June 2021, Vol. 7, No. 3, P123–P129

ORIGINAL ARTICLE

Diagnostic value of lncRNAs as potential biomarkers for oral squamous cell carcinoma diagnosis: a meta-analysis*

Yuxue Wei[1], Hua Yang[1], Xiaoqiu Liu[2] (✉)

[1] Department of Stomatology, People's Hospital of Lanling County, Linyi 276000, China
[2] Department of Stomatology, Jilin University, Changchun 130000, China

Abstract

Objective Several studies have revealed the critical role of long non-coding RNAs (lncRNAs) as biomarkers for diagnosing oral squamous cell carcinoma (OSCC). However, the data remain inconsistent. This meta-analysis was performed to summarize the potential of lncRNAs as OSCC biomarkers.

Methods We searched PubMed, Cochrane Library, Web of Science, and China National Knowledge Infrastructure databases for literature published until December 10, 2020. Study quality was assessed using Quality Assessment for Studies of Diagnostic Accuracy-2, and sensitivity, specificity, and other measures regarding lncRNAs for OSCC diagnosis were pooled using bivariate meta-analysis models. Data analyses were performed using STATA 14.0.

Results Overall, 8 studies with 981 cases and 585 controls were included in the pooled analysis. The pooled sensitivity, specificity, positive likelihood ratio, negative likelihood ratio, diagnostic odds ratio, and area under the receiver operating characteristic curve values were as follows: 0.76 [95% confidence interval (CI), 0.65–0.84], 0.90 (95% CI, 0.82–0.95), 7.5 (95% CI, 4.20–13.40), 0.27 (95% CI, 0.18–0.39), 28 (95% CI, 13.00–58.00), 0.90 (95% CI, 0.87–0.93), respectively. Deeks' funnel plot asymmetry test (P = 0.56) indicated no potential publication bias.

Conclusion Our meta-analytical evidence suggests that lncRNAs could be employed as a potential non-invasive diagnostic tool for OSCC.

Received: 24 March 2021
Revised: 21 May 2021
Accepted: 15 June 2021

Key words: lncRNA; oral squamous cell carcinoma; diagnosis; meta-analysis

Oral squamous cell carcinoma (OSCC) is the eighth most common cancer worldwide [1–2]. OSCC accounts for 95% of all oral malignancies, with a global five-year survival rate that ranges between 50% and 60%, especially in patients diagnosed at advanced stages [3–4]. Most clinical examinations and imaging techniques currently used to detect OSCC fail to reliably distinguish early OSCC [5–6]. Therefore, early diagnosis and monitoring of OSCC progression remain crucial.

Long non-coding RNAs (lncRNAs) are novel non-coding RNAs with a length of more than 200 nucleotides, which do not encode proteins [7–8]. LncRNAs are characterized by low expression, moderate sequence conservation, and high tissue specificity and play an important role in several fundamental biological processes, including transcriptional regulation, cell differentiation, and chromatin modification [9]. Notably, growing evidence implicates a close relationship between tumor occurrence and development [10–13]. Additionally, dysregulated lncRNAs promote the occurrence and metastasis of malignancies [14–15]. Reportedly, altered lncRNA expression can be detected in biological fluids in different cancer types [16–17], including OSCC [18–19]; however, no consensus has been reached regarding the clinical value of lncRNAs in OSCC diagnosis. Therefore, we conducted a bivariate meta-analysis to summarize the

✉ Correspondence to: Xiaoqiu Liu. Email: liuxq6399@163.com
* Supported by grants from the National Natural Science Foundation of China (No. 813711841014238), Jilin Province Science and Technology Department (NO. 20160519017JH).

diagnostic accuracy of lncRNAs for detecting OSCC.

Materials and methods

Literature search strategy and selection criteria

Two investigators searched PubMed, the Cochrane Library, Web of Science, and China National Knowledge Infrastructure (CNKI) databases for literature published until December 10, 2020, to identify relevant studies by employing the following terms: "lncRNAs" or "long ncRNAs" or "lincRNAs" or "long non-coding RNAs" or "long non-translated RNAs" or "long untranslated RNAs" or "long non-protein-coding RNAs" or "long intergenic non-protein coding RNAs" or "diagnostic value" or "diagnoses" or "receiver operating characteristics" or "ROC curve" or "sensitivity" or "specificity" and "OSCC" or "oral squamous cell carcinoma" or "oral cancer" or "oral tumor." Two investigators (WYX and LXQ) assessed study titles and abstracts and scanned full texts to eliminate irrelevant studies, using the following inclusion criteria: (1) Diagnostic data, including sensitivity, specificity, and the area under the receiver operating characteristic curve (AUC), were provided or could be calculated from the studies; (2) Studies included patients with OSCC and healthy controls; (3) Original research articles published in English or Chinese.

Data extraction and quality assessment

Two investigators (WYX, LXQ) independently reviewed and extracted the following information from each eligible study: first author, year, country, sample size, gender, mean age, tumor-node-metastasis (TNM) stage, type of sample, detection method, cut-off value, true positive (TP), false positive (FP), true negative (TN), and false negative (FN). The quality of included studies was assessed using Quality Assessment of Diagnostic Accuracy Studies 2 (QUADAS-2).

Statistical analysis

Statistical analyses were conducted using Stata 14.0 (Stata, College Station, TX, USA). The number of subjects with a sensitivity, specificity, diagnostic odds ratio (DOR), positive likelihood ratio (PLR), negative likelihood ratio (NLR), and their corresponding 95% confidence intervals (CIs) was calculated using a bivariate meta-analysis model. Then, summary receiver operator characteristic (SROC) curve analysis and AUC were calculated to evaluate the pooled diagnostic value of lncRNAs in OSCC detection. These data were confirmed using a hierarchical summary receiver operating characteristic (HSROC) model. The heterogeneity of eligible studies induced by the threshold effect was evaluated using Spearman correlation coefficients and ROC plane analyses. Heterogeneity of non-threshold effects was tested using Cochran's Q and inconsistency index (I^2) tests. For the Q test, $P < 0.05$ or $I^2 > 50\%$ indicated significant heterogeneity among identified studies. Moreover, Fagan's nomogram was used to assess relationships between prior-test probability, likelihood ratio, and post-test probability. Publication bias was assessed using Deeks' funnel plots.

Results

Study selection and characteristics of included studies

As shown in the flowchart (Fig. 1), a total of eight eligible studies [20–27] (981 OSCC and 585 healthy controls) evaluating 20 different lncRNAs were included in the present meta-analysis. The expression of lncRNAs was detected by reverse transcription-polymerase chain reaction (PCR) (n = 7) and TaqMan quantitative PCR (n = 1), while plasma (n = 4) or serum (n = 4) was the most common specimen assessed; in the TNM classification, four articles included patients in stages I–IV and one article included patients in stages I–III, whereas the other three failed to mention the TNM stage. According to single lncRNA expression levels, eight lncRNAs were upregulated, and data for others were unavailable. Details regarding study participants are presented in Table 1.

Quality assessment

In the present study, the methodological quality of diagnosis was assessed using QUADAS-2. All included studies presented relatively moderate-to-high quality, with QUADAS-2 scores ranging between 5 and 7 (Table

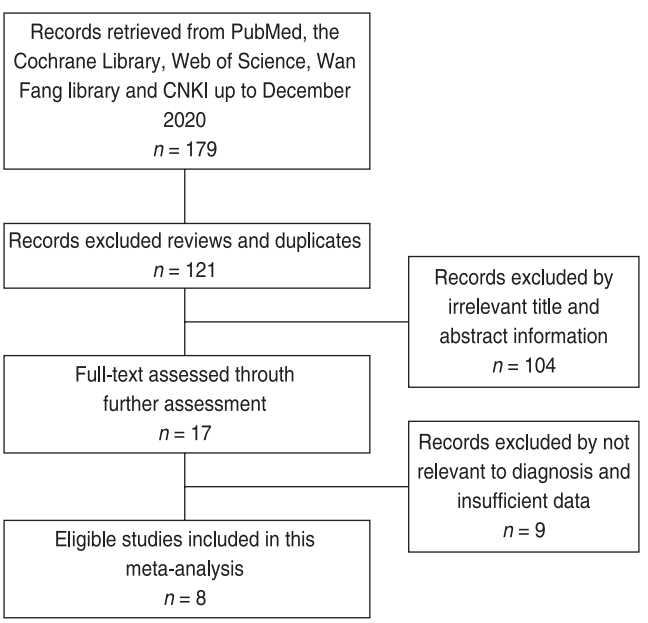

Fig. 1 Flow diagram of the study selection process

Table 1 Summary of main characteristics of included studies in this meta-analysis

First author	Year	Country	Case/ control	Sample type	Test method	Cutoff	TP	FP	FN	TN	LncRNAs Profiling	Up/Down	QUADAS-2
Zhao	2018	China	150/44	Plasma	qRT-PCR	NA	96	12	54	32	AC013268.5 RP11.65 L3.4 RP11.15A1.7	Up	5
Shao	2018	China	80/70	Serum	qRT-PCR	NA	62	11	18	59	AC007271.3	Up	6
Miao	2019	China	268/44	Plasma	qRT-PCR	1.44	157	1	111	43	LINC01629, AC083967.1, AC067863.1 AC022092.1, AC005532.1 LINC01629	NA	6
Zheng	2019	China	90/90	Serum	qRT-PCR	NA	55	7	35	83	SAMMSON	Up	7
Zhong	2019	China	116/116	Serum	qRT-PCR	NA	97	24	19	92	MIAT	Up	6
Le	2020	China	55/55	Plasma	qRT-PCR	NA	51	11	4	44	NCK-AS1	Up	7
Fan	2020	China	55/121	Serum	TaqMan-qPCR	3.29	36	5	19	116	LOC284454	Up	7
Li	2020	China	167/45	Plasma	qRT-PCR	NA	148	1	19	44	LINC01697, LINC02487 LOC105376575, AC005083.1 SLC8A1-AS1, U62317.1	NA	6

TP = true positive; FP = false positive; TN = true negative; FN = false negative; NA: Not available

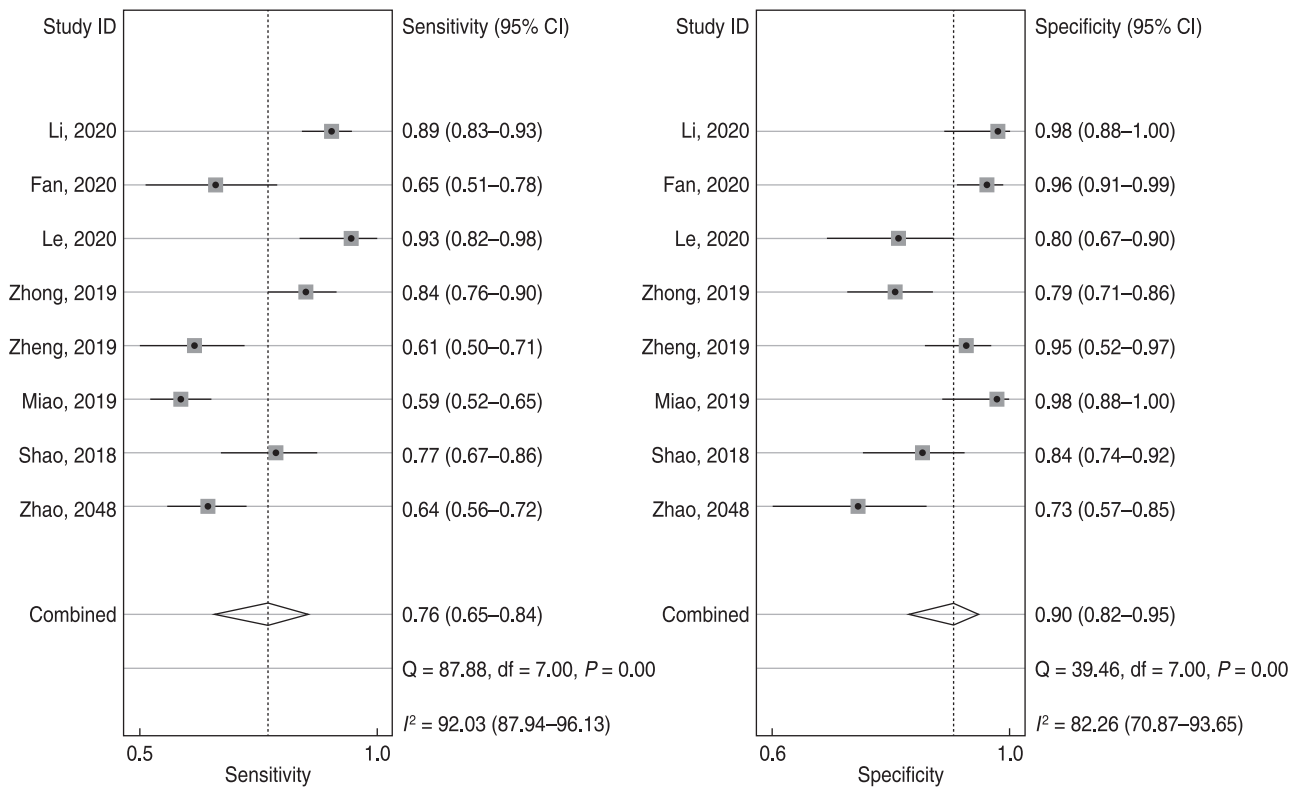

Fig. 2 Forest plots of lncRNA sensitivity and specificity for the diagnosis of OSCC

1); this indicated the reliable foundation of our meta-analysis.

Data analysis

For the eight included studies, forest plots of lncRNA sensitivity and specificity data for diagnosing OSCC are shown in Fig. 2. The pooled sensitivity and specificity of lncRNAs for diagnosing OSCC were 0.76 (95% CI, 0.65–0.84) and 0.90 (95% CI, 0.82–0.95), respectively. Additionally, the pooled PLR was 7.5 (95% CI, 4.20–13.40), NLR was 0.27 (95% CI, 0.18–0.39), and DOR was 28 (95% CI, 13.00–58.00) (Figs. 3 and 4). The overall

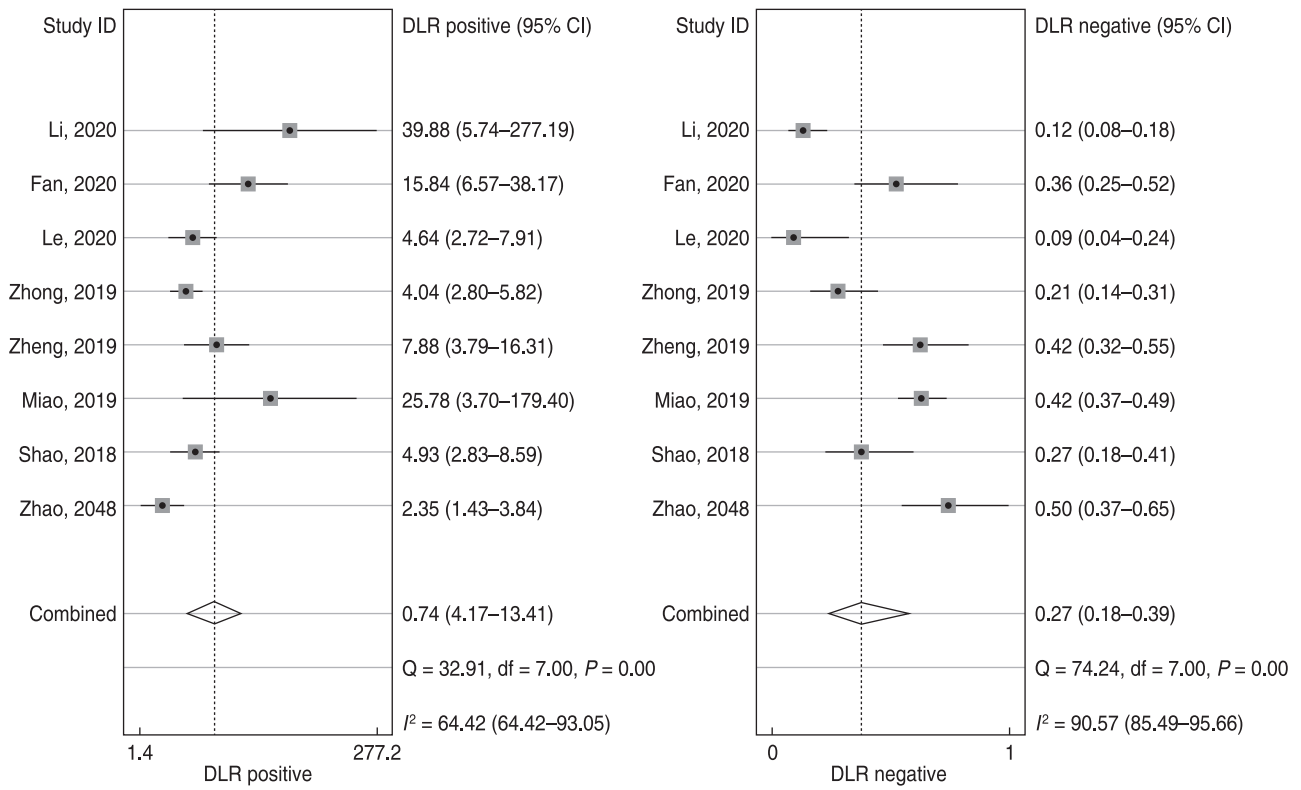

Fig. 3 Forest plots of the positive likelihood ratio (PLR) and negative likelihood ratio (NLR) of lncRNAs for the diagnosis of OSCC

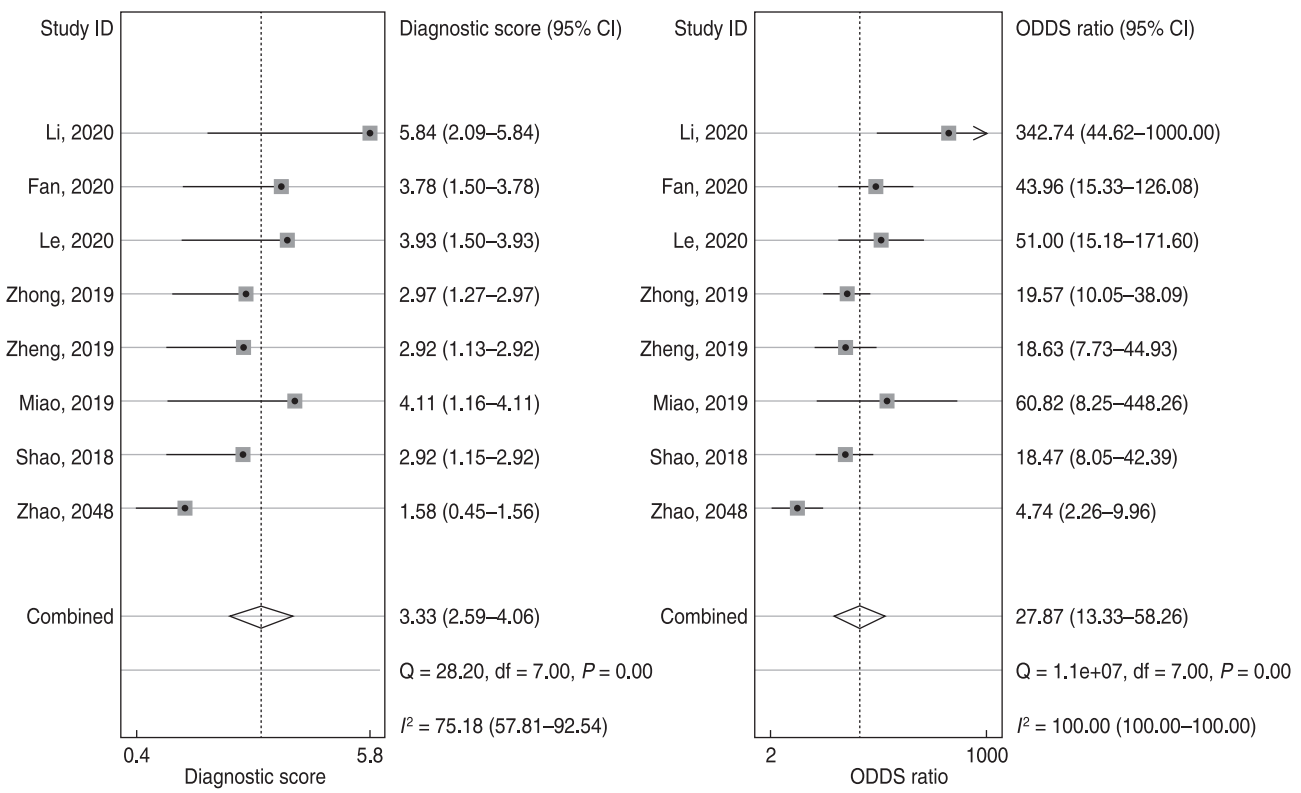

Fig. 4 Forest plots of diagnostic odds ratio (DOR) of lncRNAs for the diagnosis of OSCC

SROC curve for the eight included studies is shown in Fig. 5. The AUC of lncRNAs was 0.90 (95% CI, 0.87–0.93), which indicates that the lncRNAs were highly accurate in differentiating patients with OSCC from controls. Next, to assess the clinical utility of the index test, Fagan's nomogram was used to predict the increasing inerrability of a positive diagnosis by using the test value, which was employed for estimating post-test probabilities. As presented in Fig. 6, the pre-test probability was 20% and the positive post-test probability was increased to 65%, while the negative post-test probability was decreased to 6%. All pooled estimates indicated that lncRNAs in this analysis presented a relatively moderate-to-high accuracy in distinguishing patients with OSCC from control individuals.

Heterogeneity and publication bias

The I^2 value of the heterogeneity test was 95.95%, indicating apparent heterogeneity. Nevertheless, only eight articles were included, and subgroup and meta-regression analyses could not be undertaken in this meta-analysis. Moreover, we selected Deeks' funnel plot asymmetry test to assess publication bias (Fig. 7), which suggested no significant publication bias ($P = 0.56$).

Discussion

In OSCC, the initial stage is typically asymptomatic; therefore, early diagnosis remains a priority to improve

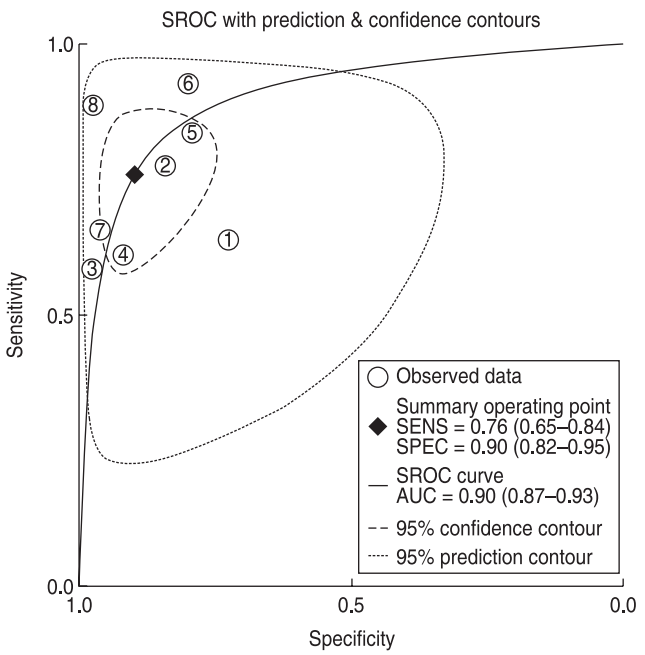

Fig. 5 Summary receiver operating characteristic (SROC) curve with pooled estimates of sensitivity, specificity, and area under the ROC curve (AUC)

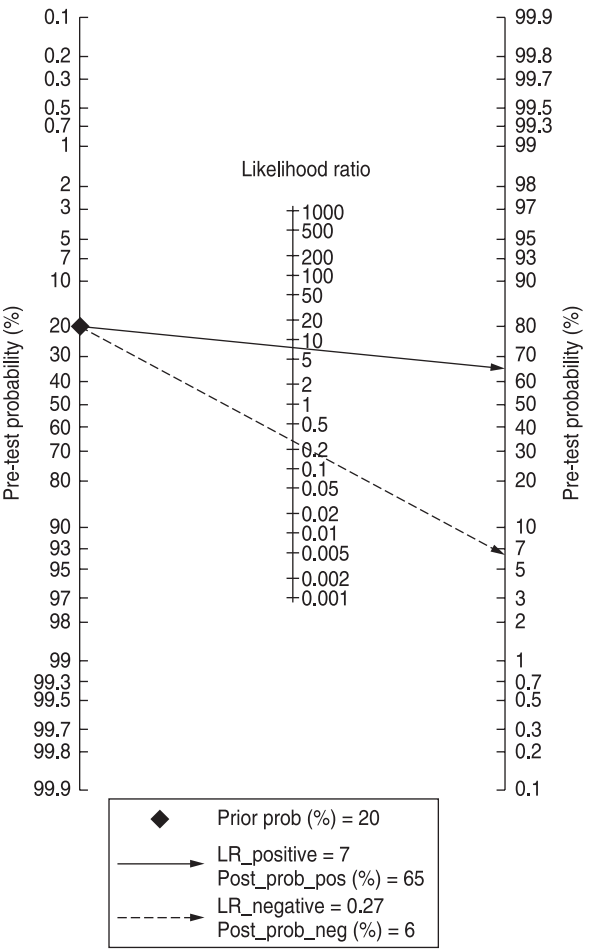

Fig. 6 Fagan's nomogram assessing the post-test probabilities

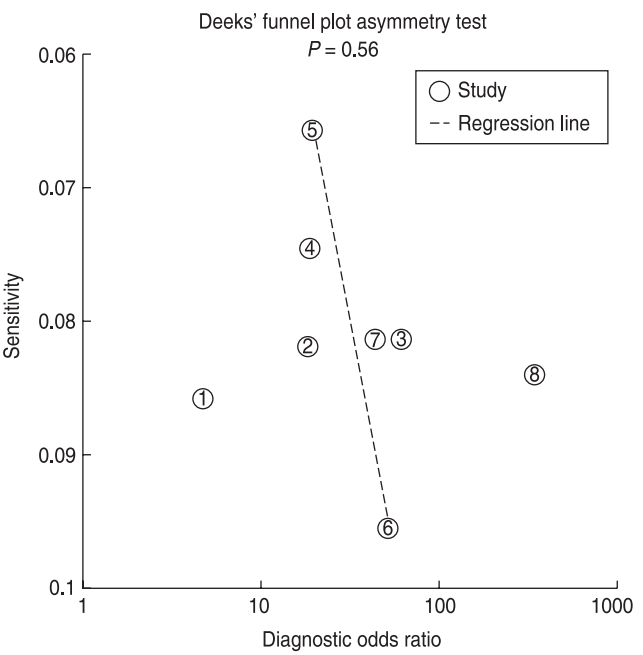

Fig. 7 Graph of Deeks' funnel plot asymmetry test

survival. Most patients with OSCC are diagnosed at late stages, resulting in a poor prognosis [19, 28]. Therefore, to optimize the survival rate and quality of life of patients with OSCC, it is essential to explore novel, practical, and non-invasive biomarkers for early detection of OSCC.

LncRNAs exert significant effects on the occurrence and development of several human diseases. Accumulating evidence suggests that altered lncRNA expression and its mutations can promote tumor occurrence and metastasis [14–15]. Furthermore, changes in lncRNA expression can be significantly associated with tumorigenesis, angiogenesis, and cell function [29]. Dysregulation of lncRNAs is reportedly involved in the occurrence, metastasis, and prognosis of cancer [8, 30]. Moreover, given their role in cancer biology and easy detection in biological fluids, lncRNAs could be potential and predictive cancer biomarkers. Circulating lncRNAs are promising new cancer biomarkers based on their role in cancer biology, and previous studies have demonstrated their feasibility as diagnostic and prognostic tools for different types of malignant tumors [30–32]. Tumor-related lncRNAs can be detected in various biological fluids, including blood [33–34].

The present review is the first evidence-based analysis to assess the diagnostic role of lncRNAs in OSCC detection. This meta-analysis included eight studies with 981 cancer cases and 585 controls, indicating that lncRNAs possess relatively high diagnostic accuracy with an overall pooled sensitivity of 0.76 (95% CI, 0.65–0.84), specificity of 0.90 (95% CI = 0.87–0.95), and AUC of 0.90 (95% CI, 0.87–0.93). Furthermore, the pooled DOR of 28 (95% CI, 13.00–58.00) suggested that lncRNAs are reliable for detecting OSCC.

Additionally, PLR and NLR were used to evaluate diagnostic accuracy. In this analysis, the pooled PLR was 7.5 (95% CI, 4.20–13.40), and the NLR was 0.27 (95% CI, 0.18–0.38); this could be attributed to the fact that patients with OSCC have a 7.5-fold higher possibility of reporting lncRNAs positive for OSCC when compared with controls, and 27% of all individuals present a negative result. As shown in Fagan's nomogram, at a pre-test probability of 20%, the positive post-test probability would increase up to 65% with a PLR of 7, while the negative post-test probability would decline to 6% with an NLR of 0.27. These results indicate the potential value of lncRNAs in OSCC detection and diagnosis.

Notably, significant heterogeneity existed among included studies in the present meta-analysis. The ROC plane showed no "shoulder arm" pattern, suggesting that the threshold effect was not a major source of heterogeneity (Fig. 8). Moreover, the Spearman correlation coefficient was -0.30 with $P = 0.09$, indicating the absence of a threshold effect. However, we could not conduct meta-regression and subgroup analyses

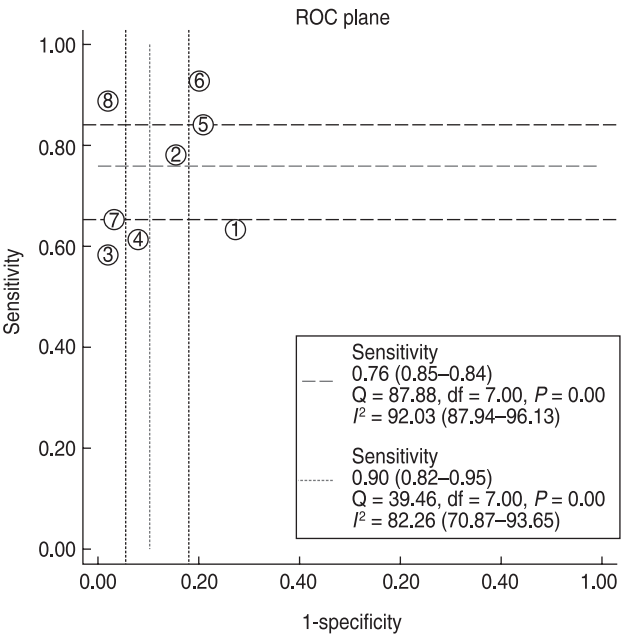

Fig. 8 Receiver operating characteristics (ROC) space to assess the threshold effect of lncRNAs

to detect the cause of heterogeneity, owing to a lack of eligible studies. Therefore, potential factors including age distribution, TNM stage, and gender proportion were not assessed as sources of heterogeneity.

However, the limitations of this study should be noted. First, our meta-analysis included a small sample size of lncRNAs in patients with OSCC. Second, the cut-off values for lncRNAs differed among included studies, which could be a potential source of heterogeneity. Third, this meta-analysis included a high proportion of Chinese populations, which may introduce unavoidable bias. Additionally, we did not determine differences in the diagnostic accuracy of lncRNAs presented in OSCCs, with respect to age distribution, TNM stage, and gender proportion. Finally, we identified the pooled lncRNA diagnostic value for OSCC but did not explore specific lncRNAs due to insufficient publications.

In conclusion, the results of this meta-analysis suggest that lncRNAs have a moderate-to-high diagnostic value in distinguishing patients with oral cancer from healthy controls, suggesting that lncRNAs can be utilized with high accuracy, particularly when performing multiple-lncRNA assays. However, large-scale prospective trials, as well as different ethnic groups, are necessary to confirm and extend our findings.

Conflicts of interest

The authors indicated no potential conflicts of interest.

References

1. Bray F, Ferlay J, Soerjomataram I, *et al*. Global cancer statistics 2018: GLOBOCAN estimates of incidence and mortality worldwide for 36 cancers in 185 countries. CA Cancer J Clin, 2018, 68: 394–424.
2. Ferlay J, Colombet M, Soerjomataram I, *et al*. Estimating the global cancer incidence and mortality in 2018: GLOBOCAN sources and methods. Int J Cancer, 2019, 144: 1941–1953.
3. Warnakulasuriya S. Global epidemiology of oral and oropharyngeal cancer. Oral Oncol, 2009, 45: 309–316.
4. Dequanter D, Shahla M, Paulus P, *et al*. Long term results of sentinel lymph node biopsy in early oral squamous cell carcinoma. OncoTargets Ther, 2013, 6: 799–802.
5. Govers TM, Schreuder WH, Klop WM, *et al*. Quality of life after different procedures for regional control in oral cancer patients: cross-sectional survey. Clin Otolaryngol, 2016, 41: 228–233.
6. Govers TM, Takes RP, Karakullukcu MB, *et al*. Management of the N0 neck in early stage oral squamous cell cancer: a modeling study of the cost-effectiveness. Oral Oncol, 2013, 49: 771–777.
7. Schmitz SU, Grote P, Herrmann BG. Mechanisms of long noncoding RNA function in development and disease. Cell Mol Life Sci, 2016, 73: 2491–2509.
8. Gutschner T, Diederichs S. The hallmarks of cancer: a long non-coding RNA point of view. RNA Biol, 2012, 9: 703–719.
9. Ponting CP, Oliver PL, Reik W. Evolution and functions of long noncoding RNAs. Cell, 2009, 136: 629–641.
10. Kim K, Jutooru I, Chadalapaka G, *et al*. HOTAIR is a negative prognostic factor and exhibits pro-oncogenic activity in pancreatic cancer. Oncogene, 2013, 32: 1616–1625.
11. Martens-Uzunova ES, Bottcher R, Croce CM, *et al*. Long noncoding RNA in prostate, bladder, and kidney cancer. Eur Urol, 2014, 65: 1140–1151.
12. Salameh A, Lee AK, Cardo-Vila M, *et al*. PRUNE2 is a human prostate cancer suppressor regulated by the intronic long noncoding RNA PCA3. Proc Natl Acad Sci U S A, 2015, 112: 8403–8408.
13. Wang YQ, He HL, Li W, *et al*. MYH9 binds to lncRNA gene PTCSC2 and regulates FOXE1 in the 9q22 thyroid cancer risk locus. Proc Natl Acad Sci U S A, 2017, 114: 474–479.
14. Bhan A, Soleimani M, Mandal SS. Long noncoding RNA and cancer: A new paradigm. Cancer Res, 2017, 77: 3965–3981.
15. Huarte M. The emerging role of lncRNAs in cancer. Nat Med, 2015, 21: 1253–1261.
16. Rapado-Gonzalez O, Majem B, Muinelo-Romay L, *et al*. Human salivary microRNAs in Cancer. J Cancer, 2018, 9: 638–649.
17. Shen Y, Ding YJ, Ma Q, *et al*. Identification of novel circulating miRNA biomarkers for the diagnosis of esophageal squamous cell carcinoma and squamous dysplasia. Cancer Epidemiol Biomarkers Prev, 2019, 28: 1212–1220.
18. Chang YA, Weng SL, Yang SF, *et al*. A three-microRNA signature as a potential biomarker for the early detection of oral cancer. Int J Mol Sci, 2018, 19: 758.
19. Momen-Heravi F, Trachtenberg AJ, Kuo WP, *et al*. Genomewide study of salivary microRNAs for detection of oral cancer. J Dent Res, 2014, 93: 86S–93S.
20. Fan C, Wang JP, Tang YY, *et al*. Upregulation of long non-coding RNA LOC284454 may serve as a new serum diagnostic biomarker for head and neck cancers. BMC Cancer, 2020, 20: 917.
21. Le F, Ou YQ, Luo P, *et al*. LncRNA NCK1-AS1 in plasma distinguishes oral ulcer from early-stage oral squamous cell carcinoma. J Biol Res (Thessalon), 2020, 27: 16.
22. Li Y, Cao XF, Li H. Identification and validation of novel long non-coding RNA biomarkers for early diagnosis of oral squamous cell carcinoma. Front Bioeng Biotechnol, 2020, 8: 256.
23. Miao TT, Si QZ, Wei Y, *et al*. Identification and validation of seven prognostic long non-coding RNAs in oral squamous cell carcinoma. Oncol Lett, 2020, 20: 939–946.
24. Shao TR, Huang JX, Zheng ZN, *et al*. SCCA, TSGF, and the long non-coding RNA AC007271.3 are effective biomarkers for diagnosing oral squamous cell carcinoma. Cell Physiol Biochem, 2018, 47: 26–38.
25. Zhao CG, Zou HR, Wang JH, *et al*. A three long noncoding RNA-based signature for oral squamous cell carcinoma prognosis prediction. DNA Cell Biol, 2018, 37: 888–895.
26. Zheng XJ, Tian X, Zhang Q, *et al*. Long non-coding RNA SAMMSON as a novel potential diagnostic and prognostic biomarker for oral squamous cell carcinoma. J Dent Sci, 2020, 15: 329–335.
27. Zhong WS, Xu Z, Wen SL, *et al*. Long non-coding RNA myocardial infarction associated transcript promotes epithelial-mesenchymal transition and is an independent risk factor for poor prognosis of tongue squamous cell carcinoma. J Oral Pathol Med, 2019, 48: 720–727.
28. Eckert AW, Kappler M, Schubert J, *et al*. Correlation of expression of hypoxia-related proteins with prognosis in oral squamous cell carcinoma patients. Oral Maxillofac Surg, 2012, 16: 189–196.
29. Huang YK, Yu JC. Circulating microRNAs and long non-coding RNAs in gastric cancer diagnosis: An update and review. World J Gastroenterol, 2015, 21: 9863–9886.
30. Qi P, Zhou XY, Du X. Circulating long non-coding RNAs in cancer: current status and future perspectives. Mol Cancer, 2016, 17, 15: 39.
31. Ke D, Li HW, Zhang Y, *et al*. The combination of circulating long noncoding RNAs AK001058, INHBA-AS1, MIR4435-2HG, and CEBPA-AS1 fragments in plasma serve as diagnostic markers for gastric cancer. Oncotarget, 2017, 8: 21516–21525.
32. Xian HP, Zhuo ZL, Sun YJ, *et al*. Circulating long non-coding RNAs HULC and ZNFX1-AS1 are potential biomarkers in patients with gastric cancer. Oncol Lett, 2018, 16: 4689–4698.
33. Zhang KC, Shi HZ, Xi HQ, *et al*. Genome-wide lncRNA microarray profiling identifies novel circulating lncRNAs for detection of gastric cancer. Theranostics, 2017, 7: 213–227.
34. Yoruker EE, Keskin M, Kulle CB, *et al*. Diagnostic and prognostic value of circulating lncRNA H19 in gastric cancer. Biomed Rep, 2018, 9: 181–186.

DOI 10.1007/s10330-021-0486-6
Cite this article as: Wei YX, Yang H, Liu XQ, *et al*. Diagnostic value of lncRNAs as potential biomarkers for oral squamous cell carcinoma diagnosis: a meta-analysis. Oncol Transl Med, 2021, 7: 123–129.

Oncology and Translational Medicine
DOI 10.1007/s10330-020-0472-2
June 2021, Vol. 7, No. 3, P130–P135

ORIGINAL ARTICLE

Construction and validation of an immune-related lncRNA prognostic model for rectal adenocarcinomas*

Danni Jian[1], Yi Cheng[2], Jing Zhang[2], Kai Qin[2] (✉)

[1] Department of Otolaryngology, Union Hospital, Tongji Medical College, Huazhong University of Science and Technology, Wuhan 430022, China
[2] Department of Oncology, Tongji Hospital, Tongji Medical College, Huazhong University of Science and Technology, Wuhan 430030, China

Abstract

Objective This study aimed to construct a prognostic model for rectal adenocarcinomas based on immune-related long noncoding RNAs (lncRNAs) and verify its prediction efficiency.

Methods Transcript data and clinical data of rectal adenocarcinomas were downloaded from The Cancer Genome Atlas (TCGA) database. Perl software (strawberry version) and R language (version 3.6.1) were used to analyze the immune-related genes and immune-related lncRNAs of rectal adenocarcinomas, and the differentially expressed immune-related lncRNAs were screened according to the criteria |log2FC| > 1 and $P < 0.05$. The key immune-related lncRNAs were screened using single-factor Cox regression analysis and lasso regression analysis. Multivariate Cox regression analysis was performed to construct an immune-related lncRNA prognostic model using the risk scores. Next, we evaluated the effectiveness of the model through Kaplan-Meier (K-M) survival analysis, ROC curve analysis, and independent prognostic analysis of clinical features. In addition, prognostic biomarkers of immune-related lncRNAs in the model were analyzed by K-M survival analysis.

Results In this study, we obtained gene expression profile matrices of 89 rectal adenocarcinomas and 2 paracancerous specimens from TCGA database and applied immunologic signatures to these transcripts. Through R and Perl software analysis, we obtained 847 immune-related lncRNAs and 331 protein-encoded immune-related genes in rectal adenocarcinomas. Eight important immune-related lncRNAs related to the prognosis of rectal adenocarcinomas were identified using univariate Cox regression and lasso regression analysis. Furthermore, four immune-related lncRNAs were identified as prognostic markers of rectal adenocarcinomas via multivariate Cox regression analysis. The prognostic risk model was as follows: risk score = (-4.084) * expression LINC01871 + (3.112) * expression AL158152.2 + (7.616) * expression PXN-AS1 + (-0.867) * expression HCP5. The independent prognostic effect of the rectal adenocarcinoma risk score model was revealed through K-M analysis, ROC curve analysis, and univariate, and multivariate Cox regression analysis ($P = 0.035$). LINC01871 ($P = 0.006$), PXN-AS1 ($P = 0.008$), and AL158152.2 ($P = 0.0386$) were closely correlated with the prognosis of rectal adenocarcinomas through the K-M survival analysis.

Conclusion We constructed a prognostic model of rectal adenocarcinomas based on four immune-related lncRNAs by analyzing the data based on TCGA database, with high prediction accuracy. We also identified two biomarkers with poor prognosis (PXN-AS1 and AL158152.2) and one biomarker with good prognosis (LINC01871).

Received: 26 October 2020
Revised: 15 March 2021
Accepted: 4 April 2021

Key words: rectal adenocarcinoma; immune-related lncRNA; prognostic model; The Cancer Genome Atlas (TCGA) database

Rectal cancer is the eighth most common cancer in the world and the tenth leading cause of cancer-related death. In 2018, there were 704,376 new cases and 310,394 deaths [1]. In recent years, the incidence of rectal cancer has increased in China [2]. Although the widespread comprehensive treatment involving total mesorectal excision (TME) surgery and chemoradiotherapy has made progress in patient survival, the long-term survival rate

✉ Correspondence to: Kai Qin. Email: qinkaitj@126.com
* Supported by a grant from the Health Commission of Hubei Province Scientific Research Project (No. WJ2019M118).

is still unsatisfactory, especially for patients with locally advanced and distant metastases, where the overall 5-year survival rate patients with rectal cancer is about 53% [3]. Therefore, there is an urgent need to identify new biomarkers to predict the prognosis of patients and guide precise treatment.

Immune-related long noncoding RNAs (lncRNAs), which are located near or overlapping the coding gene clusters of immune-related proteins, play an important role in guiding the development, differentiation, and activation of a variety of immune cells [4]. However, to date, only a few immune-related lncRNAs have been implicated in cancer [5]. Therefore, it is of great significance to study the role of immune-related lncRNAs in immune regulation. Although some reports have shown that an lncRNA is recognized as a biomarker to predict the prognosis of rectal adenocarcinomas [6-8], there are few studies on immune-related lncRNAs in rectal adenocarcinomas. In this study, immune-related lncRNAs in rectal adenocarcinomas were obtained by analyzing the transcripts and immune-related gene sets in The Cancer Genome Atlas (TCGA) database. We used univariate/multivariate Cox regression analysis to screen immune-related lncRNAs associated with the prognosis of rectal adenocarcinomas. We constructed a prognostic model composed of four immune-related lncRNAs and identified prognostic biomarkers for rectal adenocarcinoma.

Materials and methods

Patients and datasets of rectal adenocarcinomas

The transcripts and clinical data of rectal adenocarcinomas were downloaded from TCGA database (https://portal.gdc.cancer.gov/) on March 13, 2020. The screening conditions were as follows: (a) primary tumor site: rectal carcinoma; (b) project: TCGA-READ; (c) disease type: adenocarcinoma or adenoma; (d) data classification: transcriptome profiling; (e) data type: quantitative data of gene expression; and (f) workflow type: HTSeq-FPKM. The transcription data of rectal adenocarcinomas were sorted and transformed into a matrix according to the Strawberry Perl software (version 5.30.1.1). The corresponding clinical data of rectal adenocarcinomas were obtained from TCGA program (including patient number, sex, clinical stage, survival time, survival status, and TNM stage).

Immune-related genes and lncRNAs of rectal adenocarcinomas

The mRNA matrix and long noncoding RNA matrix of the coding protein were obtained by sorting the previous matrix (gene and sample names) using Perl software. We searched the immune-related gene set in the MSigDB database (http://software.broadinstitute.org/gsea/msigdb): IMMUNE_RESPONSE (M19817) and IMMUNE_SYSTEM_PROCESS (M13664), which was used to extract the immune-related genes encoding the protein. The R (version 3.6.1) and Bioconductor (https://www.bioconductor.org/) packages were used for data processing and analysis to obtain immune-related lncRNAs.

Establishment and evaluation of the prognostic model and independent prognostic analysis of clinical characteristics

The differential expression of immune-related lncRNAs in rectal adenocarcinomas was analyzed using Software Package EdgeR (http://bioconductor.org/packages/release/bioc/html/edgeR.html), filtered by the criteria |log2 FC (fold change)| > 1 and false discovery rate (FDR) < 0.05. Clinical data from TCGA were analyzed using univariate Cox proportional hazard regression (PHR), and survival-related lncRNAs were screened according to $P < 0.001$. Furthermore, through lasso-Cox analysis, the lncRNAs most related to overall survival were determined and cross-validation was performed to prevent overfitting. Then, multivariate Cox-PHR analysis was used to construct prognostic indicators and calculate risk scores. According to the median risk score, patients with rectal adenocarcinomas were divided into high- and low-risk groups. Kaplan-Meier (K-M) analysis was used to compare the differences in survival rate between the two groups. The risk score of each patient was calculated according to the expression levels of lncRNAs. The risk score model was calculated using the following formula:

$$\text{Risk score} = \sum_{i=1}^{n} \text{coefi X id}$$

To determine if the risk score could be driven by other clinical cofactors, we used a multivariate model (Cox proportional hazards) to account for age, sex, grade, clinical stage, and T stage in TCGA cohort. Receiver operating characteristic (ROC) and area under the curve (AUC) of 5-year overall survival rate and other clinical characteristics (gender, stage, TNM, and risk score) were calculated by R-package "survival ROC." Furthermore, K-M survival analysis was performed to identify lncRNAs associated with prognosis and to explore predictive lncRNAs.

Results

Differentially expressed lncRNAs in rectal adenocarcinomas

The clinical data of 90 rectal adenocarcinomas were downloaded from TCGA database (Table 1). We obtained the gene expression matrix of 89 cases of rectal

Table 1 Clinical characteristics of rectal adenocarcinomas

Clinical characteristics	No. of patients (%)
Gender	
Male	51 (56.7)
Female	39 (43.3)
Stage	
I	18 (20)
II	30 (33.3)
III	24 (26.7)
IV	14 (15.6)
Unknow	4 (4.4)
Tumor stage	
T1	4 (4.4)
T2	18 (20)
T3	62 (68.9)
T4	6 (6.7)
Fustat	
Alive	80 (88.9)
Dead	10 (11.1)
Lymph node	
N0	50 (55.6)
N1	26 (28.9)
N2	13 (14.4)
Unknow	1 (1.1)
Metastasis	
M0	70 (77.8)
M1	13 (14.4)
Unknow	7 (7.8)

adenocarcinomas; there were 2 cases of paracancerous specimens and 56754 genes were expressed. A total of 847 immune-related lncRNAs and 331 protein-encoded immune-related genes were processed and analyzed using the R language and the corresponding data packet. Using the edgeR package, 47 differentially expressed immune-related lncRNAs were screened with a threshold of $|\log2FC| > 1$ and FDR < 0.05, including 11 upregulated and 36 downregulated lncRNAs. Eight key lncRNAs related to prognosis were identified using lasso regression analysis and univariate Cox regression (Table 2).

Establishment and verification of the prognostic model of rectal adenocarcinomas

Table 2 Immune-related lncRNAs in rectal adenocarcinomas identified by univariate Cox regression analysis

Immune-related LncRNA	HR (95% CI)	*P* value
LINC01871	0.169 (0.047–0.617)	0.007
LINC02298	6.511 (1.840–23.035)	0.004
AL158152.2	4.66 (1.454–14.939)	0.01
SNHG6	4.362 (1.551–12.272)	0.005
ZFAS1	3.322 (1.383–7.984)	0.007
PXN-AS1	13.001 (1.886–89.641)	0.009
HCP5	0.262 (0.114–0.603)	0.002
Unknow	6.284 (1.890–20.892)	0.003

Table 3 Immune-related lncRNAs in rectal adenocarcinomas identified by multivariate Cox

Immune-related lncRNA	coef	R (95% CI)	*P* value
LINC01871	–4.084	0.0168 (0.001–0.433)	0.014
AL158152.2	3.112	22.457 (2.698–186.904)	0.004
PXN-AS1	7.616	20.261 (15.931–25.432)	0.002
HCP5	–0.867	0.420 (0.175–1.008)	0.052

Eight key immune-related lncRNAs, obtained by univariate Cox regression analysis, were used in the multivariate Cox-PHR regression analysis to calculate the prognosis risk score of each patient, and we constructed a risk score model consisting of four lncRNAs (Table 3): risk score = (–4.084) * expression LINC01871 + (3.112) * expression AL158152.2 + (7.616) * expression PXN-AS1 + (–0.867) * expression HCP5. K-M analysis comparing the survival difference between the high- and low-risk groups showed that the total survival time of patients in the low-risk group was significantly longer than that in the high-risk group (P= 1.93e–03; Fig. 1a). The area under the ROC curve was 0.957 (Fig. 2). Univariate/multivariate independent prognostic analysis of clinical traits showed that the prognostic risk score had an independent prognostic risk effect on rectal adenocarcinomas (P = 0.035; Table 4). The heat map, risk score, and scatter plots of survival time with respect to immune-related lncRNAs in rectal adenocarcinomas showed that the higher the risk score, the shorter the survival time and the more the death (Fig. 3).

Table 4 Univariate and multivariate Cox regression analyses of clinical characters in rectal adenocarcinomas

Clinical characteristics	Univariate Cox regression		Multivariate Cox regression	
	HR (95% CI)	*P* value	HR (95% CI)	*P* value
Age	1.12 (1.028–1.221)	0.01	1.04 (0.925–1.168)	0.512
Gender	0.559 (0.149–2.092)	0.388	0.982 (0.152–6.336)	0.985
Stage	2.355 (1.115–4.973)	0.025	9.757 (0.297–32.08)	0.201
T	2.152 (0.711–6.511)	0.175	1.562 (0.334–7.316)	0.571
M	4.206 (1.110–15.931)	0.035	0.179 (0.002–14.893)	0.446
N	2.074 (0.923–4.664)	0.078	0.587 (0.11–3.12)	0.532
Risk score	1.003 (1.001–1.005)	0.001	1.002 (1–1.003)	0.035

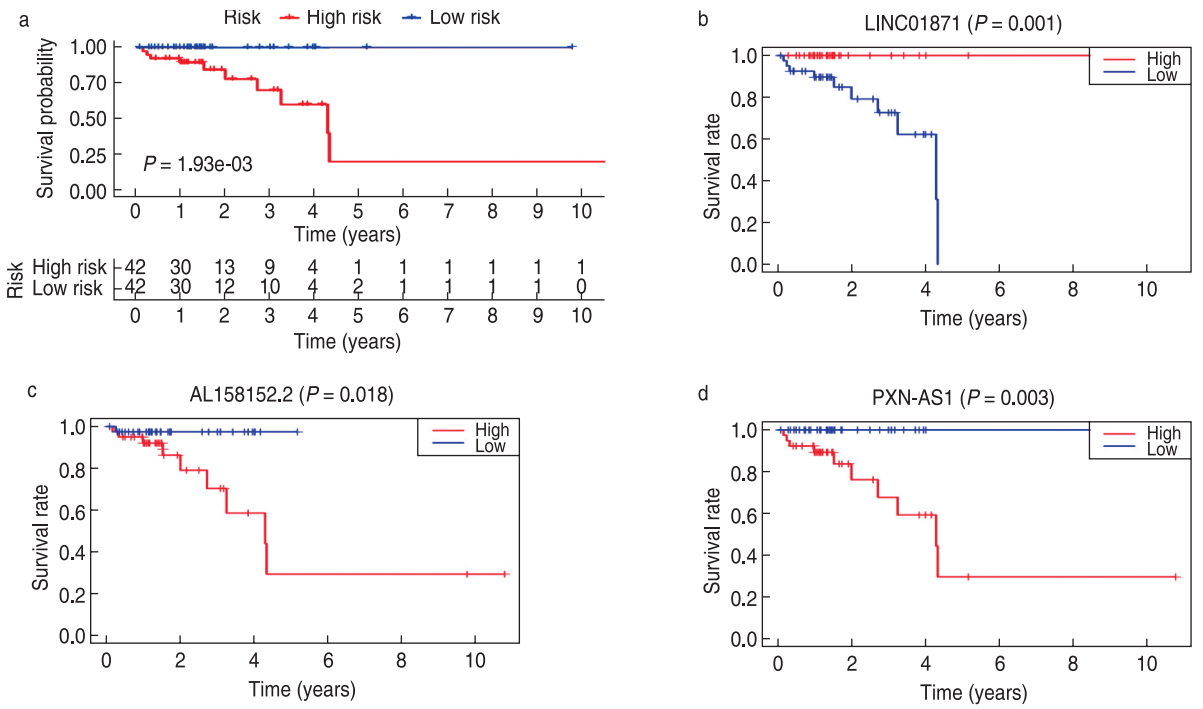

Fig. 1 Three prognostic immune-related lncRNAs identified by the multivariate Cox regression. (a) LINC01871; (b) AL158152.2; (c) PXN-AS1 and K-M survival curves of the rectal adenocarcinoma prognostic model (d)

Correlation between clinical features and key immune-related lncRNAs in the prognosis of rectal adenocarcinomas

Correlation with lymph node staging

We assessed the expression of the four immune-related lncRNAs in different lymph node stages of rectal cancer (AJCC, 8th edition) and found that the expression of AL158152.2 was positively correlated with the lymph node stage and the difference was statistically significant ($P < 0.05$). The expression of HCP5, LINC01871, and PXN–AS1 was not significantly correlated with lymph node staging ($P > 0.05$; Fig. 4a).

Correlation with the T stage and clinical stage of rectal adenocarcinomas

The results showed that there was no significant correlation among immune-related lncRNA, clinical stage, and T stage ($P > 0.05$; Figs. 4b and 4c).

Prognostic biomarkers of rectal adenocarcinomas

LINC01871 ($P = 0.001$), PXN-AS1 ($P = 0.003$), and AL158152.2 ($P = 0.018$) were associated with the prognosis in the prognostic model, as per the K-M survival analysis. LINC01871, PXN-AS1, and AL158152.2 may be independent prognostic factors, while LINC01871 may be a protective prognostic factor for rectal adenocarcinomas (Figs. 1b–1d).

Discussion

Immune-related lncRNAs are important regulators of gene expression in the immune system and play an important role in the occurrence and development of tumors [4–5, 9]. Li *et al* found that immune-related lncRNAs, which have high tissue specificity, are highly expressed in B cells and T cells [5]. Yu *et al* found that lncRNAs can be used as biomarkers to mark different stages of cancer immunity to adjust tumor immunity [10]. In recent

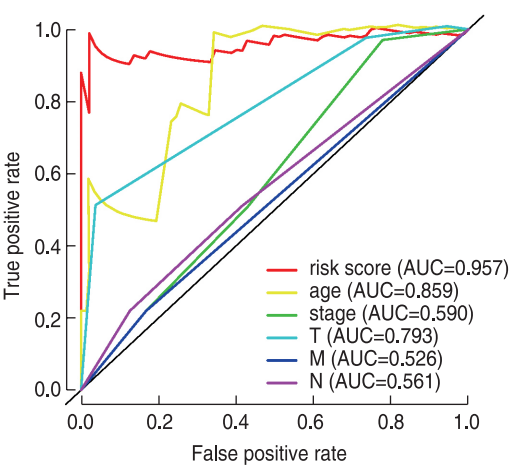

Fig. 2 Operating characteristic (ROC) curve of clinical parameters in rectal adenocarcinomas

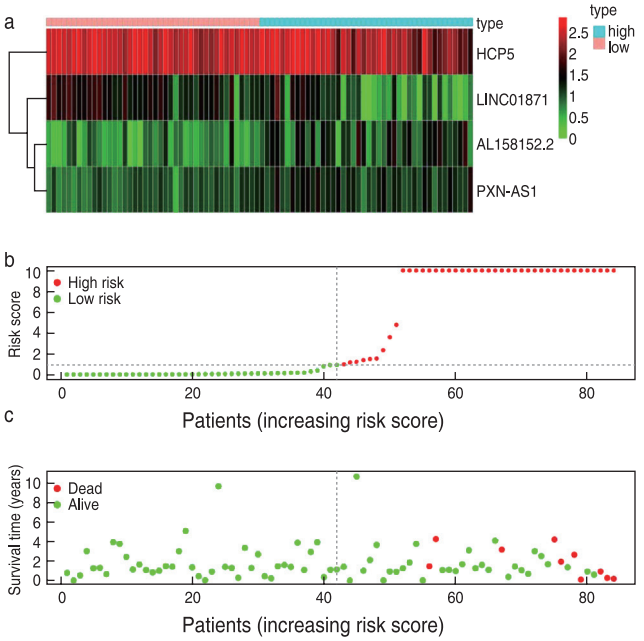

Fig. 3 Heat map (a), risk score (b) and scatter plots of survival time (c) of immune-related lncRNAs in rectal adenocarcinoma

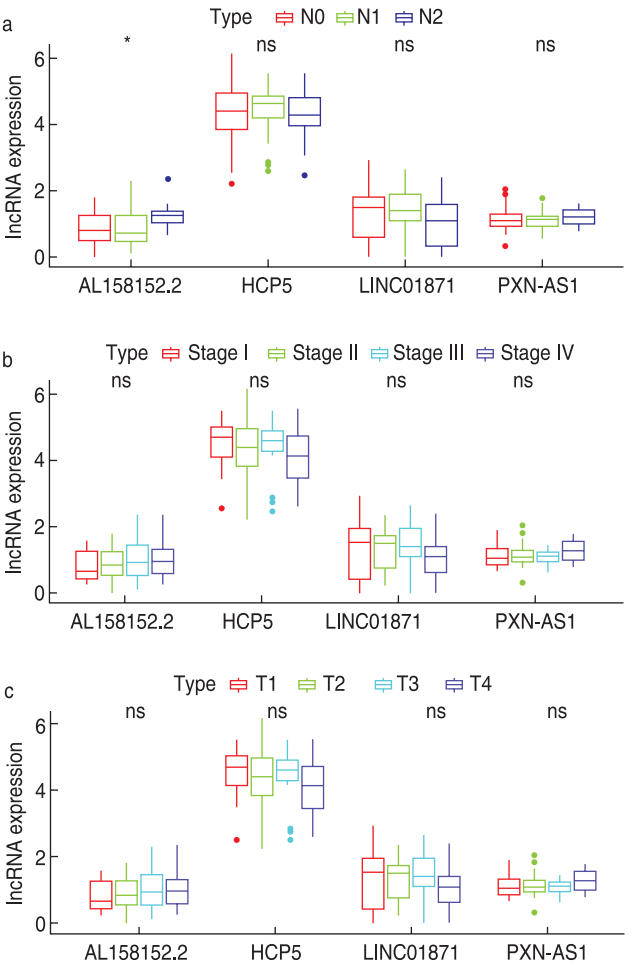

Fig. 4 The lymph node stage was positively correlated with the expression of AL158152.2, not the expressions of HCP5, LINC01871 and PXN−AS1 (a), there were no correlations between T stage, clinical stage of rectal adenocarcinomas and 4 key immune-related lncRNAs (b and c)

years, increasing evidence has shown that immune-related lncRNAs can be used as prognostic biomarkers for malignant tumors. At present, a prognostic model based on immune-related lncRNAs has been successfully constructed in a few malignant tumors, including breast cancer, head and neck squamous cell carcinoma, glioma, pancreatic cancer, and renal clear cell carcinoma [11–16]. There are many prognostic factors in rectal cancer, among which are common clinical related factors, such as surgical methods and R0 resection [3]; however, there are few reports on the prognostic role of immune-related lncRNAs. In this study, we aimed to construct a prognostic risk model of rectal adenocarcinoma based on immune-related lncRNAs and further analyze and obtain prognostic markers.

In the present study, a prognostic model was constructed by analyzing rectal adenocarcinoma samples from TCGA database. Risk score = (-4.084) * expression LINC01871 + (3.112) * expression AL158152.2 + (7.616) * expression PXN-AS1 + (-0.867) * expression HCP5. It had a high accuracy. LINC01871 is a protective immune-related lncRNA, while PXN-AS1 and AL158152.2 are harmful prognostic markers. At present, there are few reports on the prognostic immune-related lncRNAs in rectal adenocarcinomas. Tao *et al* found that NKILA, an immune-related lncRNA encoded by a gene on chromosome 20q13, was expressed at low levels in various human tumors, such as breast, lung, and rectal cancers. NKILA inhibits proliferation, migration, and invasion of rectal cancer cells by inhibiting NF-κB signaling, which is related to clinical progress and prognosis [17]. Zhao *et al* obtained a prognostic risk model of rectal cancer consisting of five lncRNAs (AC079789.1, AC106900.2, AL121987.1, AP004609.1, and LINC02163), in which AC106900.2 and LINC02163 are immune-related lncRNAs, but their functions are still unknown [7]. He *et al* found that HCP5, EPB41L4A-AS1, SNHG12, and LINC00649 are significantly related to the occurrence and prognosis of colorectal cancer through the competitive endogenous RNA network mediated by lncRNA, among which HCP5 and SNHG12 are immune-related lncRNAs. Studies have shown that SNHG12 can increase the expression of cell cycle-related proteins and inhibit the expression of caspase-3 in colorectal cancer and human osteosarcoma. In addition, silencing the expression of SNHG12 inhibited the proliferation of triple-negative breast cancer cells. It was found that SNHG12, as miR-199a/b-5p, regulates

the expression of MLK3 in hepatocellular carcinoma and affects the activation of the NF-κB pathway [18]. Therefore, SNHG12 may be a potential biomarker. The lncRNA HLA complex P5 (HCP5) is located at 6P21.33, which is homologous to the retrovirus gene sequence [19]. HCP5, which is considered a susceptibility gene site for HCV-related liver cancer, is downregulated in ovarian cancer,. HCP5 targets miR-139-5p and inhibits the expression of miR-139-5p. The miR-139-5p/ZEB1/Wnt signaling pathway is involved in the occurrence and development of EMT in CRC [20]. It was reported that HCP5 is highly expressed in glioma tissues and can promote the proliferation, migration, and invasion of glioma cells, inhibit apoptosis, and promote malignant biological behavior of glioma cells [18]. The lncRNA PXN-AS1-L is upregulated in hepatocellular carcinoma, nasopharyngeal carcinoma, lung cancer, and glioma, and promotes tumor occurrence by upregulating PXN [16, 18, 20–22]. In addition, we know nothing about the function and mechanism of LINC01871 and AL158152.2. However, the conclusion of this study was based on TCGA database, and we lacked domestic data to verify the prediction model and markers of immune-related lncRNAs in rectal adenocarcinomas.

In summary, we constructed a prognostic model of rectal adenocarcinomas based on the expression levels of four immune-related lncRNAs (LINC01871, PXN-AS1, HCP5, and AL158152.2) by analyzing TCGA database and immune-related gene sets, which have high prediction accuracy. Two negative prognostic biomarkers (PXN-AS1 and AL158152.2) and positive prognostic biomarker (LINC01871) were identified. However, the mechanism of action in rectal adenocarcinomas needs to be further explored.

Conflicts of interest

The authors indicated no potential conflicts of interest.

References

1. Bray F, Ferlay J, Soerjomataram I, *et al.* Global cancer statistics 2018: GLOBOCAN estimates of incidence and mortality worldwide for 36 cancers in 185 countries. CA Cancer J Clin, 2018, 68: 394–424.
2. Arnold M, Sierra MS, Laversanne M, *et al.* Global patterns and trends in colorectal cancer incidence and mortality. Gut, 2017, 66: 683–691.
3. Khalfallah M, Dougaz W, Jerraya H, *et al.* Prognostic factors in rectal cancer: where is the evidence? Tunis Med, 2017, 95: 79–86.
4. Geng H, Tan XD. Functional diversity of long non-coding RNAs in immune regulation. Genes Dis, 2016, 3: 72–81.
5. Li Y, Jiang T, Zhou W, *et al.* Pan-cancer characterization of immune-related lncRNAs identifies potential oncogenic biomarkers. Nat Commun, 2020, 11: 1000.
6. Zhang Z, Wang S, Ji D, *et al.* Construction of a ceRNA network reveals potential lncRNA biomarkers in rectal adenocarcinoma. Oncol Rep, 2018, 39: 2101–2113.
7. Zhao K, Wang M, Kang H, *et al.* A prognostic five long-noncoding RNA signature for patients with rectal cancer. J Cell Biochem, 2019 Nov. 10.
8. Liu H, He YK, Li QL, *et al.* Expression and clinical significance of lncRNA AC010145.4 in patients with rectal cancer. Chin J Cancer Prev Treat (Chinese), 2018, 25: 1558–1561.
9. Atianand MK, Caffrey DR, Fitzgerald KA. Immunobiology of long noncoding RNAs. Annu Rev Immunol, 2017, 35: 177–198.
10. Yu WD, Wang H, He QF, *et al.* Long noncoding RNAs in cancer-immunity cycle. J Cell Physiol, 2018, 233: 6518–6523.
11. Khadirnaikar S, Kumar P, Pandi SN, *et al.* Immune associated LncRNAs identify novel prognostic subtypes of renal clear cell carcinoma. Mol Carcinog, 2019, 58: 544–553.
12. Shen Y, Peng X, Shen C. Identification and validation of immune-related lncRNA prognostic signature for breast cancer. Genomics, 2020, 112: 2640–2646.
13. Wei C, Liang Q, Li X, *et al.* Bioinformatics profiling utilized a nine immune-related long noncoding RNA signature as a prognostic target for pancreatic cancer. J Cell Biochem, 2019, 120: 14916–14927.
14. Wang W, Zhao Z, Yang F, *et al.* An immune-related lncRNA signature for patients with anaplastic gliomas. J Neurooncol, 2018, 136: 263–271.
15. Zhou M, Zhang Z, Zhao H, *et al.* An immune-related six-incRNA signature to improve prognosis prediction of glioblastoma multiforme. Mol Neurobiol, 2018, 55: 3684–3697.
16. Wu S, Dai X, Xie D. Identification and validation of an immune-related RNA signature to predict survival of patients with head and neck squamous cell carcinoma. Front Genet, 2019, 10: 1252.
17. Tao F, Xu Y, Yang D, *et al.* LncRNA NKILA correlates with the malignant status and serves as a tumor-suppressive role in rectal cancer. J Cell Biochem, 2018, 119: 9809–9816.
18. Jiang L, Wang R, Fang L, *et al.* HCP5 is a SMAD3-responsive long non-coding RNA that promotes lung adenocarcinoma metastasis via miR-203/SNAI axis. Theranostics, 2019, 9: 2460–2474.
19. Yang C, Sun J, Liu W, *et al.* Long noncoding RNA HCP5 contributes to epithelial-mesenchymal transition in colorectal cancer through ZEB1 activation and interacting with miR-139-5p. Am J Transl Res, 2019, 11: 953–963.
20. Zhang Z, Peng Z, Cao J, *et al.* Long noncoding RNA PXN-AS1-L promotes non-small cell lung cancer progression via regulating PXN. Cancer Cell Int, 2019, 19: 20.
21. Jia X, Niu P, Xie C, *et al.* Long noncoding RNA PXN-AS1-L promotes the malignancy of nasopharyngeal carcinoma cells via upregulation of SAPCD2. Cancer Med, 2019, 8: 4278–4291.
22. Shang F, Du SW, Ma XL. Upregulation of lncRNA PXN-AS1-L is associated with unfavorable prognosis in patients suffering from glioma. Eur Rev Med Pharmacol Sci, 2019, 23: 8950–8955.

DOI 10.1007/s10330-020-0472-2
Cite this article as: Jian DN, Cheng Y, Zhang J, *et al*. Construction and validation of an immune-related lncRNA prognostic model for rectal adenocarcinomas. Oncol Transl Med, 2021, 7: 130–135.

Oncology and Translational Medicine
DOI 10.1007/s10330-020-0447-7

June 2021, Vol. 7, No. 3, P136–P140

ORIGINAL ARTICLE

A study of the potential adverse effects of electrosurgical smoke on medical staff during malignant tumor surgery*

Zhaoxia Luo[1], Xiuze Li[2], Shuhua Li[3], Bo Hou[1] (✉)

[1] Operation Room, Mianyang Central Hospital, Mianyang 621000, China
[2] Department of Anesthesiology, Mianyang Central Hospital, Mianyang 621000, China
[3] Department of Otolaryngology, Mianyang Central Hospital, Mianyang 621000, China

Abstract

Objective The aim of this study was to investigate the potential adverse effects of electrosurgical smoke on medical staff performing malignant tumor surgery.

Methods This study was divided into two parts: *in vitro* and *in vivo* experiments. The human thyroid cancer cell line, ARO, was cultured and passaged. The tumor cells were burned with an ultrasonic scalpel, and the surgical smoke was absorbed by a transwell membrane. The captured particles were diluted in 3 mL of culture medium, and cell survival was assessed under a microscope. DNA was extracted from the cells for genotyping. BALB/c mice were used to construct thyroid cancer xenograft models. The tumor tissues were dissected on day 14 using an ultrasonic scalpel. The smoke from the electrosurgical procedure was collected on a transwell membrane. The membrane was washed in 2 mL of rinsing solution, and the solution was then injected into the right armpit of 10 mice. After sacrifice, the tumor tissues were removed and stained with hematoxylin and eosin (HE).

Results Viable ARO cells could be seen on the first day after culturing cell fragments from surgical smoke, and vigorous cell proliferation could be seen on the 17th day of incubation. The genotype of the cells cultured in the presence of smoke particles was identical to the genotype of the original cells. Tumor growth was observed in four out of 10 mice injected with the smoke particle rinse. HE staining showed a significantly increased number of nuclei in the tumor tissue, which was consistent with the general morphological characteristics of malignant tumors.

Conclusion Viable tumor cells were detected in surgical smoke generated by ultrasonic scalpel dissection, and these cells had growth activity. Thus, it is necessary to protect patients and medical staff from electrosurgical smoke.

Received: 22 July 2020
Revised: 25 January 2021
Accepted: 15 March 2021

Key words: electrosurgery; ultrasonic scalpel; malignant tumor; smoke

Electrocautery, radiofrequency ablation, and ultrasonic scalpels are the commonly used electrosurgical techniques and tools for cutting, dissecting, and solidifying tissues during surgery [1]. Operating rooms do not have special devices to protect against electrosurgical smoke, even though patients and the operating room medical staff are exposed to surgical smoke generated by electrosurgical equipment [2]. Surgical smoke is composed of the gaseous by-products of evaporated tissues and is mainly composed of 95% water vapor and 5% combustion particles, which contain a large number of chemical substances, blood and tissue particles, viruses, or bacteria [3]. The nature of surgical smoke differs according to differences in the energy of the device being used and the tissue being cut [4]. Other possible influencing factors include the type of operation, the skill of the surgeon, and the power level of the instruments and devices. Surgical smoke can produce irritating gases and release potentially harmful substances [5]. Previous studies have raised concerns about the risk of infection, mutation, and the diffusion of malignant

✉ Correspondence to: Bo Hou. Email: hhh1471232021@163.com
* Supported by grants from the Sichuan Youth Science and Technology Fund (No. 1886521) and the Mianyang Science and Technology Plan Project (No. 17YFZ-0016).

cells during electrosurgical procedures [6]. Exposure to surgical smoke has adverse effects on the cardiovascular and respiratory systems. Surgical smoke has been shown to be cytotoxic, genotoxic, and mutagenic, and it is also a potential biological hazard [7]. However, there are few studies on the potentially harmful effects of residual malignant tumor cells in surgical smoke. Therefore, the purpose of this study was to explore the effects of residual malignant tumor cells in surgical smoke on medical staff and determine whether these cells still have growth potential.

Materials and methods

Experimental cells, animals, and instruments

The human thyroid cancer cell line, ARO, was purchased from the Kunming Cell Bank, Chinese Academy of Sciences. Roswell Park Memorial Institute (RPMI) 1640 medium was purchased from Wuhan Sanying Biotechnology Co., Ltd (Wuhan, China). Fetal bovine serum was purchased from Hangzhou Sijiqing Company (Hangzhou, China). Hematoxylin and eosin and immunohistochemical staining kit purchased from Beijing Jin Zijing Biomedical Technology Co., Ltd. (Beijing, China). A Reflex Ultra 45 radiofrequency ablation system and an ultrasonic scalpel were purchased from Shanghai Zhiheng Medical Device Co., Ltd. (Shanghai, China). Semi-permeable polyester membranes were purchased from Shenzhen Boanno Technology Co., Ltd (Shenzhen, China). Twenty SPF BALB/c mice were obtained from the Institute of Field Surgery, the Third Affiliated Hospital of the Third Military Medical University, China (animal certificate no.: 0001517, laboratory animal license no.: syxk [Yu] 2017-0005). Adaptive feeding was performed for 2 weeks, with free access to food and drinking water. All experiments were conducted in accordance with the Guide for the Care and Use of Laboratory Animals published by the National Institutes of Health.

In vitro experiments

In vivo and *in vitro* experiments were performed in a standard animal operating room. ARO cells were cultured in RPMI 1640 medium supplemented with 10% fetal bovine serum (FBS) and 1% penicillin and streptomycin. All tumor cells were maintained in an incubator at 37 °C, with 5% carbon dioxide. The cells were passaged every 3 days. Cells were digested with 25% trypsin for 3 min, and then, the single cell suspensions were obtained by pipetting. Cells were passaged at a concentration of approximately 2×10^6 cells/mL. The tumor cells in the culture medium were burned with an ultrasonic scalpel, and the resulting surgical smoke was absorbed by a vacuum pump (15 cmHg) connected to a syringe equipped with a transwell membrane. The membrane was located 5 or 10 cm away from the target cell line (Fig. 1). The smoke-collection membrane had a dense double-layer structure to effectively separate the gaseous smoke. The particles captured on the transwell membrane were diluted with 3 mL of RPMI medium. The diluted medium was cultured in an incubator at 37 °C, and cell survival was assessed by observation under a microscope. Genotyping was performed to determine whether the cells in the surgical smoke were the same as the original tumor cells.

In vivo experiments

In vivo experiments were divided into two parts. In the first part, 1×10^5 ARO cells were injected into the right armpits of 10 BALB/c mice. The growth of cancer cells was then observed in these mice. After 14 days, the tumor tissue was dissected with an ultrasonic scalpel, under 3% halothane anesthesia administered using a mask. The tumor tissue was dissected with an ultrasonic scalpel according to the standard procedure used for human malignant tumor surgery. The tumor tissue was dissected with 2 cm of normal tissue around the tumor tissue. A transwell membrane system was used to collect the electrosurgical smoke generated during the procedure. After collection, the smoke was eluted in 2 mL of TBST (Tris-buffered saline with Tween solution). In the second part of the experiment, the collected rinsing solution was injected into the right armpits of 10 BALB/c mice, and tumor growth was observed over a period of 3 weeks. At the end of the experimental period, the anesthetized mice were sacrificed via an intraperitoneal injection of pentobarbital. The site of the tumor was scraped clean, the subcutaneous nodules were fully exposed, and the tumor tissue was completely removed.

Hematoxylin and eosin (HE) and immunohistochemical staining

Tumor tissue was embedded in paraffin, sectioned, baked, and cryopreserved after cooling (each piece was cut at 4 μm thickness intervals and baked at 60 °C in 30 min). Tissue sections were dewaxed with xylene and then hydrated through an ethanol gradient. They were then stained with hematoxylin for 30–60 s, washed for 5 min, stained with eosin for 30 s, and washed again for 5 min. After dehydration through an ethanol gradient, the sections were dried, incubated in xylene, and sealed with neutral gum. Stained sections were observed under an Olympus® Bx50 optical microscope (Olympus, Tokyo, Japan), and images were captured.

Results

Result of *in vitro* culture of membrane particles

After culturing cell fragments within surgical smoke, viable ARO cells could be seen on the first day. On the

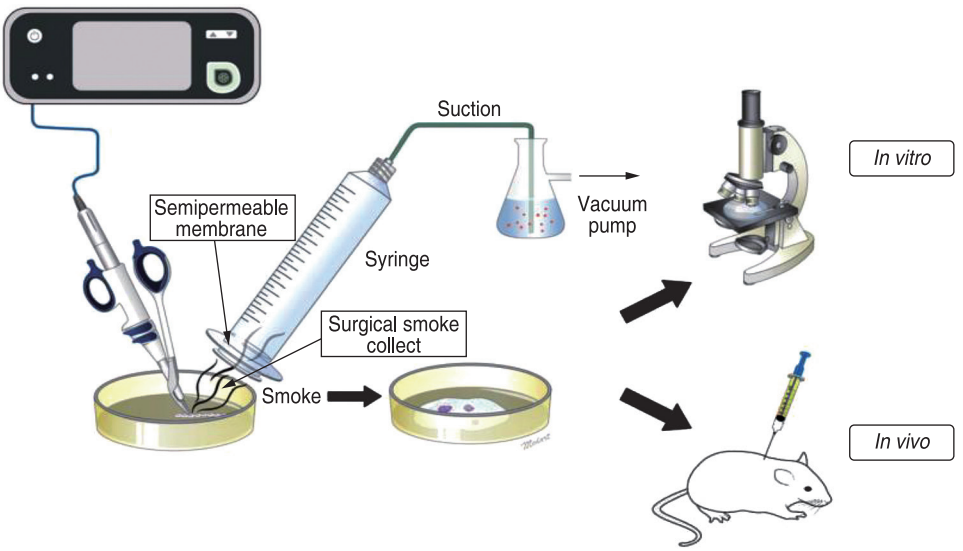

Fig. 1 *In vitro* and *in vivo* experimental models

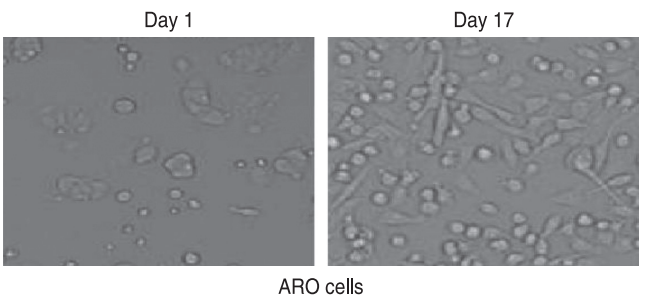

Fig. 2 Cultured cells from membrane particles

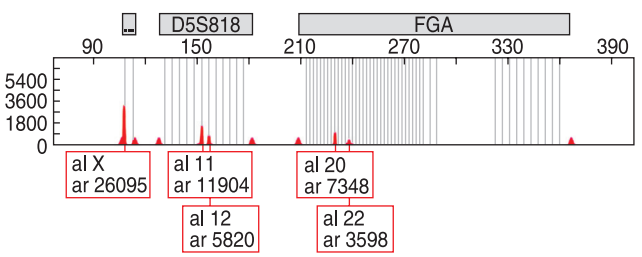

Fig. 3 Alleles detected in the ARO cell line

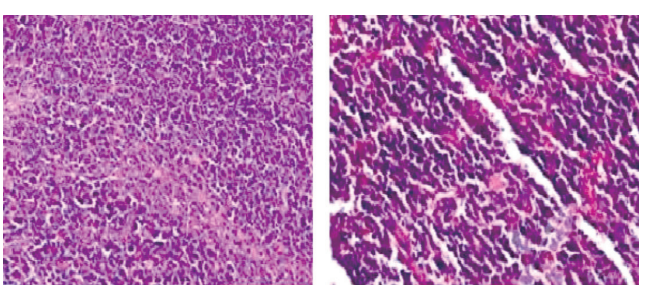

Fig. 4 Hematoxylin and eosin staining of mouse tumor tissue

17th day, vigorous cell proliferation could be seen, and the cells almost entirely covered the surface of the culture plate (Fig. 2). This indicated that a certain number of tumor cells survived in surgical smoke, and as they were not completely inactivated, they had strong growth potential.

Genotyping analysis

Genotyping analysis showed that the cells in the smoke particles collected using the membrane system were genetically identical to the original ARO cells (Fig. 3).

Tumor growth and HE staining in mice

Tumor growth was observed in four out of 10 mice injected with the smoke particle rinse. All palpable masses were biopsied for morphological evaluation. HE staining showed abnormal nuclei and a rough cytoplasm (Fig. 4).

Discussion

More than 600 different organic compounds are contained in the smoke produced by instruments used in surgical procedures. Most of these compounds have adverse effects on human health. Long-term exposure to this polluted environment may induce the development of various diseases of the respiratory, digestive, reproductive, nervous, blood, and immune systems. Surgical smoke may also have bioactive substances, such as virus particles, active cell fragments, and DNA fragments. HIV can remain active for 14 days in surgical smoke and only becomes completely inactive after 28 days.

The working principle of the ultrasonic scalpel involves the conversion of electrical energy into

mechanical energy through a special conversion device. The high-frequency ultrasonic vibration of the ultrasonic knife head can vaporize water in the contact tissues and cells, break the hydrogen bonds in proteins, and cut the tissue after solidification [8]. Ultrasonic scalpels have fast and slow gears. The fast gear is mainly used for tissue cutting, and the slow gear is mainly used for hemostasis. Its application in laparoscopic surgery has obvious advantages, and it is the main surgical instrument used in laparoscopic surgery, especially for gastric and colorectal cancer, for which it is used in more than 95% of the cases [9]. During high-temperature operation, the target cells are heated to the boiling point, resulting in membrane rupture and the dispersion of fine particles in the surrounding area. Ultrasonic scalpels use ultrasonic energy to destroy tissue through cavitation, and they produce a dense cloud of cell debris, which may contain living cells [10]. The heat generated by the ultrasonic scalpel is the result of internal friction caused by high-frequency vibration (approximately 55 000 times/s). High-temperature aerosols are more likely to carry infectious and active substances than low-temperature aerosols [11]. The present study demonstrated that there may be viable malignant cells in the surgical smoke produced by ultrasonic scalpels. This suggests that malignant tumor cells can be atomized onto tumor-bearing tissues via the use of an ultrasonic scalpel, and to some extent, it explains the recurrence of tumors at sites distant from the tumor extraction site after laparoscopic resection [12].

There is evidence that live bacteria and viruses are present in surgical smoke. Capizzi and others [13] reported that 5 strains of coagulase-negative *staphylococci* grew after laser resurfacing, among the 13 strains of bacterial culture. Garden [14] detected complete viral DNA sequences in smoke collected during the laser treatment of human papilloma virus-infected verrucae. The infectivity of these particles was confirmed by inoculating them onto the skin of calves. It has been reported that a surgeon was infected with laryngeal papilloma after using a surgical laser to treat condyloma acuminata of the anus and genitalia [15]. Although there are still disputes about the existence of living cells in surgical smoke, some studies have failed to screen out atomized cells in the peritoneal cavity during laparoscopic surgery. Other studies have shown that there are cell-sized fragments with intact morphology, but not viable cells, in surgical smoke. According to Johnson *et al* [16], in the surgical smoke generated by an ultrasonic scalpel, there are almost no intact cells, and no living cells. Fletcher [17] found that melanoma cells survive in the smoke produced by the electric cauterization of mouse melanoma cells. Therefore, many researchers believe that living cells, especially malignant cells, which have greater vitality, may survive in surgical smoke. Previous studies have used surgical fumes inhaled directly through long tubes. However, in the present study, transwell membranes with a pore size smaller than the size of cells, were used to increase the number of cells collected. When surgical smoke passes through the membrane, the gas is collected by a vacuum pump, and cells larger than the pores are filtered out and collected. Because of this, cell collection may be more efficient in this study than that in the previous studies.

Even with the use of smoke extractors, operating room staff can usually detect the smell of burnt tissue when performing electrical dissection procedures. This indicates that the surgical smoke is not fully removed from the room. The direct resection of a tumor mass is rare, because surgeons usually dissect the tumor tissue along with normal tissue 5 cm from the edge of the tumor [18]. However, owing to a distorted surgical field, an extensive malignant tumor, or surgical error, tumor masses may be directly removed. Therefore, it is necessary to control surgical smoke and use smoke extraction systems to protect the surgical team members and patients. At the same time, surgical fumes from the scalpel may contain viable tumor cells, and there is a theoretical risk of metastasis to anyone in close vicinity of the procedure.

In conclusion, this study found that there are viable tumor cells in the surgical smoke generated by ultrasonic scalpel dissection, and these cells have growth activity. Therefore, it is necessary to protect patients and medical staff from electrosurgical smoke.

Conflicts of interest

The authors indicated no potential conflicts of interest.

References

1. Golda N, Merrill B, Neill B. Intraoperative electrosurgical smoke during outpatient surgery: a survey of dermatologic surgeon and staff preferences. Cutis, 2019, 104: 120–124.
2. Romano F, Milani S, Gustén J, *et al*. Surgical smoke and airborne microbial contamination in operating theatres: Influence of ventilation and surgical phases. Int J Environ Res Public Health, 2020, 17: 5395.
3. Hamed H. Underwater-seal evacuation of surgical smoke in laparoscopy during the COVID-19 pandemic: A feasibility report of a simple technique. Br J Surg, 2020, 107: e640–e641.
4. Chiswell C, Akram Y. Impact of environmental tobacco smoke exposure on anaesthetic and surgical outcomes in children: a systematic review and meta-analysis. Arch Dis Child, 2017, 102: 123–130.
5. Chapman LW, Korta DZ, Lee PK, *et al*. Awareness of surgical smoke risks and assessment of safety practices during electrosurgery among US dermatology residents. JAMA Dermatol, 2017, 153: 467–468.
6. Bratu AM, Petrus M, Patachia M, *et al*. Quantitative analysis of laser surgical smoke: Targeted study on six toxic compounds. Rom J Phys, 2015, 60: 215–227.
7. Michaelis M, Hofmann FM, Nienhaus A, *et al*. Surgical smoke-hazard perceptions and protective measures in German operating rooms. Int J Environ Res Public Health, 2020, 17: 515.

8. Dalal AJ, McLennan AS. Surgical smoke evacuation: a modification to improve efficiency and minimise potential health risk. Br J Oral Maxillofac Surg, 2017, 55: 90–91.
9. Karjalainen M, Kontunen A, Saari S, *et al*. The characterization of surgical smoke from various tissues and its implications for occupational safety. PloS One, 2018, 13: e0195274.
10. Steege AL, Boiano JM, Sweeney MH. Secondhand smoke in the operating room? Precautionary practices lacking for surgical smoke. Am J Ind Med, 2016, 59: 1020–1031.
11. Ilce A, Yuzden GE, Yavuz van Giersbergen M. The examination of problems experienced by nurses and doctors associated with exposure to surgical smoke and the necessary precautions. J Clin Nurs, 2017, 26: 1555–1561.
12. Kontunen A, Karjalainen M, Lekkala J, *et al*. Tissue identification in a porcine model by differential ion mobility spectrometry analysis of surgical smoke. Ann Biomed Eng, 2018, 46: 1091–1100.
13. Capizzi PJ, Clay RP, Battey MJ. Microbiologic activity in laser resurfacing plume and debris. Lasers Surg Med, 1998, 23: 172–174.
14. Garden JM, O'Banion MK, Bakus AD, *et al*. Viral disease transmitted by laser-generated plume (aerosol). Arch Dermatol, 2002, 138: 1303–1307.
15. Chavis S, Wagner V, Becker M, *et al*. Clearing the air about surgical smoke: An education program. AORN J, 2016, 103: 289–296.
16. Johnson GK, Robinson WS. Human immunodeficiency virus-1 (HIV-1) in the vapors of surgical power instruments. J Med Virol, 1991, 33: 47–50.
17. Fletcher JN, Mew D, DesCôteaux JG. Dissemination of melanoma cells within electrocautery plume. Am J Surg, 1999, 178: 57–59.
18. Dobrogowski M, Wesolowski W, Kucharska M, *et al*. Health risk to medical personnel of surgical smoke produced during laparoscopic surgery. Int J Occup Med Environ Health, 2015, 28: 831–840.

DOI 10.1007/s10330-020-0447-7
Cite this article as: Luo ZX, Li XZ, Li SH, *et al*. A study of the potential adverse effects of electrosurgical smoke on medical staff during malignant tumor surgery. Oncol Transl Med, 2021, 7: 136–140.

Oncology and Translational Medicine
DOI 10.1007/s10330-020-0465-5

June 2021, Vol. 7, No. 3, P141–P147

ORIGINAL ARTICLE

Antitumor and vascular effects of apatinib combined with chemotherapy in mice with non-small-cell lung cancer

Hui Cao[1] (✉), Shili Wang[1], Yaohui Liu[2]

[1] Department of Pharmacy, Zigong Fourth People's Hospital, Zigong 643000, China
[2] Department of Pharmacy, Zigong First People's Hospital, Zigong 643000, China

Abstract

Objective The aim of this study was to investigate the antitumor and vascular effects of apatinib use combined with chemotherapy on mice with non-small-cell lung cancer (NSCLC).

Methods First, 60 tumor-bearing nude mice were randomly divided into control, low-dose, and high-dose groups. Four nude mice per group were sacrificed before administration and on days 1, 3, 7, and 10 after administration. HIF-1α expression in tumor tissues was detected. Second, 32 nude mice were randomly divided into control, premetrexed, synchronous, and sequential groups. The weights and tumor volumes of mice were recorded.

Results (1) HIF-1α expression decreased significantly on days 3 and 7 after low-dose apatinib treatment. There was no significant difference in HIF-1α expression in the high-dose apatinib group ($P > 0.05$). MMP-2 and MMP-9 expression levels in the low-dose apatinib group were significantly lower than those in the control group ($P < 0.05$). (2) In the low-dose apatinib group, the microvessel density increased gradually from days 3 to 7 post-treatment, while that in the high-dose apatinib group decreased significantly. (3) The inhibitory effect of sequential therapy using low-dose apatinib and pemetrexed was optimal, while that of synchronous treatment was not better than that of pemetrexed usage alone. Sequential treatment using low-dose apatinib and pemetrexed exerted the best antitumor effect. (4) The expression levels of p-AKT, p-mTOR, p-MEK, and p-ERK in the sequential group were significantly lower than those in the other three groups ($P < 0.05$).

Conclusion Apatinib usage involves certain considerations, such as dose requirements and time window for vascular normalization during lung cancer treatment in nude mice, suggesting that dynamic contrast-enhanced magnetic resonance imaging and other tests can be conducted to determine the vascular normalization window in patients with lung cancer and to achieve the optimal anti-vascular effect.

Received: 4 November 2020
Revised: 25 November 2020
Accepted: 20 December 2020

Key words: non-small-cell lung cancer (NSCLC); apatinib; pemetrexed

Lung cancer is the leading cause of cancer-related deaths worldwide, with nearly 1.2 million individuals succumbing to lung cancer every year [1]. Non-small-cell lung cancer (NSCLC) accounts for more than 80% of the lung cancer cases. Although chemotherapy can improve the outcome and quality of life of patients to some extent, the prognosis remains poor, and the median survival time is often less than 10 months [2]. Tumor growth depends on tumor angiogenesis; hence, anti-angiogenesis strategies play an important role in tumor treatment [3]. The traditional view is that antiangiogenic drugs can reduce tumor blood vessel formation, leading to tumor necrosis and "starvation" of the tumor. Short-term use of antiangiogenic drugs can be a good therapeutic strategy [4], while long-term use may lead to development of necrosis of blood vessels in the central area of the tumor, resulting in hypoxia. According to the theory of tumor angiogenesis normalization proposed by Jain *et al* [5], tumor angiogenesis is a complex process, and the imbalance between pro-angiogenic factors and angiogenesis inhibitors is a key factor. Apatinib, a small-molecule tyrosine kinase inhibitor, selectively inhibits the phosphorylation between vascular endothelial growth factor receptor 2 (VEGFR-2) and tyrosine

✉ Correspondence to: Hui Cao. Email: benbenda3321@163.com

through competitive binding with the tyrosine residue of the ATP binding site in VEGFR-2 on cells [6]. Kinase activity blocks the transmission of the VEGF/VEGFR-2 signaling pathway and inhibits tumor angiogenesis, thus inhibiting tumor growth [7]. PI3K-AKT-mTOR is one of the three major signaling pathways that have been identified to play crucial roles in cancer progression. mTOR is a key kinase downstream of PI3K/AKT, which regulates tumor cell proliferation, growth, survival, and angiogenesis. Cancer cells evade normal biochemical systems that regulate the balance between apoptosis and survival. PI3K-AKT-mTOR generally acts to promote survival through inhibition of expression of pro-apoptotic factors and activation of expression of anti-apoptotic factors. Cells contain PTEN phosphatase, which is used to negatively regulate PI3K expression. A reduction in PTEN expression indirectly stimulates PI3K-AKT-mTOR activity, thereby contributing to oncogenesis in humans. A series of clinical trials conducted on advanced lung cancer have preliminarily confirmed that apatinib can effectively decelerate lung cancer growth. However, the specific mechanism of its effect on tumor angiogenesis remains unclear.

Materials and methods

Cell lines

Human lung cancer cell line A549 was purchased from the cell bank of Chinese Academy of Sciences (Shanghai, China). A549 cells were cultured in the RPMI-1640 medium (Hyclone, Logan, USA) containing 10% fetal bovine serum, 100 U/mL penicillin, 50 mg/mL streptomycin, and 2 mmol/L glutamine; further, they were passaged and incubated in a 37°C incubator.

Establishment of xenograft tumor model in mice

Specific pathogen-free male BALB/C nude mice, aged 4–5 weeks, were purchased from the Biomedical Research Institute of Nanjing University (Nanjing, China). Approximately 2×10^6 A549 cells were suspended in 0.2 mL phosphate-buffered saline and injected subcutaneously into the right chest wall of each nude mouse. Tumor formation was observed within 10 days of injection. There was no significant difference observed in the average volumes of transplanted tumors in nude mice before intervention. In the first experiment, 60 tumor-bearing nude mice were randomly divided into three groups (20 mice per group); in the control group, normal saline was provided orally for 10 days once a day; in the low-dose apatinib group, intragastric administration of 60 mg/kg apatinib once a day, for 10 continuous days, was performed; in the high-dose apatinib group, intragastric administration of 120 mg/kg apatinib once a day, for 10 continuous days, was performed. Four nude mice per group were sacrificed before administration and on the 1st, 3rd, 7th, and 10th day after administration. In the second experiment, 32 tumor-bearing nude mice were randomly divided into 4 groups (8 mice per group); in the control group,mice were injected with normal saline of 0.5 mL.; in the pemetrexed group, intraperitoneal injection of pemetrexed 150 mg/kg was performed; in the apatinib and pemetrexed synchronous group, continuous oral administration of apatinib 60 mg/kg for 14 days along with intraperitoneal injection of pemetrexed on the first day at the same dose was performed; in the apatinib followed by pemetrexed group, first, vascular normalization was induced using apatinib for a certain period, and then pemetrexed was intraperitoneally injected during the vascular normalization window. The same abovementioned dose (60 mg/kg) was used. The time of vascular normalization was determined according to the results obtained in the first stage. Nude mice were treated for 14 days. The body weights and tumor volumes were recorded by the same person every 3 days.

Western blotting

Sonolysis of the tumor tissue was performed using a mild fluorophenyl buffer solution. A bicinchoninic acid protein detection kit was used to determine the total protein concentration. The equivalent protein amount was transferred onto a polyvinylidene fluoride membrane after subjecting the proteins to 10% sodium dodecyl sulfate polyacrylamide gel electrophoresis (SDS-PAGE). The membrane was incubated overnight with anti-mTOR, anti-p-mtor, anti-AKT, anti-erk, anti-mrk, anti-p-erk, and anti-p-mrk (diluted at 1:500) primary antibodies. The secondary antibody linked with horseradish peroxidase was added and the membrane was incubated for 3 h. After washing the membrane with Tris-Buffered Saline and Tween 20 buffer, blots were developed using enhanced chemiluminescence. Developed blots were imaged and the Image J software was used to analyze the images.

Immunohistochemistry

Immunohistochemical staining: The transplanted tumor tissue was fixed using 4% paraformaldehyde, dehydrated, and embedded in paraffin. Serial sections (3 mm thick) were obtained from each paraffin-embedded section; they were baked at 65°C for 1 h, and then dewaxed using xylene. The slides were dehydrated using ethanol, and the antigens were and repaired under high pressure with EDTA antigen repair solution. Peroxidase was removed using 3% H_2O_2 and samples were pre-treated using 5% bovine serum albumin for 30 min. They were incubated with anti HIF-1α primary antibody at 4°C overnight, and sections were incubated with biotin secondary antibody at room temperature

(25℃) for 20 min. The target protein was stained using diaminobenzidine, a peroxidase substrate. The staining intensity was estimated by three independent observers in five random regions per section.

Preparation of sample for electron microscopy analysis

The transplanted tumor tissues of mice were fixed using 3% glutaraldehyde at 4°C for 4 h, washed using 0.1 M sodium dicarboxylate buffer, and then soaked in 1% citric acid for 2 h. Then, tissues were washed twice using 0.1 M sodium dicarboxylate buffer and dehydrated using an ethanol gradient. Tissues were infiltrated with propylene oxide, completely embedded in the embedding solution, and incubated at 40°C for 12 h. The slides were then transferred to the insert plate and incubated at 60°C for 48 h. The ultrastructure of the organs was observed by transmission electron microscopy (Jeol, Japan).

Statistical analysis

All data have been expressed as mean ± standard deviation. The data were analyzed using the GraphPad prism software version 5.0. The two datasets were compared using a two-tailed unpaired Student's t-test. Multiple comparisons were performed using two-way analysis of variance and Bonferroni's post-hoc test. $P < 0.05$ was considered statistically significant.

Results

The effect of apatinib on HIF-1α expression in tumor tissues

In tumor tissues, hypoxia inducible factor (HIF) can induce an increase in angiopoietin expression, resulting in increased neovascularization, morphological variations in neovascularization, insufficiency of function, and formation of an incomplete basement membrane with uneven thickness. Therefore, HIF expression can be used as an indicator of tumor angiogenesis. The results of immunohistochemistry showed that HIF-1α expression decreased significantly on the 3rd and 7th days after treatment with lose-dose apatinib (60 mg/kg). There was no significant difference in the expression of HIF-1α in the high-dose apatinib group ($P > 0.05$; Fig. 1).

Electron microscopic observation of the ultrastructure of blood vessels

Electron microscopic observation showed that the vascular structure of the transplanted tumor was complete and exhibited regular characteristics on the 3rd and 7th days after treatment with low-dose apatinib, and the cellular structure and vascular basement membrane features were complete without formation of any gaps. When the vascular structure was disordered, a mature cell structure was not observed. At other time points and in high-dose groups, the vascular basement membrane showed incomplete formation (Fig. 2).

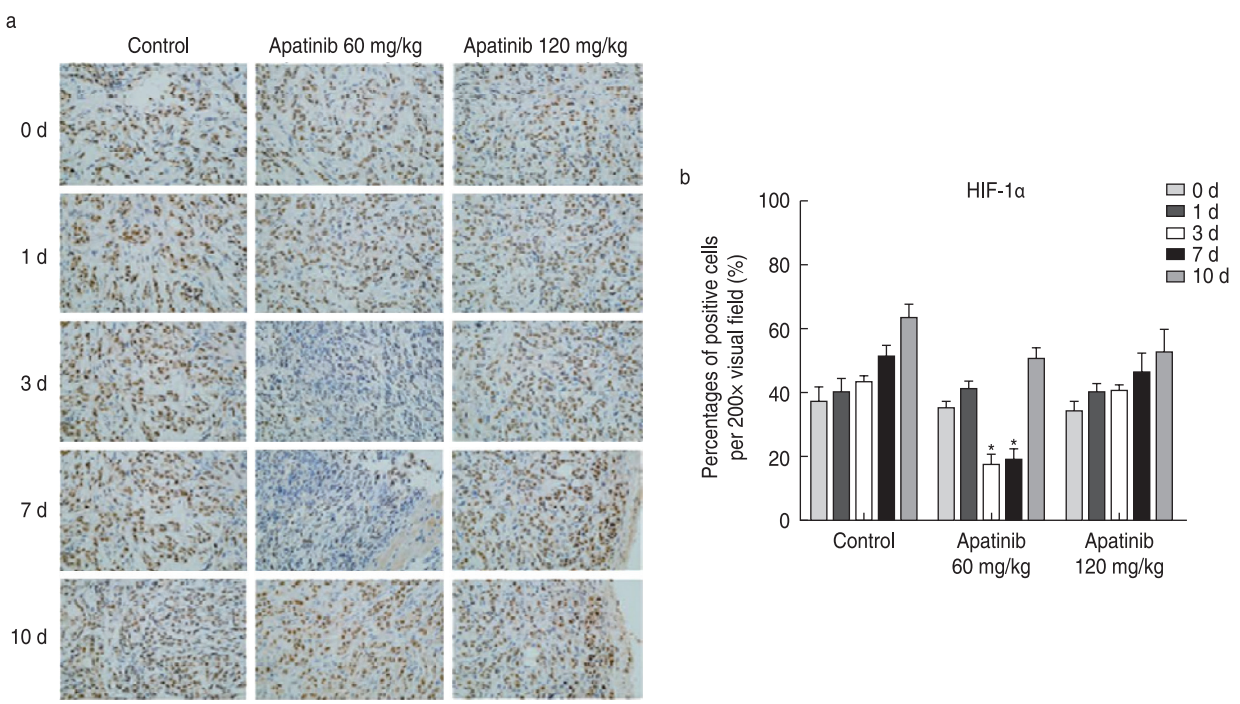

Fig. 1 Effect of apatinib on HIF-1α expression in tumor tissues. (a) Immunohistochemistry showing the expression of HIF-1α in tumor tissues; (b) Percentage of HIF-1 α expression positive cells

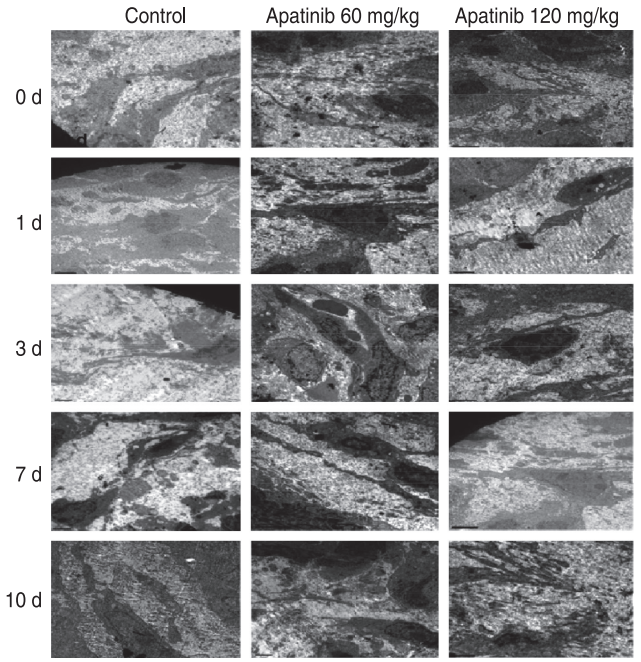

Fig. 2 Electron microscopic observation of the vascular tissue ultrastructure

Expression of MMP-2 and MMP-9 in transplanted tumor tissues

Western blotting results showed that compared with other groups, the low-dose apatinib group exhibited significantly decreased expression levels of MMP-2 and MMP-9 during days 3–7 ($P < 0.05$). MMP-2 and MMP-9 expression levels demonstrated no significant changes at other time points or in the high-dose apatinib group ($P > 0.05$; Fig. 3).

The effect of apatinib on microvessel density (MVD) in transplanted tumor tissues

MVD was detected via immunohistochemistry. The results showed that the MVD in the low-dose apatinib group increased gradually from days 3 to 7 post-treatment, and there was no significant difference during other time periods ($P > 0.05$; Fig. 4). The MVD of the high-dose apatinib group decreased significantly. This finding provides an explanation for the observation of low-dose apatinib-mediated induction of vascular normalization, while high-dose apatinib significantly destroyed the vascular structure of the transplanted tumor tissue, resulting in a significant reduction in blood vessels in the tumor tissue; thus, no time window exists for vascular normalization.

Inhibitory effect of apatinib in combination with chemotherapy on transplanted tumors

The inhibitory effect of sequential therapy with low-dose apatinib and pemetrexed was optimal, while that of synchronous treatment was not better than that of pemetrexed alone. According to the tumor inhibition curve, compared with the growth of the control group, that of the other three groups was significantly inhibited. The tumor volumes significantly differed, and the sequential treatment group had the best inhibitory effect, which was significantly different from that of

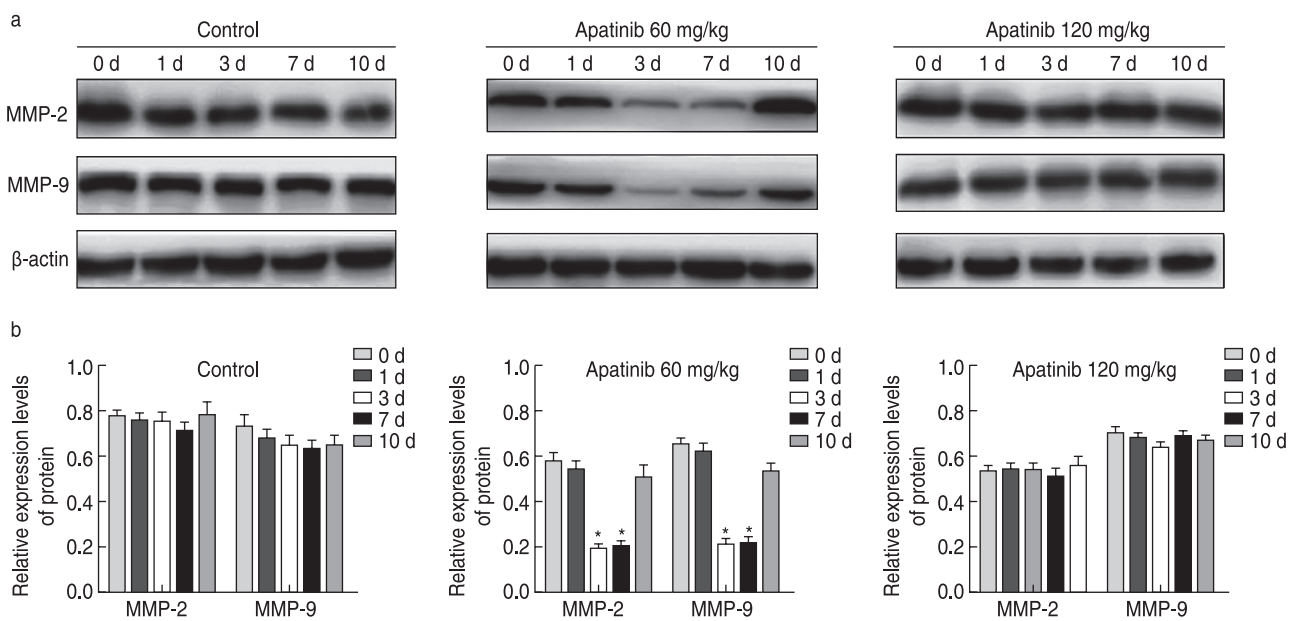

Fig. 3 MMP-2 and MMP-9 expression in transplanted tumor tissues. (a) Western blot analysis of the expression of MMP-2 and MMP-9 in transplanted tumor tissue; (b) Relative expression of MMP-2 and MMP-9 in transplanted tumor tissues

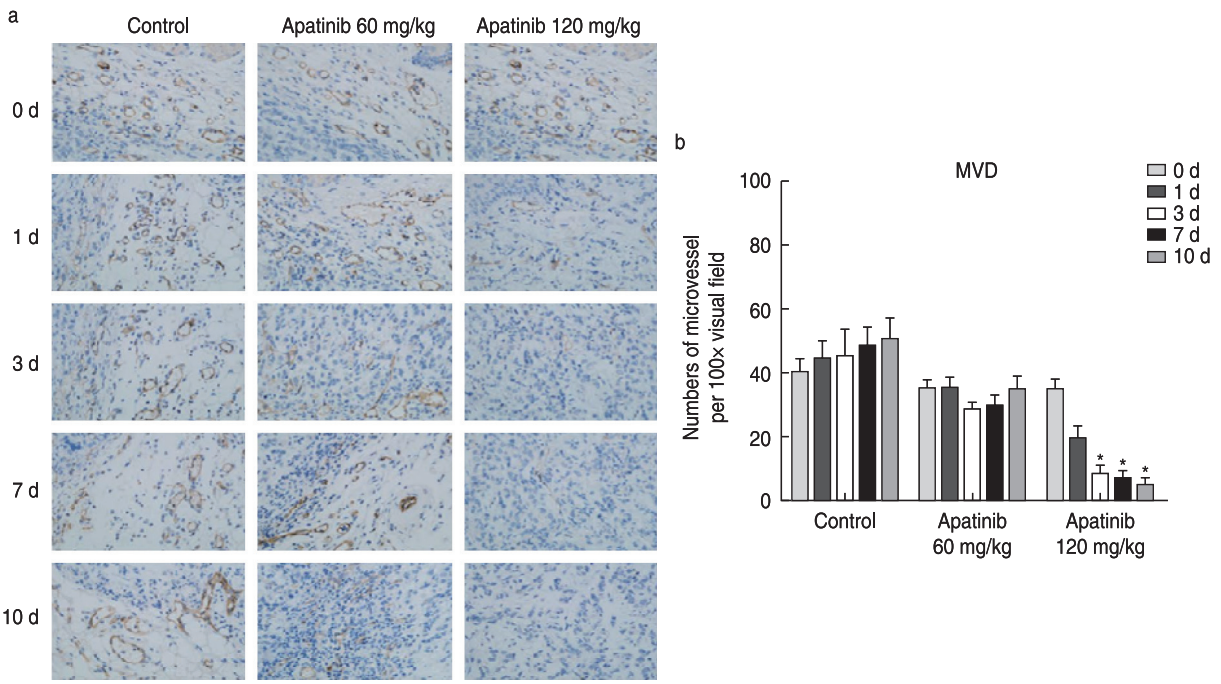

Fig. 4 Effect of apatinib on MVD in transplanted tumor tissues. (a) Immunohistochemical detection of the effect of apatinib on microvessel density in transplanted tumor tissues; (b)The number of microvessels in the transplanted tumor tissues

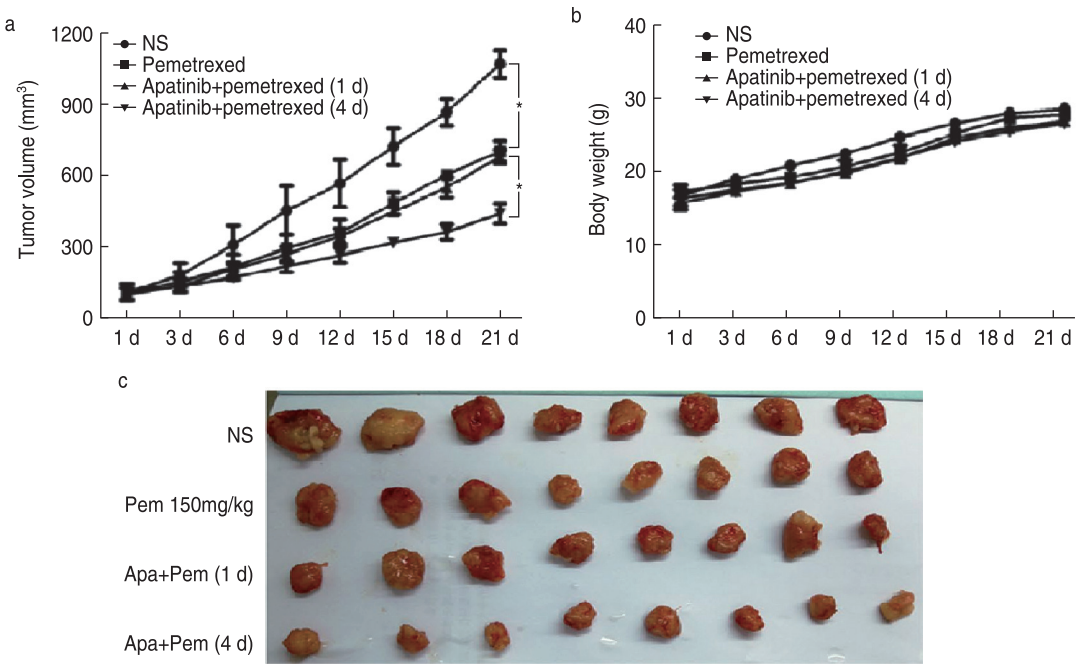

Fig. 5 Inhibitory effect of apatinib combined with chemotherapy on transplanted tumors. (a) Effect of apatinib combined with chemotherapy on the volume of transplanted tumors; (b) Effect of apatinib combined with chemotherapy on the weight of transplanted tumors; (c) Inhibitory effect of apatinib in combination withchemotherapy on transplanted tumors

synchronous treatment ($P < 0.05$; Fig. 5).

Expression of related signaling pathway factors in transplanted tumor tissue

The PI3K-AKT-mTOR signaling pathway plays an important role in cancer stem cell self-renewal and development of resistance to chemotherapy or

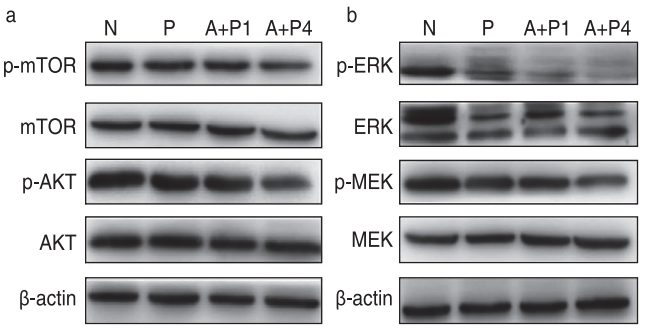

Fig. 6 Effect of apatinib on protein expression of related signaling pathways. (a) Western blot analysis of the effect of apatinib on the expression of PI3k-Akt-mTOR pathway protein; (b) Western blot analysis of the effect of apatinib on the expression of MEK-ERk-MNk pathway protein

radiotherapy, which has been suggested to be attributable for treatment failure, cancer recurrence, and metastasis. The expression levels of p-AKT, p-mTOR, p-MEK, and p-ERK in the sequential group were significantly lower than those in the other three groups ($P < 0.05$; Fig. 6). This suggests that sequential therapy using low-dose apatinib and pemetrexed may exert biological effects through the above-mentioned signaling pathways and may inhibit the growth of xenografts.

Discussion

Since the first antiangiogenic drug bevacizumab was administered for clinical use, antiangiogenic therapy has become an important strategy to treat malignant tumors. Particularly, the application of small-molecule antiangiogenic drugs via oral administration to cancer patients has demonstrated appreciable effects. Apatinib is a specific VEGFR-2 receptor antagonist, which competitively binds to VEGFR-2 receptors, blocks the VEGF-mediated signaling pathway, inhibits tumor angiogenesis, and thus controls tumor growth [8]. Presently, more than 30 clinical studies have examined the treatment of advanced lung cancer with apatinib. Most patients present with progressive NSCLC, while a few present with small-cell lung cancer. Most treatments focus on third-line therapy as the suitable approach. Apatinib monotherapy also includes apatinib use combined with chemotherapy or targeted drug therapy. In all clinical studies, monotherapy demonstrated poor efficacy [9]. The median progression-free survival (PFS) was less than 3 months, and the disease control rate was less than 50%. Therefore, the National Comprehensive Cancer Network guideline no longer recommends utilization of apatinib monotherapy for lung cancer [10]. According to the efficacy of apatinib usage combined with chemotherapy reported in the treatment of advanced lung cancer, compared with apatinib usage alone, the combination therapy can improve the PFS and overall survival (OS) of patients to a certain extent, but the OS time remains short.

Traditionally, antiangiogenic drugs inhibit blood flow mainly by inhibiting blood vessel formation in tumors, resulting in tumor "starvation." Antiangiogenic drugs can effectively control tumor growth for a certain period, but tolerance to therapy and tumor recurrence occurs inevitably [11]. At this juncture, combination therapy may be an effective strategy, including combined chemotherapy, targeted therapy, or immunotherapy. However, the clinical results of apatinib usage combined with chemotherapy for the treatment of advanced lung cancer did not significantly improve PFS and OS, which might be related to the mode of administration. Conventional doses of antiangiogenic drugs can effectively reduce tumor angiogenesis. During the administration of combined chemotherapy drugs, due to the rapid reduction in tumor neovascularization, especially in the tumor center, the effective concentration of local chemotherapy drugs is observed to be lower than expected, which markedly affects the tumor sensitivity to these drugs. Additionally, ischemia, hypoxia, and acidosis further affect the metabolism and transportation of drugs, resulting in exertion of poor treatment effects [12]. Astrid *et al.* [13] found that bevacizumab reduced docetaxel administration flow and net flow within 5 h in NSCLC patients, and these effects lasted for a period of 4 days. This further indicates that antiangiogenic drugs can easily induce local chemotherapy drug transport and reduce the effective blood concentration of the drug.

Based on these results, the combination of antiangiogenic drugs and chemotherapy drugs is not recommended. Since Jain first proposed the "vascular normalization theory" in 2005, accumulating studies have supported this perspective. After treatment with anti-vascular drugs, tumor blood vessels exhibit "normalized" characteristics within a certain period; that is, tumor blood vessels and cell morphology exhibit normal features, and the integrity of the basement membrane structure is partially restored, to improve hypoxia and acidosis in the tumor [14]. This state reduces the interstitial pressure in the tumor tissue, thus improving the transport, local effective concentration, and efficacy of chemotherapy drugs in the tumor. Our findings further confirm this phenomenon. Tumor tissues release various factors that promote growth of new blood vessels. Under the effect of VEGF, the most crucial angiogenic factor, tumor blood vessels grow rapidly, and vascular distortion, disorder, local expansion, leakage, and increased interstitial pressure occur. Increased pressure can lead to development of ischemia and hypoxia, and increased HIF expression, resulting in the establishment of a series of biological effects. Apatinib is the most specific VEGFR-2 inhibitor,

which can effectively reduce the effect of VEGF [15]. In this experiment, we observed that HIF-1α expression in the transplanted tumor tissue decreased significantly after 3–7 days of low-dose apatinib administration. These results indicate that after the intervention using low-dose apatinib, the local hypoxic state of the transplanted tumor tissue was significantly improved, and the tumor vascular structure was relatively complete, thus realizing transient normalization. In the high-dose apatinib group, we did not observe a clear window of vascular normalization. Immunohistochemistry results also showed that MVD was significantly decreased in the high-dose apatinib group, especially in the center of the transplanted tumor. The MVD decreased and there was no neovascularization, indicating that MVD did not return to normalcy. Therefore, we believe that the appearance of the vascular normalization window is related to the timing of antiangiogenic drug administration as well as the dose [16]. To further confirm that the window of vascular normalization during treatment with antiangiogenic drugs in combination with chemotherapy could effectively improve the therapeutic effect of chemotherapeutic drugs, we constructed a nude mouse model using transplanted tumors. The results showed that pemetrexed chemotherapy on day 4 following low-dose apatinib administration could significantly reduce the transplanted tumor volume. Therefore, sequential therapy with low-dose apatinib and pemetrexed can effectively inhibit the proliferation and promote the apoptosis of the transplanted tumor. Moreover, the PI3k-AKT-mTOR and the MEK-ERk-MNk signaling pathways play biological roles in these outcomes. It is suggested that the window of tumor vessel normalization is not observed immediately after application of an appropriate dose of antiangiogenic drugs, and the addition of chemotherapeutic drugs during this window can effectively improve their efficacy.

In conclusion, this study reports that there a certain dose is required for apatinib use and there exists a time window for vascular normalization in the treatment of lung cancer in nude mice, which suggests that DCE-MRI and other tests can be conducted to determine the vascular normalization window in patients. Furthermore, we should also follow the principle of individualized administration to enable treatment of each patient within the appropriate window of vascular normalization.

Conflicts of interest

The authors indicated no potential conflicts of interest.

References

1. Roman M, Baraibar I, Lopez I, *et al*. KRAS oncogene in non-small cell lung cancer: clinical perspectives on the treatment of an old target. Mol Cancer, 2018, 17: 1–14.
2. Wei X, Shen X, Ren Y, *et al*. The roles of microRNAs in regulating chemotherapy resistance of non-small cell lung cancer. Current Pharm Design, 2017, 23: 5983–5988.
3. Wilner KD, Usari T, Polli A, *et al*. Comparison of cardiovascular effects of crizotinib and chemotherapy in ALK-positive advanced non-small-cell lung cancer. Future Oncol, 2019, 15: 1097–1103.
4. Bacic I, Karlo R, Zadro A S, *et al*. Tumor angiogenesis as an important prognostic factor in advanced non-small cell lung cancer (Stage IIIA). Oncol Lett, 2017, 15: 2335–2339.
5. Jain R K. Antiangiogenic therapy for cancer: current and emerging concepts. Oncology, 2005, 19: 7–15.
6. Liu S, Su L, Mu X, *et al*. Apatinib inhibits macrophage-mediated epithelial–mesenchymal transition in lung cancer. RSC Advances, 2018, 8: 21451–21459.
7. Zhang H, Cao Y, Chen Y, *et al*. Apatinib promotes apoptosis of the SMMC-7721 hepatocellular carcinoma cell line via the PI3K/Akt pathway. Oncol Lett, 2018, 15: 5739–5743.
8. Liu M, Wang X, Li H, *et al*. The effect of apatinib combined with chemotherapy or targeted therapy on non-small cell lung cancer in vitro and vivo. Thorac Cancer, 2019, 10: 1868–1878.
9. Huang M, Gong Y, Zhu J, *et al*. A phase I dose-reduction study of apatinib combined with pemetrexed and carboplatin in untreated EGFR and ALK negative stage IV non-squamous NSCLC. Invest New Drugs, 2020, 38: 478–484.
10. Lan C Y, Wang Y, Xiong Y, *et al*. Apatinib combined with oral etoposide in patients with platinum-resistant or platinum-refractory ovarian cancer (AEROC): a phase 2, single-arm, prospective study. Lancet Oncol, 2018, 19: 1239–1246.
11. Nagano T, Tachihara M, Nishimura Y. Molecular mechanisms and targeted therapies including immunotherapy for non-small cell lung cancer. Curr Cancer Drug Targets, 2019, 19: 595–630.
12. Liu Z, Ou W, Li N, *et al*. Apatinib monotherapy for advanced non-small cell lung cancer after the failure of chemotherapy or other targeted therapy. Thorac Cancer, 2018, 9: 1285–1290.
13. Van der Veldt AA, Lubberink M, Bahce I, *et al*. Rapid decrease in delivery of chemotherapy to tumors after anti-VEGF therapy: implications for scheduling of anti-angiogenic drugs. Cancer Cell, 2012, 21: 82–91.
14. Wang J, Ma S, Chen X, *et al*. The novel PI3K inhibitor S1 synergizes with sorafenib in non-small cell lung cancer cells involving the Akt-S6 signaling. Invest New Drugs, 2019, 37: 828–836.
15. Nielsen S H, Willumsen N, Brix S, *et al*. Tumstatin, a matrikine derived from collagen type IVα3, is elevated in serum from patients with non–small cell lung cancer. Transl Oncol, 2018, 11: 528–534.
16. Chen Y, Mathy NW, Lu H. The role of VEGF in the diagnosis and treatment of malignant pleural effusion in patients with non-small cell lung cancer (Review). Mol Med Rep, 2018, 17: 8019–8030.

DOI 10.1007/s10330-020-0465-5
Cite this article as: Cao H, Wang SL, Liu YH. Antitumor and vascular effects of apatinib combined with chemotherapy in mice with non-small-cell lung cancer. Oncol Transl Med, 2021, 7: 141–147.

Call For Papers
Oncology and Translational Medicine

(CN 42-1865/R, ISSN 2095-9621)

Dear Authors,

Oncology and Translational Medicine (OTM), a peer-reviewed open-access journal, is very interested in your study. If you have unpublished papers in hand and have the idea of making our journal a vehicle for your research interests, please feel free to submit your manuscripts to us via the Paper Submission System.

Aims & Scope

- Lung Cancer
- Liver Cancer
- Pancreatic Cancer
- Gastrointestinal Tumors
- Breast Cancer
- Thyroid Cancer
- Bone Tumors
- Genitourinary Tumors
- Brain Tumor
- Blood Diseases
- Gynecologic Oncology
- ENT Tumors
- Skin Cancer
- Cancer Translational Medicine
- Cancer Imageology
- Cancer Chemotherapy
- Radiotherapy
- Tumors Psychology
- Other Tumor-related Contents

Contact Us
Editorial office of Oncology and Translational Medicine
Tongji Hospital
Tongji Medical College
Huazhong University of Science and Technology
Jie Fang Da Dao 1095
430030 Wuhan, China
Tel.: 86-27-69378388
Email: dmedizin@tjh.tjmu.edu.cn;
dmedizin@sina.com

Oncology and Translational Medicine (OTM) is sponsored by Tongji Hospital, Tongji Medical College, Huazhong University of Science and Technology, China (English, bimonthly).

OTM mainly publishes original and review articles on oncology and translational medicine. We are working with the commitment to bring the highest quality research to the widest possible audience and share the research work in a timely fashion.

Manuscripts considered for publication include regular scientific papers, original research, brief reports and case reports. Review articles, commentaries and letters are welcome.

About Us

- Peer-reviewed
- Rapid publication
- Online first
- Open access
- Both print and online versions

For more information about us, please visit:
http://otm.tjh.com.cn

中国科技核心期刊

（中国科技论文统计源期刊）

收录证书

CERTIFICATE OF SOURCE JOURNAL

FOR CHINESE SCIENTIFIC AND TECHNICAL PAPERS AND CITATIONS

ONCOLOGY AND TRANSLATIONAL MEDICINE

经过多项学术指标综合评定及同行专家评议推荐，贵刊被收录为“中国科技核心期刊”（中国科技论文统计源期刊）。

特颁发此证书。

中国科学技术信息研究所

Institute of Scientific and Technical Information of China

北京复兴路 15 号 100038　　www.istic.ac.cn

2020年12月

证书编号：2019-G616-0093

有效期至：2021年12月